# Development of Novel Environmentally-Friendly Bio-based Polymers Derived from Natural Cardanol

A dissertation submitted

to Tokyo University of Agriculture and Technology

fulfillment of the requirements for the degree of

DOCTOR OF PHILOSOPHY

in

Engineering

PIRADA SUDPRASERT

Department of Bio-Functions and Systems Science

Graduate School of Bio-Applications and Systems Engineering

# Publication

1. **Pirada Sudprasert**, Shotaro Kariya, Kenji Ogino, Suwabun Chirachanchai, Shinji Kanehashi, Synthesis and Characterization of Novel Bio-based Epoxy Polymers Derived from Natural Phenolic Compound, *J. Appl. Polym. Sci.*, Accepted on 16th May 2022.

   (Chapter 2)

2. **Pirada Sudprasert**, Kenji Ogino, Shinji Kanehashi, Cellulose Nanofiber-reinforced CNSL-derived Epoxy Nanocomposites, *J. Fiber Sci. Technol.*, Accepted on 20, May 2022.

   (Chapter 3)

3. Kan Kato, **Pirada Sudprasert**, Hiromu Saito, Takeshi Shimomura, Kenji Ogino, Shinji Kanehashi, Novel UV-curable bio-based polymers derived from non-edible phenolic biomass, *Chem. Lett.*, Accepted on 5th May 2022.

   (Chapter 4)

# Acknowledgement

Throughout the writing of this dissertation, I have received a great deal of support and assistance. I want to take a moment to thank them.

First and foremost, I would like to express my deep sense of thanks and gratitude to my supervisor Prof. Dr. Kenji Ogino and my advisor Assoc. Dr. Shinji Kanehashi, Department of Bio-Functions and Systems Science, Graduate School of Bio-Applications and Systems Engineering, Tokyo University of Agriculture and Technology (TUAT) for their day-to-day supervision, invaluable suggestions, constructive criticism and keen interest to carry out this research work. Their immense knowledge, plentiful experience and scientific integrity and dedication have been inspiring throughout my graduate study.

My warm thanks are conveyed to all the participants in this study. Their views, opinions and information helped me to understand the depth of the issues. I would like to conclude by expressing my sincere gratitude to 'Ministry of Higher Education, Science, Research and Innovation, Royal Thai Government Scholarship' for providing financial assistance throughout my stay and study in Japan.

I am profoundly indebted to my family, for their love, encouragement and motivation during the time. Without their support and encouragement, it would be very hard to complete my work. I would also like to thank my beloved friends, my laboratory's friends who helping me not only the experiment but also the valuable experience living in Japan, my Thai friends who study in Japan, we always share the feeling and beside together, my friends in Thailand who remind me, I am never alone and we can do the great things after my graduation.

# Declaration

I declare that this thesis is my own work, and it has not been previously submitted for any other degree or diploma. To the best of my knowledge and belief, any previously written or published materials used in this thesis by way of background information, are duly acknowledged in the text of the thesis

# Table of Contents

# List of Figures

# List of Tables

# List of Abbreviations

| | |
|---|---|
| SDGs | Sustainable Development Goals |
| CNSL | Cashew Nut Shell Liquid |
| CNF | Cellulose nanofiber |
| FRP | Epoxy resins as a matrix in fiber-reinforced polymer |
| EC | Epoxy Cardanol |
| ECP | Epoxy Cardanol Prepolymer |

# Dissertation Summary

Recently, worldwide environmental problems such as global warming, depletion of fossil resources, plastic pollution have been solved to establish sustainable economy. Development of chemicals and polymers from renewable resources has received great attention to mitigate these environmental concerns. The use of biomass resources is highly significant for the reduction in greenhouse gases as well as saving fossil resources. Particularly, utilization technology of non-edible biomass resources has received much attention since these resources are not competitive as food. Among agricultural biomass resources, plant oil is one of the candidates for the feedstocks of bio-based materials, since plant oils have various nature such as abundant renewable resources, cost effectiveness, availability of chemical reaction, etc. CNSL is obtained from cashew nuts shells which are biomass waste in cashew nuts industry. This plant oil possesses very unique properties such as phenolic compound having long alkyl side chain, antimicrobial property, antioxidant property, and UV absorption property, etc.

Here, effective utilization technology of CNSL was investigated to develop novel functional bio-based polymer.

In Chapter 1, introduction of this thesis is described. Research background and literature review of recent CNSL work are summarized in this chapter.

In Chapter 2, novel bio-based epoxy polymer was developed. The epoxy polymers were prepared from all cardanol-based epoxy and amine components at room temperature without any organic solvent. Molecular weight of epoxy cardanol prepolymer and thermal treatment improved the drying thermal and mechanical properties. Therefore, environmentally-friendly preparation protocols without formaldehyde, heavy metal catalyst, and organic solvent for novel all cardanol-based epoxy polymers was developed.

In Chapter 3, novel bio-based epoxy composite was developed. The epoxy composites were prepared from all cardanol-based epoxy and amine components with cellulose nanofiber (CNF). CNF immobilization with amine components provided better improvement of thermal and mechanical properties of the composites. The result indicated that hydrophobic CNF can be reacted with phenalkamine to give the CNF immobilization with phenalkamine and worked effectively as reinforced materials in cardanol-based epoxy polymer.

In Chapter 4, novel bio-based photocurable polymer was developed. The polymer was prepared from allyl cardanol and thiol compound via thiol-ene photoclick reaction at room temperature without any organic solvent. The resultant UV-cured polymers showed flexible transparent self-standing nature, thermal stability, and long-term stability (i.e., anti-aging) as compared with other cardanol-based polymers. This is because that thiol-ene reaction proceeded effectively among S-H and C=C, leading to be more highly crosslinked structure. Furthermore, thermal treatment of UV-cured polymers improved aging behavior because S-S bonds were formed between unreacted S-H groups after thermal treatment.

In chapter 5, Conclusion of this thesis is described. The strategy for the utilization of CNSL investigated in this thesis provides various fundamental research benefits in academia and industry. The significance of this research is believed to broaden the utilization of CNSL for novel bio-based polymer synthesis and their applications for sustainable economy to mitigate recent global environmental problems.

# CHAPTER 1: Introduction

## 1.1 Bio-materials to achieve SDGs: Sustainable Development Goals

The 17 Sustainable Development Goals (SDGs) with their targets are at the heart of the United Nations 2030 Agenda for Sustainable Development [1] and were accepted by the United Nations General Assembly's 193 member states in 2015. SDGs were developed to create foundations in sustainable development, with the goal of progressing toward global health and well-being, advocating the abolition of all forms of inequity and poverty, supporting climate action, quality education, gender equality, peace, and social justice. The goals are expressed explicitly in their targets (ranging from five to twelve targets per goal). The Sustainable Development Goals (SDGs) are formed from the three pillars of sustainable development: the economic, social, and environmental sectors, in order to ensure humankind's sustainability on Earth.

Despite the fact that the SDGs are acknowledged as a priority, their implementation is not proceeding as intended, developing at varied rates and with a variety of problems, owing in part to the present pandemic setting. Indeed, COVID-19 has caused an unanticipated worldwide catastrophe, with catastrophic consequences for the lives and health of nearly the entire world population [2]. The epidemic has delayed economic development, risen unemployment, and exacerbated poverty and starvation [3].

Materially dedicated, they play a crucial role in all aspects of human life: their consumption has been steadily increasing in recent years, reaching an unsustainable material footprint per capita, which is predicted to expand further in the next decades [4]. Materials extraction, manufacture, consumption, and end-of-life alternatives, in particular, have a significant influence on the economic, social, and environmental pillars [5].

Materials are clearly linked to several of the SDGs. For example, raw material exploitation, which should be related to the well-being of the population living in a natural resource-rich region, can cause pollution, GHG emissions, and stress on Earth. Advanced materials are

also important in the advancement of technology, innovation, and resources in all disciplines (from medicine to engineering and agriculture to artificial intelligence).

This implies a direct relationship between the various SDGs and the various stages of raw material management. Then, for global sustainability, raw material replacement with sustainable resources is required [5].

"Raw materials" are critical in a variety of industrial applications, such as chemicals, forestry and agriculture, medicine, industrial metals, and mining Natural resources are extracted and produced, with often negative effects on the natural environment. In our planet, there are about 100,000 different materials [6] and suitable materials selection is critical. Depending on the needed functional features and the ultimate cost, many aspects might be considered while choosing among different materials.

Today, more emphasis must be placed on sustainability within the context of the SDGs. Materials created from renewable resources are considered sustainable. Examples include recycled metals, bio-based polymers, and sustainable energy sources. People are becoming increasingly aware of the environmental part of sustainability challenges, and while the economic dimension of sustainable development is also well acknowledged, the social dimension is the lesser-known pillar. "Social sustainability" is associated with social results and principles such as equality, social responsibility, children's work, gender equality, community resilience, poverty eradication, and so on [7]. These are the more difficult to describe and quantify sustainability challenges, which can be summed by the notion of "inclusive growth," i.e., economic growth must be properly distributed throughout society members and generate opportunity for all.

It is also vital to emphasize that it is not feasible to totally prevent mining. Raw resources have always been necessary for mankind to exist on this planet. Furthermore, it is now obvious that the extraction of specific minerals containing specific elements, such as copper and rare earth elements, will be required in order to make significant progress toward greenhouse gas reduction objectives. Mining raw materials is still important; thus, in certain circumstances, a pertinent issue should be not only if such minerals can be given,

but also at what cost, taking into account environmental and social aspects [8]. Additionally, metals recycling can benefit metals' future availability by reducing the need for virgin resources. According to the United Nations, "sustainable consumption and production promote resource and energy efficiency, sustainable infrastructure, and giving access to essential services, green and dignified jobs, and a higher quality of life for everyone. " Its implementation helps to achieve overall development plans, reduce future economic, environmental and social costs, strengthen economic competitiveness, and reduce poverty" (Goal 12: Ensure Sustainable Consumption and Production Patterns) [9]. Then, sustainable materials and innovation in their production must be in accordance with the SDGs, and this review indicates that they are (directly or indirectly) linked to all of them.

"Composites materials," for example, in Europe, packaging accounts for 39.6 % of total plastics (often composites materials) demand, demonstrating that packaging is the most significant sector for plastics demand [10]. It is obvious that packaging has the disadvantage of generating plastic trash in Europe. As a result, the packaging industry urgently needs to introduce more sustainable packaging materials [5], derived from renewable sources. The research effort addressing alternative packaging (including SDGs 2-9-11-12-14-15) available from sustainable resources (for example, starch, poly(lactic acid), chitosan) is now quite active, with the main goal of finding viable alternatives to polymers generated from fossil fuels [11].

Cellulose is another material that may be utilized to create new sustainable composites [12,13] capable of producing films for a variety of applications where biodegradability is desired [14], as in single-use items (SDGs 1-2-7). Another pressing requirement is to develop new fillers (rather than only matrices) to replace natural ones such as calcite [5], nanocellulose crystals, for example, can be constructed [15], as fillers capable of improving mechanical, barrier, and thermal properties, surface wettability, and drug release capabilities. Other sustainable composites have been generated from agro-food waste (for example, coffee silverskin, a coffee waste) and utilized as reinforcing agents in biopolymer-based materials [16]. Finally, stabilized fly ash was used as a calcite (or talk)

alternative in the fabrication of polypropylene composites [17], demonstrating that the mechanical properties of raw materials and finished products may be preserved.

"Bio-Based and Food-Based Materials" are concerned with the most valuable and appropriate solutions to produce chemicals, which necessitate the use of various synthetic pathways, overcoming the difficulties associated with the use of commercial solvents and harsh conditions. Several examples can be discovered in the field of biomaterials, where materials are primarily synthesized to create novel sustainable and safe molecules for medical applications. New sustainable approaches for converting polyesters into functionalized oligomeric derivatives that may be utilized to print personalized biomedical devices, for example, have recently been presented [18].

Following the principles of green chemistry, new drug delivery composites for the controlled release of antibiotics have been developed (SDG 3) [19], and new drug delivery techniques that are more efficient have been proposed. Other materials for diagnostic and therapeutic agents have been realized, with reduced toxicity and the avoidance of some undesirable side effects of the chemicals used in pharmacy. In certain circumstances, water has been employed as a green solvent instead of poorer sustainable commercial reactants (SDG 12). Some of these materials can be derived from waste, byproducts, or crops, so contributing to the achievement of SDG 11 objectives [20,21].

In 2012, up to 30% of food production in the European Union was not consumed, and 88 million tons of food are presently wasted each year [22]. As a consequence, avoiding and eliminating food waste, as well as finding alternative applications for it, are vital, urgent tasks that should be approached from a resource efficiency perspective that regards food waste as feedstock for new materials.

In some cases, biomaterials can be useful for both bio-remediation and fuel production. A novel chemical method called as "Azure Chemistry" has just been proposed to achieve this goal [23], to restore or reconstruct ecosystems using fully environmentally-friendly and sustainable materials and technology, microalgal, for example, was employed as a filler in the manufacturing of bioplastic (SDGs 14-15) [24]. To complete the cycle following their

usage in bio-remediation, these microalgae can be exploited as a biofuel source (SDG 11) [25].

As previous mentioned, the growing concern in reducing the environmental effect produced by traditional plastics is helping to the emergence of more sustainable plastics with the goal of reducing the consumption of non-renewable resources for their manufacturing. Thus, enhanced bio-based polymer manufacturing and use in recent years has positioned biopolymers as one of the most viable solutions to achieve the sustainable development aim of replacing existing petroleum polymers with more sustainable materials in a variety of industrial sectors [26].

### 1.2 Cashew nut shell liquid (CNSL), Cardanol

Currently, this feedstock is widely employed as a raw material or after proper modification in a variety of sectors, including surfactants, lubricants, paints, household items, wastewater purification, textiles, and applications in coatings and resins [27–29]. Among these renewable raw resources, "Cashew nut shell liquid (CNSL)", an industrial waste and pollutant from the cashew nut (*Anacardium occidentale)* processing sector, has piqued the interest of researchers due to its widespread availability and ease of separation in high yields.

CNSL is a greenish-yellow to brownish viscous liquid obtained by thermal treatment of cashew nut shell, with an estimated annual industrial production of 450,000 metric tons [30]. Cashew nut trees were originally native to north-eastern Brazil, are now extensively distributed across the world's tropical areas, including India, Brazil, Bangladesh, Tanzania, Kenya, Mozambique, and Southeast Asia [31]. The cashew nut grows on the exterior of the cashew apple, an edible fruit. The cashew nut shell is leathery and contains a viscous reddish-brown liquid that accounts for roughly 67 % of the nut weight [32–34].

CNSL is among the most precious aromatic bio-feedstocks. It is high in phenolic compounds with unsaturated aliphatic chains, such as anacardic acid, cardol, cardanol, and 2-methylcardol [35]. CNSL is unique for a wide range of applications due to its phenolic residues and most hydrophobic long alkyl chains. It has practical applications, such as

brake lining compounds, in addition to its natural antibacterial and antitermite qualities [36], flame-resistant materials [37], surfactants [38], plasticizers [39], lubricants [40], resins [41], CNSL nanomaterials [42], soft materials [43], doping agents [44], and other medical applications [45].

Because CNSL is a non-edible oil, it has no detrimental impact on food production and availability when compared to other food crop-based bio-feedstock. Traditionally, several chemical processes such as the hot oil process, solvent extraction, mechanical extraction, vacuum distillation, and supercritical fluid bath have been used to extract the CNSL from raw cashew nut shells.

### 1.2.1 CNSL: Extraction and Chemical Composition

CNSL is a reddish-brown dark oil with a distinct odor that is widely regarded as one of the most important natural sources of non-isoprenoid phenolic lipids. Anacardic acid, cardanol, cardol, and 2-methylcardol are the primary chemical components found in CNSL, the structures illustrate in Figure 1.1.

These phenolic compounds have a peculiar chemical structure, having an alkyl side chain of 15 carbon atoms in meta-position in compared to their hydroxyl group (s). Another intriguing feature is that these alkyl side chains can have varied degrees of unsaturation, varying from none to 3 double bonds with cis (or Z) orientation (Figure 1.1).

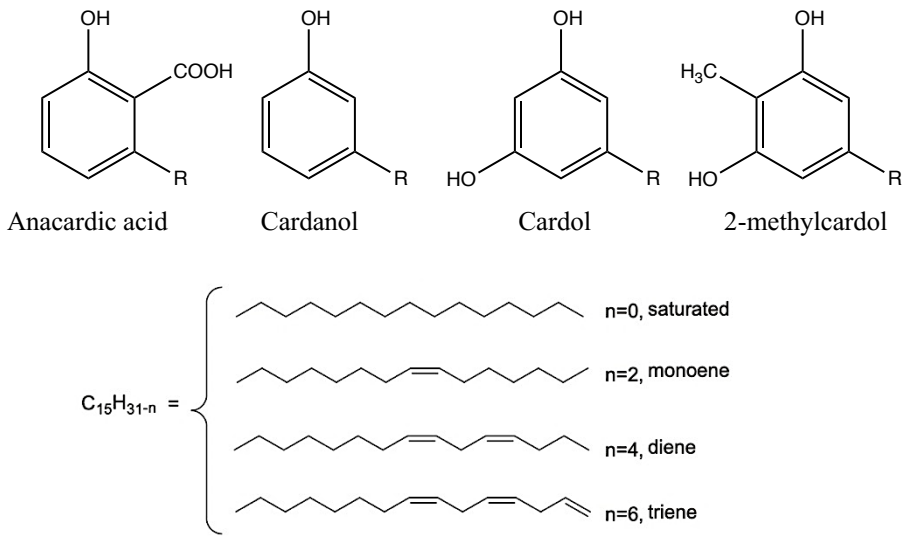


Figure 1.1 Chemical structure of the main components of CNSL.

CNSL may have variable chemical compositions depending on the technique of extraction and therefore be categorized into two types: solvent-extracted CNSL (natural CNSL) and technological CNSL (tCNSL).

Natural CNSL is prepared by using a solvent extraction technique (often Soxhlet, supercritical carbon dioxide, or subcritical water) to get its contents under moderate circumstances and without encouraging any chemical modification. Natural CNSL hence represents the original composition found in nature, which is mostly constituted of anacardic acids (60-70%), cardols (10-20%), cardanols (3-10%), 2-methylcardols (2-5%), and other minor elements [46,47]. Technical CNSL, on the other hand, is a by-product of the cashew nut industrial processing. Because the primary purpose of the cashew industry is to extract the lucrative kernel, CNSL is a secondary product.

Technical CNSL was initially used as a source of phenolic chemicals for the manufacture of phenol/formaldehyde polymers. With advancements in the chemistry of these phenolic lipids, tCNSL now promises to be an economically viable source of phenolic components. CNSL is extracted in the industry by an automated procedure that includes high temperatures to crack the shell and collect the cashew kernel. Cashew nutshells are submerged in the CNSL and heated to 180–190 °C in this "hot-oil process". Under these

conditions, anacardic acid in natural CNSL undergoes a decarboxylation reaction, converting itself to cardanol, resulting in technical CNSL, which is chemically distinct from natural CNSL and is composed primarily of cardanol (60-70%), cardol (10-20%), 2-methylcardol (2-5%), polymeric materials (5-10%), and other minor constituents. Table 1.1 describes several natural and technological CNSL compositions documented in the literature.

Initially, these variations may be explained by the fact that CNSL is a natural product, and hence its composition varies depending on geographical coordinates, climate, and soil conditions. Other important factors which could influence to composition discrepancies include extraction processes and analytical methodologies. Chemical compounds will have different affinities for the mobile phase depending on the extraction strategy (solvent utilized, temperature, duration, etc.), affecting their concentration in the completed product [48].

Table 1.1 Chemical composition of natural and technical CNSL

| Compound | Natural CNSL | | | Technical CNSL | | |
|---|---|---|---|---|---|---|
| | Tyman, 1996 [49] (%) | Oliveira et al., 2011 [50] (%) | Paramashivappa et al., 2001 [35] (%) | Tyman, 1996 [49] (%) | Andrade et al., 2011 [51] (%) | Kumar et al., 2002 [52] (%) |
| Anacardic acid | 71.65 | 62.90 | 63.00 | - | - | - |
| Cardanol | 5.10 | 6.99 | 10.50 | 67.80 | 40.26 | 67.00 |
| Cardol | 22.30 | 23.98 | 22.50 | 18.20 | 29.95 | 22.00 |
| 2-Methylcardol | 1.10 | - | - | 3.30 | - | - |

### 1.2.2 Cardanol-Based Functional Materials

Cardanol is an aromatic biomonomer generated from CNSL; it is environmentally friendly, affordable, and widely available as agricultural waste in many regions of the world. Anacardic acid is typically decarboxylated into cardanol and isolated as a pale-yellow liquid when CNSL is treated with high temperature (180-220 °C) under vacuum (3-4 millimeter torr). It was made up of a variety of cardanol compounds with variable degrees of unsaturation in the meta-positioned side chain

Cardanol has unique structural properties; it is a phenol-based monomer with a meta-substituted unsaturated alkyl side chain (C15) and many functionalization sites. The phenolic hydroxyl group leads the following incoming groups into the aromatic ring's ortho and/or para locations, allowing for more synthetic flexibility. The system's amphiphilicity and lipid nature are induced by the unsaturated/saturated hydrophobic alkyl chain with odd-numbered carbons. The phenolic hydroxyl group and the cis double bonds on the side chains are also suitable for functionalization with other monomers. Cardanol is a valuable starting material for the synthesis of different derivatives due to the difficulty of synthesizing phenols with a long unsaturated carbon chain at meta-position and its low price and availability [32–34].

Cardanol's potential as a starting material derives from its distinct chemical structure. Cardanol is widely used as a renewable feedstock for the production of many functional materials, particularly in places where cashew nut trees are abundantly cultivated. Cardanol's active sites (aromatic ring, hydroxyl group, and unsaturation in side chains) react with other molecules to produce a variety of functional materials. Esterification, alkylation, etherification, propoxylation, polymerization, and phosphatation all benefit from the phenolic hydroxyl group. Side chain unsaturation can be employed in hydrogenation, epoxidation, metathesis, and hydrosilylation processes, conclusion in Figure2. On an aromatic ring, several substitution (bromination, nitration, sulfation, and amination), condensation, and hydrogenation processes can take place. These properties are widely used in the design and development of a wide range of materials, including epoxy resins, phenolic resins, acrylics, rubbers, polyurethanes, paints, and varnishes that use cardanol as a bio-monomer [36–45].

A comprehensive list of products generated from cardanol is the very commercially valuable cardanol-based polymers underlined. Condensation of formaldehyde with cardanols resulted in the formation of several resins [53]. These resins' mechanical properties may be easily controlled by exploiting unsaturation in the side chains [54]. Furthermore, these materials exhibit excellent hardness, elasticity, and superfine adhesive properties.

Epoxy-type resins are synthesized from cardanol copolymers with phenols and glycidyl ethers. These resins are among the best modified phenolic epoxy resins available as an alternative to regular synthetic epoxy resins. They provide high flexibility and temperature resistance while maintaining oil bleeding qualities [36]. Another important utilization cardanol is the creation of benzoxazines with superior thermal, physical, and mechanical qualities such as minimal moisture absorbtion, chemical and flame resistance, and nearly no shrinking. These polymers are created using the Mannich-type condensation of cardanol, formaldehyde, and various primary amines [55].

Cardanol-porphyrin derivatives were also effective for a variety of applications; they were created by either simple reaction or condensation of cardanol aldehydes with pyrroles [56]. Cardanol-derived porphyrin composites are also employed to enhance TiO2 photocatalytic activity in photodegradation processes [57].

Sulfation of saturated cardanol is widely documented in the literature; it may be accomplished using sufficient sulfuric acid at ambient temperatures in halogenated solvents or by treating the phenolic hydroxyl group with ethylene sulfate. The sulfated salts of cardanol can be employed as surfactants, and their surfactant characteristics appear to be similar to those of commercially available detergents, such as dodecylbenzene sulfonate [58–60].

Cardanol's unsaturated C15 hydrocarbon side chain is universally acknowledged for its crosslinking characteristics. Cardanol-azo benzene self-polymerization produces very transparent liquid crystalline material films. These materials exhibited thermotropic as well as lyotropic characteristics [61].

Another essential category cardanol functionalization is phosphorylation of the hydroxyl group of phenol. These phosphorylated cardanols are commonly known as an excellent rubber plasticizer [62]. Cardanol polymers combined with formaldehyde yielded rubbery-type gel products that can be employed in cement hardening [36].

Cardanol has also been used to create thermoplastic polyurethanes with excellent thermal and mechanical qualities [39,63]. These environmentally-friendly cardanol-derived

polymeric coatings have found use in the paint, enamel, and varnish industries [31]. Most polymeric coatings are synthesized by autooxidation or crosslinking of oily materials.

Due to the benefit of double bonds in the side chain, cardanol auto-oxidizes quickly at room temperature and creates strong, clear, scratch- and wrinkle-free polymeric films [62]. Cardanol-based amphiphilic compounds were discovered to have outstanding self-assembly capabilities in a variety of nanostructures. Cardanyl glycolipid molecules, for example, generated nanotubes, twisted ribbons, tapes, and other forms that might be useful in catalysis, inclusion chemistry, and nanofabrication [43].

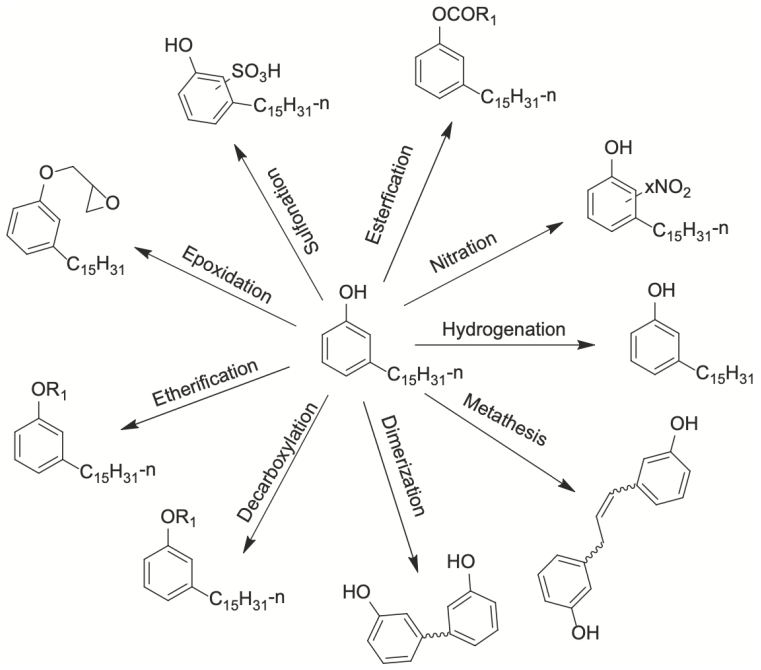


Figure 1.2 Possible reactions of cardanol [64].

## 1.3 Chemicals and Polymers

### 1.3.1 Thermosetting cardanol resins

There is a greater emphasis on the importance of green chemistry in the chemical industry. Cardanol phenol has raised significant interest in the development of thermosetting materials with improved characteristics and applications [65]. Light, heat, and chemical initiators were used to cure these materials. Cardanol-based thermoset products, such as phenolic, epoxy, polyester, and polyurethane resins, offer advantages over petroleum-based thermosetting materials because they are a unique and suitable sustainable feedstock, have a cost-performance foundation, and have excellent eco-friendliness characteristics [66]. Previous research exploited rosin as a natural substance to manufacture enhanced epoxy resins, curing agents, vinyl ester resins, polyester, alkyd, and polyurethane [67–71]

Cardanol and related polymers have been found to have intriguing structural properties for chemical modification and polymerization into specialty polymers. Cardanol-formaldehyde resins outperform ordinary phenolic resins in terms of flexibility (due to the internal plasticization effect of the lengthy chain), which improves processability. Because it works as a water-repellent group, the inclusion of extended alkyl groups improves the weathering resilience of cardanol polymers [72].

Moreover, cardanol polymers offer advantageous qualities such as heat and electrical resistance, antibacterial capabilities, and insect resistance. Natural fibers, such as ramie, flax, and hemp fibers, have been added to cardanol–formaldehyde resins in some situations to overcome the steric hindrance and decreased intermolecular interactions conferred by the C15 side chain for fabric structural purposes. It was also stated that an epoxy resin based on bisphenol A diglycidyl ether was mixed with the cardanol-formaldehyde resins to lower the quantity of water generated during the process and the porosity of the cardanol-formaldehyde resins [73].

A novel benzoxazine prepolymer derived from cardanol was recently used to make phenolic resins in the presence of formaldehyde and an amine. Cationic catalysts such as PCl5 enable for faster polymerization of cardanol-based benzoxazine monomer at room

temperature. The benzoxazine-based phenolic family has demonstrated exceptional capabilities as advanced composites, including strong thermal properties and flame retardancy, as well as mechanical performance and molecular design flexibility [73].

Epoxy thermosets are the most frequent polymers, with over 3 million tons manufactured, and have a variety of uses in coating, adhesives, and composites. Petroleum derivatives are most typically used to make epoxy resins. Recently, bio-based feedstocks have been employed extensively to create epoxy from plastic waste and natural materials as low-cost sources [67–71].

To generate epoxy resins, the phenolic hydroxyl group of cardanol or unsaturated double bonds on the C15 alkyl side chain can be treated with epichlorohydrin (ECH) or epoxidized, respectively. Furthermore, polyphenol derived from cardanol is utilized to make epoxy resins. Cardanol was used to partially or completely replace phenol in thermoset resins such as novolac resins [74], vinyl esters [75,76], and also in epoxy resins modification [77].

Based on CNSL and its derivatives, the production of many types of epoxy compounds. At 95 °C, the hydroxyl group of cardanol was reacted with ECH to create epoxy using ZnCl2 as a catalyst under basic conditions. Cardolite Corporation sells this product commercially. Cardolite resins (commercial epoxy based on cardanol) have been treated with bisphenol A to produce adhesives with increased impact strength and shear resistance [78–80]. Cardanol was also used to synthesize curing agents for epoxy resins, such as polyamines [33] and cardanol-based self-curing epoxy [81] to modified in surface coatings. By reacting with chloroperbenzoic acid, perbenzoic acid, and performic acid, the double bonds of the alkyl group linked to the cardanol phenyl group can be epoxidized to yield polyepoxy cardanol [82–84]. These double bonds might also be epoxidized in toluene using enzymes such as Candida antarctica lipase, acetic acid, and hydrogen peroxide (95 % yield) [85]. Cardanol-based modified epoxy resins were made in two steps: phenolation of the aliphatic chain (C15H31), followed by reactivity of the phenol hydroxyl groups with epichlorohydrin. When compared to diglycidyl ether based on bisphenol A, the modified epoxy based on cardanol performed well after curing with polyamines [86].

### 1.3.2 Curing agents

The reactive groups belonging to the molecules of an epoxy resin may react with a variety of curing agents, including amines, anhydrides, acids, mercaptans, imidazoles, phenols, and isocyanates, to produce covalent intermolecular connections and therefore build a three-dimensional network. Because of the improved environmentally freindly of amine-epoxy cured resin, primary and secondary amines are the most often employed curing agents among these compounds: aliphatic or cycloaliphatic amines for limited epoxy systems as adhesives or coatings, and aromatic amines to manufacture matrices for fiber-reinforced composites [87].

Aliphatic amines are often combined with epoxy resins at room temperature, resulting in a system with a greater curing rate and shorter curing life (i.e. gel and vitrification durations) than cycloaliphatic or aromatic polyamines. Aliphatic amines are extremely reactive curing agents that, when combined with epoxy molecules, produce dense cross-linked networks because to the small distance between active sites. As a consequence, it is feasible to create cured systems with strong resistance to alkalis and certain inorganic acids, good resistance to water and solvents (but less against many organic solvents), outstanding bonding performance, and good mechanical characteristics, but poor flexibility. The qualities of these epoxy systems that normally cure at ambient temperature are enhanced by performing a post-curing treatment at high temperatures [55,78,88–90].

Aromatic amines react with epoxy resins more slowly than aliphatic or cycloaliphatic amines. By combining these curing agents with an epoxy resin, the resultant system has a lengthy curing time and requires extended durations at high temperatures to achieve optimal characteristics. Curing aromatic amine, in particular, requires two heating steps: the first at a low temperature (about 80°C) to limit heat production, and the second at a higher temperature (typically between 150°C and 170°C). The cured epoxy systems generated by utilizing aromatic amines as hardeners exhibit outstanding heat resistance, mechanical and electrical capabilities, and chemical resistance, notably against alkalis [91].

Phenalkamine is produced through the Mannich reaction of cardanol with certain amines, which results in a partly bio-based polymer (Fig 1.3). The reaction mostly produces monomeric compounds with low molecular weight. Phenalkamine's aromatic backbone is responsible for its great chemical resistance. Because the aliphatic side chain is hydrophobic, these resins may be water-resistant. Because of the phenolic-OH group, phenalkamine is particularly active even at low temperatures. The high crosslinked density is due to the amine side chain. Aside from low-temperature curing (with a practical pot life), their capacity to resist moisture while curing makes them perfect for temperature-insensitive cure. When employed as a crosslinking agent in an epoxy system, the curing characteristics are determined by the amine value [55].

Furthermore, the ultimate characteristics of the cured epoxy are determined by the polyamine structure, which might be aliphatic or aromatic. The molecular weight of the resulting phenalkamine is determined by the cardanol, formaldehyde, and amine ratio. Higher molecular weight phenalkamines dry the surface quicker than lower molecular weight equivalents. The curing, mechanical, thermal, and anticorrosive characteristics of epoxy-based coatings are affected by the molecular weight and structure of phenalkamine curing agents.[89] Despite the ideal characteristics, inherent constraints such as poor color stability exist. Cardanol butyl ether and its phenalkamine based on diethylene triamine were recently produced. Low molecular weight compounds produced by equimolar concentrations of all three reactants were employed as epoxy cross-linkers. They determined that cardanol butyl ether yields light colored phenalkamines but is less reactive as an epoxy curing agent than typical phenalkamine [89,92]. As a consequence, cardanol derivatives and phenalkamines were developed.

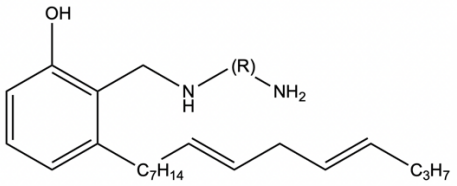


Figure 1.3 Chemical structure of Phenalkamine.

### 1.3.3 Bio-derived epoxy resins

Over the past decade, major research efforts have been directed toward the synthesis of polymers using renewable resources. This is mostly due to rising petrochemical pricing and increased environmental concerns. As with other plastic materials, scientists are now investigating the formulation and characterization of bio-derived thermosetting resins: specifically, the replacement of bisphenol-A-based epoxy resins by materials obtained from natural sources poses a problem.

Cardanol, a phenol-based byproduct of the cashew nut industry, is one of the most often utilized precursors in the production of several kinds of epoxy bio-based resins. CNSL, the international abbreviation for alkyl phenolic oil, is used to produce cardanol. CNSL obtained from the most widely distributed roasted mechanical processes of the cashew sector accounts for almost 25% of total nut weight, and its global output (Africa, Asia, and South America being the primary producer regions) is projected to be over 300,000 tons per year [73].

By coupling an epoxy monomer and an acid-based catalyst with a resole chemical, a thermosetting resin containing roughly 40% cardanol by weight has been synthesized [93]. This final product was created by cardanol and formaldehyde in the presence of a basic catalyst. The formulation, which had sufficient qualities and curing temperatures, was reinforced with natural fibers (short ramie, flax, hemp fibers, and a jute fabric) to produce samples that were then evaluated in tensile and flexural configurations.

Two diverse novolac resins (with unreacted cardanol contents of 35% and 20% by weight, respectively) were utilized as curing agents for a DGEBA epoxy resin. Calorimetric tests revealed that novolac/epoxy resin weight ratios less than 60/40 resulted in resin cross-linking due to an increase in the amount of secondary hydroxyl groups accessible for cross-linking reactions. The mechanical qualities improved when the epoxy resin quantity was increased. The heat resistance of the cured resin in a nitrogen environment, on the other hand, did not vary considerably with novolac quantity, and only a one-step mass loss

corresponding to a single thermal degradation process, occurring at temperatures greater than 400°C, was detected [74].

A paint based on an epoxy–cardanol resin has been developed and then described to compare its performance (physicomechanical characteristics, chemical resistance, and corrosion protection efficiency) to paints prepared with unmodified epoxy resin. It was discovered that the new bio-based paints had stronger anticorrosive qualities than unmodified paints, and so the cardanol-based epoxy resin provides an excellent binder medium for paint formation [94].

### 1.3.4 Thiol-ene reaction for epoxy resins

A novel paradigm for chemical reactions was revealed in 2001, which focuses on high selective (stereospecificity and stereoselectivity) and easy reactions without side products under mild circumstances (solventless or aqueous solvent).[95] Several efficient reactions capable of producing various synthetic compounds and materials have been classified as "click reactions" [96,97] This reaction prompted researchers to focus on additional "click-reactions," such as thiol-ene [98–101]. This last, long-known reaction is simply a thiolation of a C=C double bond followed by a proton exchange. It is very beneficial in the synthesis of polymers and materials [102–104].

Thiol-ene reaction, the reaction of thiols with -ene compounds has been used to generated crosslinkage of epoxy, and it is one of the greatest developments and creating these molecules. Indeed, due to growing environmental concerns and limited petrochemical resource availability, there has been a significant surge in demand for amines produced from renewable resources [105,106]. It expands the possibilities for modifying vegetable oils and fatty acid derivatives, as well as the manufacture of functional monomers and polymers [107–110].

Amidation, thiol-ene click reaction, and esterification were used to develop a polyfunctional tung oil-derivate reactive diluent (TDMM). The thiol-ene click reaction conditions were initially optimized: 2 wt% 1173 as photoinitiator, a molar ratio of thiols to C C double bonds of 12:1, a mercury lamp power of 300 W, and a reaction period of 6 h.

When compared to the monomer acrylated epoxidized soybean oil (AESO) and commercial pentaerythritol triacrylate, the resultant TDMM had a viscosity of 105 CP (PETA). The rheological behavior of the AESO-TDMM mixture system enhanced when combined with high viscosity monomer AESO. After that, AESO was treated using photo-initiator 819 and a portable UV-LED light source with varying doses of TDMM. These mixing systems have a high bio-content ranging from 61-81 %. Notably, adding TDMM into AESO improved Tg and storage modulus. The high cross-linking density and long fatty chain of as-synthesized TDMM contributed to the improvement in mechanical strength. Furthermore, TDMM and the corresponding UV-LED cured films had excellent physical and chemical characteristics. Overall, tung oil-based reactive diluent had tremendous promise in the UV-LED curable coatings sector owing to its superior characteristics as well as the benefit of high bio-content [111].

The use of thiol-ene coupling in the synthesis of a variety of polyfunctional primary amines. These amines were created by thiol-ene coupling cysteamine hydrochloride to triallyl pentaerythritol under UV light. The triallyl pentaerythritol direct coupling has a poor yield. This poor yield is due to amine solubility in water. To generate insoluble amine in water and therefore raise the overall yield of the procedure (and particular the extraction yield), a first step of grafting of hydrophobic backbone by esterification of triallyl pentaerythritol's hydroxyl group was attempted. These amines were then investigated to identify their function- ality. BADGE was used to create epoxy/amine compounds with known functionality. According to these findings, the functionality of the synthesized amines ranges between 2.5 and 2.9. Finally, epoxy/amine compounds were created using two bio-based epoxy: di-epoxidized cardanol and phloroglucinol tris epoxidized cardanol (PGTE). Thermal characterizations of the materials suggest that these networks might be used in a variety of applications ranging from coatings to composites [78].

By UV, free-radical-initiated thiol-ene coupling between the double bond moieties of the cardanol long carbon side chain and thiol functional groups, industrial-grade cardanol and 2-mercaptoethanol were reacted to form hydroxyl-functionalized cardanol. The reaction period influenced the average hydroxyl number of the hydroxyl-functionalized cardanol,

with hydroxyl values varying between 168-201 mg KOH $g^{-1}$. This cardanol was then employed as a polyol in the preparation of cardanol-based polyurethane using hexamethylene diisocyanate and an NCO/OH ratio of one. Cardanol modified with 10-undecylenate was utilized as a raw material to manufacture cardanol-based polyols, including the long carbon chain of 10-undecylenate, to compare the impact of cardanol-based polyols with the qualities of cardanol-based polyurethane. The research demonstrated that cardanol-based polyols with this long carbon chain may enhance the hydrophobic and mechanical characteristics of cardanol-based polyurethane [112].

Thiol-ene coupling was used to synthesize a di-acrylic UV oligomer based on cardanol, followed by a ring opening reaction employing glycidyl methacrylate. In commercial epoxy acrylate resin, the produced oligomer was substituted from 10-50% wt%. The coatings were applied to wood panels and their mechanical and chemical characteristics were evaluated. The coatings' adherence was shown to decrease when the concentration of cardanol-based UV oligomer was increased. Furthermore, when the quantity of produced UV oligomer rose, a longer duration was needed to obtain a significant degree of crosslinking. Furthermore, the inclusion of UV oligomer reduced pencil hardness and gloss values. The chemical structure of commercial epoxy acrylate and cardanol-based UV oligomer might explain such a trend in characteristics (GMA-CDS). When the hard and rigid structure of bisphenol-A-based epoxy acrylate was replaced with less compact GMA-CDS, the curing time and water absorption increased but pencil hardness, gloss, and adhesion properties decreased. Nonetheless, coatings produced by substituting 30 wt% of commercial epoxy acrylate demonstrated comparable mechanical and chemical characteristics [113].

## 1.4 Composites (Cellulose nanofiber (CNF), Epoxy resins as a matrix in fiber-reinforced polymer (FRP) composites, etc.)

### 1.4.1 Cellulose nanofiber (CNF)

CNF, also known as micro (nano) fibrillated cellulose, is a material made up of cellulose microfibrils as an elementary unit. CNF may be defined as a fibrous substance having a width of 4–20 nm and an L/D ratio greater than 100. Non-cellulose components are frequently absent from CNF. Producing CNF from higher plant cell walls requires the removal of microfibrils. Raw material purification and fibrillation are common production methods. The existence of numerical inconsistencies in the literature [114–125].

Purification of plant raw materials is done to remove non-cellulose components such as pectin, hemicellulose, and lignin as cell wall components. While hemicellulose does not appreciably hinder fibrillation, the high quantity of lignin left does. Chemical pulping through heating and bleaching procedures is widespread for woody raw materials. Delignification (Wise technique, peracetic acid treatment) and hemicellulose extraction with alkali are also performed. CNFs, like CNCs, may be produced from a variety of cellulosic sources [126], that include wood [127], tunicates [128], banana [129], pineapple leaf [130], bamboo [131], cotton [132], algae [133], sludge [134], other industrial residues [135]. Their proportions are greatly influenced by the cellulose source.

Due to the excellent characteristics of CNF, the creation of polymer nanocomposites employing CNF as a nanofiller has prompted a great deal of scientific interest in recent years [136]. However, like with CNCs, there is a limited potential that CNF's hydrophilicity will consider it incompatible with the hydrophobic polymer matrix. To produce the desired nanocomposites, some kind of polymer-CNF interaction must be included. When reinforcing composites using polymers, the CNF dispersion may be homogenized. However, unlike rod-like CNC systems, interweaving of nanofibers may be induced in the event of homogeneity by blades revolving at high speeds. This requires the whole attention.

There are two distinct methods: covalent and non-covalent interactions. Polymer/CNF Nanocomposite with Covalent Interactions, such as etherification, the –OH groups of CNF were also effectively employed for coupling with polymer epoxide moieties. Ansari and colleagues discovered that CNF greatly contributes to the curing of epoxy (EP)/CNF nanocomposite [137]. The –OH groups of the CNF interacted with the epoxy units during the curing process, resulting in a crosslinked nanocomposite with three times the stiffness and strength of the pure nanocomposite. Furthermore, Tg increased gradually as CNF level increased, indicating covalent interaction between EP and CNF. Furthermore, the nanocomposite demonstrated much decreased moisture absorption. Surface-modified CNF may also be employed in crosslinking operations to create EP/CNF nanocomposite. The surface modification of CNF by polyethylenimine (PEI), a branching polymer with many amine groups, allowed for the crosslinking reaction between amine and epoxy units, which resulted in a 237.6 % increase in Young's modulus [138].

Peptidic Coupling, Due to the presence of the –COOH group at C6, TEMPO-oxidized CNF (TOCN) gives the opportunity to graft polymers onto the nanofibers via amide (–CONH) bond formation. The peptidic coupling approach along with the other approaches to incorporate covalent interaction between the polymer and CNF [139–141]. The TEMPO technology has a wide variety of applications in the CNF manufacturing industry.

### 1.4.2 Epoxy resins as a matrix in fiber-reinforced polymer (FRP) composites

The utilize of nanoparticles or nanofillers in the production of high-performance and/or functional polymer materials has already become an important topic of current study not only in academia but also in industry. The choice of nanofiller for creating nanocomposites has created environmental issues in the last decade. There is a huge need for sustainable and biodegradable nanofillers. In this respect, cellulose nanomaterials have piqued the attention of researchers due to their natural abundance and biodegradability, as well as a slew of other essential intrinsic properties that contribute to functionality expression and material performance improvement.

Because of the unique properties of those nanoparticles, such as abundant surface –OH groups and their related ease of surface modification, high strength, (possibly) cheap cost, and renewability, the fabrication of polymer nanocomposites employing nanocelluloses has grown in popularity. However, these nanoparticles have several drawbacks, such as significant moisture absorption and poor compatibility with the hydrophobic polymer matrix. To obtain the required performance and functions, it has therefore been necessary to induce any kind of contact, either covalent or non-covalent, between the polymer and nanocellulose. The kind and extent of the interaction are the primary determinants of nanocellulose dispersibility in the polymer matrix and, therefore, the ultimate characteristics of the nanocomposite.

The original specialist disciplines of the researchers who have contributed to the nano-cellulose sector are diverse: physical chemistry such as colloids and interfaces, mechanical engineering, wood science, plant biology, and so on. The last several years, there have been provided an overview of the structure and characteristics of cellulosic nanoparticles [114] and their surface modification [115–117]. The colloidal behavior of nanocellulose has also been studied in terms of its characteristics [118,142]. It should be emphasized that those results are extremely suggestive for researchers getting into the area of nanocellulose.

There are several publications that summarize the developments in polymer nanocomposites reinforced by nanocellulose, such as the synthesis and characteristics of cellulosic bio-nanocomposites [119], achieved mechanical properties [120], the comparison of mechanical reinforcement with the type and content of nanocellulose [121], and the processing of nanocellulosic composites [123,124,143]. Additionally, polymer-grafted nanocellulose is useful in the fabrication of polymer/nanocellulose composites in specific instances [144,145].

Epoxy resins are more costly than other thermosetting polymers (such as polyester or vinyl ester resins), but they have stronger mechanical qualities as well as greater resistance to moisture absorption and corrosive liquids and conditions. When compared to other thermoset polymers, their high physical qualities and durability in service combine to give a superior cost-performance ratio. Epoxy resins also exhibit excellent electrical resistance

and good performance at high temperatures, owing to their greater heat deflection temperatures as compared to polyester matrices, as well as their high glass transition temperatures (Tg). Furthermore, they exhibit excellent adhesion to a variety of substrates (including metal and plastic) as well as fibers utilized as reinforcement in composite materials (e.g., glass, carbon and Kevlar). Another advantage of epoxy resins is that they shrink very little during the curing process. Polyester and vinyl ester resins shrink up to 12% volumetrically (specific shrinkage volumetric reductions for polyester and vinyl ester resins are 5-12% and 5-10%, respectively), and since the resin continues to cure over lengthy periods of time, this impact may not be immediately apparent. Epoxy resins, on the other hand, shrink by less than 5%. [146].

Thus, epoxy resins exhibit various features that have made them the finest choice among thermosetting resins for the majority of technical applications: There is no emission of volatile and dangerous products during the curing process reaction, there is flexibility in the choice of monomers to obtain a variety of products ranging from low Tg rubbers to high Tg materials, and there is very little or no volume contraction during the curing process for some blends. Due to the polar groups in the structure, the resin system has great adhesion qualities to a variety of materials, and the ability to introduce various modifiers to generate a resin system with a variety of useful properties (e.g., electrical or thermal). However, these resins have drawbacks such as poor fracture development resistance, brittleness, and limited UV resistance [147].

### 1.4.3 CNFs reinforced epoxy composites

Epoxy resins are a significant family of thermosetting polymers with many uses in coatings, adhesives, electronics, and other fields [148]. However, as compared to other regularly used fillers such as glass fibers, cellulose fibers often provide less augmentation of the mechanical characteristics of the composites. The mechanical behavior of composites is highly influenced by the dispersion of fillers in the matrix as well as the interfacial contact between them [149]. However, the many hydroxyl groups on the cellulose molecules provide high polarity and thick hydrogen bonding in its structure [143]. As a result, CNF compatibility and dispersion were not met in several polymeric matrices,

particularly at high loading circumstances [150]. These flaws impair the mechanical characteristics of the composites and significantly restrict the uses of cellulose in composite materials. As a result, poor dispersion and compatibility between cellulose fibers and polymer matrix become critical concerns that must be addressed in order to generate high-performance composites.

CNF/epoxy composites with large volume fractions have been developed. Impregnation of a wet porous CNF network with an acetone/epoxy/amine solution yielded 15-50vol% CNF. Infrared spectroscopy investigations demonstrated a considerable increase in the curing rate of epoxy (EP) in the presence of CNF. The CNF offered exceptionally effective reinforcement (at 15 vol percent, stiffness and strength increased thrice to 5.9 GPa and 109 MPa, respectively), while ductility was conserved. Furthermore, the glass transition temperature rose with increasing CNF concentration (from 68 °C in clean epoxy to 86 °C in 50 vol percent composite) and had strong thermal degradation stability in nitrogen till 250 °C. Most notably, the moisture sorption values for the 15 vol percent CNF/EP were low, even similar to pure epoxy. This material's mechanical characteristics did not alter when the relative humidity rose (90 percent RH). As a cellulose-based composite, NFC/EP offers a unique combination of high strength, modulus, ductility, and moisture stability. The success is due to the controlled nanoscale distribution of CNF and strong CNF/EP interface contacts without the need of expensive coupling chemicals. Chemically and morphologically diverse plant fiber architectures exhibit substantially greater moisture absorption, as well as non-uniform fiber distribution and poor fiber/matrix interface interactions [137].

The surface-modified CNF with polyethyleneimine (PEI) resulted in abundant amine groups on the surface of CNFs, resulting in a lower hydrogen bond density between CNFs and, as a result, fewer CNF agglomerates. The amine groups might also react with the epoxy to provide an efficient curing agent, increasing the density of interfacial crosslinking and strengthening interfacial adhesion. CNFs-PEI/Epoxy nanocomposites had tensile strength and Young's modulus that were 88.1 percent (104.72 MPa) and 237.6 percent (3.41 GPa) greater than plain epoxy, respectively. The nanocomposites' tensile storage modulus

rose considerably at temperatures below and over Tg (30°C). The coefficient of thermal expansion of the CNFs-PEI/Epoxy nanocomposites was 22.2 ppm $K^{-1}$, which was much lower than the coefficient of thermal expansion of the plain epoxy (88.6 ppm $K^{-1}$). Furthermore, the thermal conductivity of the nanocomposites was reported to increase. The nanocomposites' remarkable and balanced features may give potential applications in automotive, construction, and electrical devices [138].

Immobilization of epoxy monomer and amine curing agents on the surface of cellulose nanofibers was achieved. FTIR analyses revealed that the epoxy monomer was physically attached to the surface of the CNF. Meanwhile, the amine curing agent began a chemical reaction with CNF to create active amide groups while leaving some amine groups unreacted. Epoxy coatings containing both epoxy immobilized CNF (EiCNF) and amine curing agent immobilized CNF (AiCNF) demonstrated self-healing capabilities. At the presence of water, EiCNF existing in the injured site de-formed and released epoxy monomer into the scratch. The epoxy monomer was released and interacted with the $-NH_2$ or amide groups in the AiCNF to produce an epoxy network that healed the scratch [151].

The epoxy composites were developed from CNF which was generated from Bleached Softwood Kraft (NBSK). The morphology, XRD, and elemental content of the produced CNFs filler reveal that it is nano in size and contains exclusively C and O elements. The influence of varied CNFs filler loadings (0.5, 0.75, and 1%) on tensile, impact, and flexural characteristics. The composite with 0.75 %CNF had the maximum tensile strength of 26.7 MPa and the smallest Young's modulus of 1.3 GPa. However, considerable increases in mechanical characteristics seem to have been seen for 0.75 %CNFs due to homogeneous and fine dispersion of CNFs filler within epoxy matrix with no trace of agglomerations and micro-voids. In compared to the remainder of the nanocomposites, the SEM and TEM pictures support the presence of toughening processes for 0.75 %CNF/epoxy nanocomposites. The XRD pattern demonstrated that there is no discernible difference in the intensity of diffraction peaks and crystallinity of the epoxy nanocomposites compared to pure epoxy composites. The integration or functionalization of CNFs filler to the epoxy

matrix via physical bonding is supported by FTIR research, and no new chemical bond formation was found for any epoxy nanocomposites [152].

Photocuring techniques have also been modified for the enhancement of CNFs reinforced epoxy composites. Because of its low energy consumption, room temperature operation with rapid reaction speeds, and avoidance of solvents, photopolymerization is regarded as a green technique. The photocuring of a commercially available epoxidized cardanol and its application in reinforcement with microfibrillated cellulose (MFC) for the manufacture of entirely biobased composites are the focus of this study. Filtration was used to create wet MFC mats, which were subsequently impregnated with resin. The impregnated mats were then exposed to UV light. FT-IR spectroscopy was utilized to evaluate the photocuring of epoxidized cardanol and composites. The thermomechanical characteristics of composites were evaluated using thermogravimetric analysis, differential scanning calorimetry, and dynamic mechanical analysis. It was the ability to create completely cured composites, however a high photo-initiator concentration was required, probably owing to a photo-initiator side reaction with MFC [153].

## 1.5 References


1. Org, S. U. Transforming Our World: The 2030 Agenda for Sustainable Development United Nations.
2. Bontempi, E. First data analysis about possible COVID-19 virus airborne diffusion due to air particulate matter (PM): The case of Lombardy (Italy). Environmental Research **186**, (2020).
3. Nations, U. Sustainable Development Outlook 2020: Achieving SDGs in the wake of COVID-19: Scenarios for policymakers.
4. Ribeiro, P. J. G. & Pena Jardim Gonçalves, L. A. Urban resilience: A conceptual framework. Sustainable Cities and Society vol. 50 (2019).
5. Bontempi, E. Raw Materials and Sustainability Indicators. in Raw Materials Substitution Sustainability 1–28 (Springer International Publishing, 2017). doi:10.1007/978-3-319-60831-0_1.
6. Ljungberg, L. Y. Materials selection and design for development of sustainable products. Materials and Design **28**, 466–479 (2007).
7. Eizenberg, E. & Jabareen, Y. Social sustainability: A new conceptual framework. Sustainability (Switzerland) **9**, (2017).

8. Parra, C., Lewis, B. & Ali, S. Mining, Materials, and the Sustainable Development Goals (SDGs): 2030 and Beyond. (2020). doi:10.1201/9780367814960.
9. Chan, S., Weitz, N., Persson, Å. & Trimmer, C. Stockholm Environment Institute SDG 12: Responsible Consumption and Production-A Review of Research Needs 1 1 SDG 12: Responsible Consumption and Production A review of research needs Annex to the Formas report Forskning för Agenda 2030: Översikt av forskningsbehov och vägar framåt. (2018).
10. Fortunati, E. et al. Effect of hydroxytyrosol methyl carbonate on the thermal, migration and antioxidant properties of PVA-based films for active food packaging. Polymer International **65**, 872–882 (2016).
11. Bilo, F. et al. A sustainable bioplastic obtained from rice straw. Journal of Cleaner Production **200**, 357–368 (2018).
12. Sawalha, S. et al. Improving 2D-organization of fullerene Langmuir-Schäfer thin films by interaction with cellulose nanocrystals. Carbon N Y **167**, 906–917 (2020).
13. He, X. et al. Citric Acid as Green Modifier for Tuned Hydrophilicity of Surface Modified Cellulose and Lignin Nanoparticles. ACS Sustainable Chemistry & Engineering **6**, (2018).
14. Aliotta, L., Gigante, V., Coltelli, M. B., Cinelli, P. & Lazzeri, A. Evaluation of mechanical and interfacial properties of bio-composites based on poly(lactic acid) with natural cellulose fibers. International Journal of Molecular Sciences **20**, (2019).
15. Fortunati, E. & Torre, L. Cellulose nanocrystals in nanocomposite approach: Green and high-performance materials for industrial, biomedical and agricultural applications. in vol. 1736 20012 (2016).
16. Sarasini, F. et al. Effect of different compatibilizers on sustainable composites based on a PHBV/PBAT matrix filled with coffee silverskin. Polymers (Basel) **10**, (2018).
17. Assi, A. et al. A circular economy virtuous example-use of a stabilized waste material instead of calcite to produce sustainable composites. Applied Sciences (Switzerland) **10**, (2020).
18. Foli, G., Degli Esposti, M., Morselli, D. & Fabbri, P. Two-Step Solvent-Free Synthesis of Poly(hydroxybutyrate)-Based Photocurable Resin with Potential Application in Stereolithography. Macromolecular Rapid Communications **41**, (2020).
19. Ghedini, E. et al. Sulfadiazine-based drug delivery systems prepared by an effective sol–gel process. Journal of Sol-Gel Science and Technology **83**, 618–626 (2017).
20. Kierkowicz, M. et al. Filling Single-Walled Carbon Nanotubes with Lutetium Chloride: A Sustainable Production of Nanocapsules Free of Non-Encapsulated Material. ACS Sustainable Chemistry & Engineering **5**, (2017).
21. Baldassarre, F. et al. Application of calcium carbonate nanocarriers for controlled release of phytodrugs against Xylella fastidiosa pathogen. Pure and Applied Chemistry **92**, (2019).
22. Stenmarck, A. et al. Estimates of European food waste levels.

23. Zanoletti, A., Bilo, F., Depero, L. E., Zappa, D. & Bontempi, E. The first sustainable material designed for air particulate matter capture: An introduction to Azure Chemistry. Journal of Environmental Management **218**, 355–362 (2018).
24. Ciapponi, R., Turri, S. & Levi, M. Mechanical reinforcement by microalgal biofiller in novel thermoplastic biocompounds from plasticized gluten. Materials **12**, (2019).
25. Angioni, S. et al. Photosynthetic microbial fuel cell with polybenzimidazole membrane: synergy between bacteria and algae for wastewater removal and biorefinery. Heliyon **4**, 560 (2018).
26. Balart, R., Garcia-Garcia, D., Fombuena, V., Quiles-Carrillo, L. & Arrieta, M. P. Biopolymers from natural resources. Polymers vol. 13 (2021).
27. Bentsen, N. S. & Felby, C. Biomass for energy in the European Union-a review of bioenergy resource assessments. http://www.biotechnologyforbiofuels.com/content/5/1/25 (2012).
28. Ben-Iwo, J., Manovic, V. & Longhurst, P. Biomass resources and biofuels potential for the production of transportation fuels in Nigeria. Renewable and Sustainable Energy Reviews vol. 63 172–192 (2016).
29. Pimentel, D., Hepperly, P., Hanson, J., Douds, D. & Seidel, R. Environmental, energetic, and economic comparisons of organic and conventional farming systems. Bioscience **55**, 573–582 (2005).
30. Performance and Emission Characteristics of a DI Diesel Engine Fuelled with Cashew Nut Shell Liquid ( CNSL )-Diesel Blends C. in (2011).
31. Baghel, M. & Baid, R. CNSL (cashew nut shell liquid) - A versatile renewable natural resource. Plant Archives **7**, 497–501 (2007).
32. Voirin, C. et al. Functionalization of cardanol: towards biobased polymers and additives. Polym. Chem. **5**, 3142–3162 (2014).
33. Lubi, M. C. & Thachil, E. T. Cashew nut shell liquid (CNSL) - A versatile monomer for polymer synthesis. Designed Monomers and Polymers **3**, 123–153 (2000).
34. Balachandran, V. S., Jadhav, S. R., Vemula, P. K. & John, G. Recent advances in cardanol chemistry in a nutshell: from a nut to nanomaterials. Chem. Soc. Rev. **42**, 427–438 (2013).
35. Paramashivappa, R., Kumar, P. P., Vithayathil, P. J. & Rao, A. S. Novel Method for Isolation of Major Phenolic Constituents from Cashew (Anacardium occidentale L.) Nut Shell Liquid. Journal of Agricultural and Food Chemistry **49**, 2548–2551 (2001).
36. Devi, A. & Srivastava, D. Studies on the blends of cardanol-based epoxidized novolac type phenolic resin and carboxyl-terminated polybutadiene (CTPB), I. Materials Science and Engineering A **458**, 336–347 (2007).
37. Ravichandran, S., Bouldin, R. M., Kumar, J. & Nagarajan, R. A renewable waste material for the synthesis of a novel non-halogenated flame retardant polymer. Journal of Cleaner Production **19**, 454–458 (2011).
38. Scorzza, C., Nieves, J., Vejar, F. & Bullón, J. Synthesis and physicochemical characterization of anionic surfactants derived from cashew nut shell oil. Journal of Surfactants and Detergents **13**, 27–31 (2010).

39. Anilkumar, P. & Jayakannan, M. Fluorescent Tagged Probing Agent and Structure-Directing Amphiphilic Molecular Design for Polyaniline Nanomaterials via Self-Assembly Process. The Journal of Physical Chemistry C **111**, 3591–3600 (2007).
40. Rios, M. A. D. S., Sales, F. A. M. & Mazzetto, S. E. Study of antioxidant properties of 5-n-pentadecyl-2-tert-amylphenol. Energy and Fuels **23**, 2517–2522 (2009).
41. Pillai, C. K. S., Prasad, V. S., Sudha, J. D., Bera, S. C. & Menon, A. R. R. Polymeric resins from renewable resources. II. Synthesis and characterization of flam retardant prepolymers from cardanol. Journal of Applied Polymer Science **41**, 2487–2501 (1990).
42. John, G. & Vemula, P. Design and development of soft nanomaterials from biobased amphiphiles. Soft Matter **2**, (2006).
43. John, G., Masuda, M., Okada, Y., Yase, K. & Shimizu, T. Nanotube Formation from Renewable Resources via Coiled Nanofibers**. Adv. Mater vol. 13 (2001).
44. Radhakrishan, S., Rao, C. R. K. & Vijayan, M. Electrochemical synthesis and studies of polypyrroles doped by renewable dopant cardanol azophenylsulfonic acid derived from cashew nutshells. Journal of Applied Polymer Science **114**, 3125–3131 (2009).
45. Toyomizu, M., Sugiyama, S., Jin, R. L. & Nakatsu, T. α-glucosidase and aldose reductase inhibitors: Constituents of cashew, Anacardium occidentale, nut shell liquids. Phytotherapy Research **7**, 252–254 (1993).
46. Gedam, P. H. & Sampathkumaran, P. S. Cashew nut shell liquid: Extraction, chemistry and applications. Progress in Organic Coatings **14**, 115–157 (1986).
47. Patel, R. N., Bandyopadhyay, S. & Ganesh, A. Extraction of cashew (Anacardium occidentale) nut shell liquid using supercritical carbon dioxide. Bioresource Technology **97**, 847–853 (2006).
48. Yuliana, M., Tran-Thi, N. Y. & Ju, Y. H. Effect of extraction methods on characteristic and composition of Indonesian cashew nut shell liquid. Industrial Crops and Products **35**, 230–236 (2012).
49. Preface. in Synthetic and Natural Phenols (ed. Tyman, J. H. P.) vol. 52 viii (Elsevier, 1996).
50. Oliveira, M. S. C. et al. Antioxidant, larvicidal and antiacetylcholinesterase activities of cashew nut shell liquid constituents. Acta Tropica **117**, 165–170 (2011).
51. Andrade, T. D. J. A. D. S. et al. Antioxidant properties and chemical composition of technical Cashew Nut Shell Liquid (tCNSL). Food Chemistry **126**, 1044–1048 (2011).
52. Phani Kumar, P., Paramashivappa, R., Vithayathil, P. J., Subba Rao, P. v & Srinivasa Rao, A. Process for Isolation of Cardanol from Technical Cashew (Anacardium occidentale L.) Nut Shell Liquid. Journal of Agricultural and Food Chemistry **50**, 4705–4708 (2002).
53. Sultania, M., Rai, J. S. P. & Srivastava, D. Process modeling, optimization and analysis of esterification reaction of cashew nut shell liquid (CNSL)-derived epoxy resin using response surface methodology. Journal of Hazardous Materials **185**, 1198–1204 (2011).

54. Mwaikambo, L. Y. & Ansell, M. P. Cure characteristics of alkali catalysed cashew nut shell liquid-formaldehyde resin.
55. Pathak, S. K. & Rao, B. S. Structural effect of phenalkamines on adhesive viscoelastic and thermal properties of epoxy networks. Journal of Applied Polymer Science **102**, 4741–4748 (2006).
56. Mele, G. et al. Polycrystalline TiO2 impregnated with cardanol-based porphyrins for the photocatalytic degradation of 4-nitrophenol. Green Chemistry - GREEN CHEM **6**, (2004).
57. Vasapollo, G. et al. Use of novel cardanol-Porphyrin hybrids and their tio2-Based composites for the photodegradation of 4-Nitrophenol in water. Molecules **16**, 5769–5784 (2011).
58. Souza Jr, F., Soares, B., Hatna, S., Barra, G. & Herbst, M. Influence of plasticizers (DOP and CNSL) on mechanical and electrical properties of SBS/polyaniline blends. Polymer (Guildf) **47**, 7548–7553 (2006).
59. Kattimuttathu I, S., Foerst, G., Schubert, R. & Bartsch, E. Synthesis and micellization properties of new anionic reactive surfactants based on hydrogenated cardanol. Journal of Surfactants and Detergents **15**, 207–215 (2012).
60. Bruce, I. E., Mehta, L., Porter, M. J., Stein, B. K. & Tyman, J. H. P. Anionic surfactants synthesised from replenishable phenolic lipids. Journal of Surfactants and Detergents **12**, 337–344 (2009).
61. Paul, R. K. & Pillai, C. K. S. Melt/Solution Processable Polyaniline with Functionalized Phosphate Ester Dopants and Its Thermoplastic Blends. J Appl Polym Sci vol. 80 (2001).
62. Menon, A. R. R., Pillai, C., Bhattacharya, A. K., Nando, G. & Gupta, B. R. Rheology of phosphorylated cashew nut shell liquid prepolymer modified natural rubber. KGK-Kautschuk und Gummi Kunststoffe **53**, 35–41 (2000).
63. Mythili, C. v, Retna, A. M. & Gopalakrishnan, S. Synthesis, mechanical, thermal and chemical properties of polyurethanes based on cardanol. Bull. Mater. Sci vol. 27 (2004).
64. Anilkumar, P. Cashew nut shell liquid: A goldfield for functional materials. Cashew Nut Shell Liquid: A Goldfield for Functional Materials (Springer International Publishing, 2017). doi:10.1007/978-3-319-47455-7.
65. Raquez, J. M., Deléglise, M., Lacrampe, M. F. & Krawczak, P. Thermosetting (bio)materials derived from renewable resources: A critical review. Progress in Polymer Science (Oxford) vol. 35 487–509 (2010).
66. Stewart, R. Going green: eco-friendly materials and recycling on growth paths. Plastics Engineering vol. 64 16+ (2008).
67. Atta, A. M., El-Kafrawy, A. F., Aly, M. H. & Abdel-Azim, A. A. A. New epoxy resins based on recycled poly(ethylene terephthalate) as organic coatings. Progress in Organic Coatings **58**, 13–22 (2007).
68. Atta, A. M., Elsaeed, A. M., Farag, R. K. & El-Saeed, S. M. Synthesis of unsaturated polyester resins based on rosin acrylic acid adduct for coating applications. Reactive and Functional Polymers **67**, 549–563 (2007).
69. Atta, A. M., El-Saeed, S. M. & Farag, R. K. New vinyl ester resins based on rosin for coating applications. Reactive and Functional Polymers **66**, 1596–1608 (2006).

70. Atta, A. M., Mansour, R., Abdou, M. I. & Sayed, A. M. Epoxy resins from rosin acids: Synthesis and characterization. Polymers for Advanced Technologies **15**, 514–522 (2004).
71. Atta, A. M., Mansour, R., Abdou, M. I. & El-Sayed, A. M. Synthesis and characterization of tetra-functional epoxy resins from rosin. Journal of Polymer Research **12**, 127–138 (2005).
72. Yadav, R. & Srivastava, Dr. D. Kinetics of the acid-catalyzed cardanol–formaldehyde reactions. Materials Chemistry and Physics - MATER CHEM PHYS **106**, 74–81 (2007).
73. Maffezzoli, A. et al. Synthesis of a novel cardanol-based benzoxazine monomer and environmentally sustainable production of polymers and bio-composites. Green Chemistry - GREEN CHEM **9**, (2007).
74. Campaner, P., D'Amico, D., Longo, L., Stifani, C. & Tarzia, A. Cardanol-based novolac resins as curing agents of epoxy resins. Journal of Applied Polymer Science **114**, 3585–3591 (2009).
75. Sultania, M., Rai, J. S. P. & Srivastava, D. Kinetic modeling of esterification of cardanol-based epoxy resin in the presence of triphenylphosphine for producing vinyl ester resin: Mechanistic rate equation. Journal of Applied Polymer Science **118**, 1979–1989 (2010).
76. Sultania, M., Rai, J. & Srivastava, Dr. D. Studies on the synthesis and curing of epoxidized novolac vinyl ester resin from renewable resource material. European Polymer Journal - EUR POLYM J **46**, 2019–2032 (2010).
77. Unnikrishnan, K. & Thachil, E. Studies on the Modification of Commercial Epoxy Resin using Cardanol-based Phenolic Resins. Journal of Elastomers and Plastics - J ELASTOM PLAST **40**, 271–286 (2008).
78. Darroman, E., Bonnot, L., Auvergne, R., Boutevin, B. & Caillol, S. New aromatic amine based on cardanol giving new biobased epoxy networks with cardanol. European Journal of Lipid Science and Technology **117**, 178–189 (2015).
79. Darroman, E., Durand, N., Boutevin, B. & Caillol, S. New cardanol/sucrose epoxy blends for biobased coatings. Progress in Organic Coatings **83**, 47–54 (2015).
80. Caillol, S. et al. New biobased epoxy materials from cardanol. European Journal of Lipid Science and Technology **116**, (2014).
81. Shukla, R. & Kumar, P. Self-curable epoxide resins based on cardanol for use in surface coatings. Pigment & Resin Technology **40**, 311–333 (2011).
82. Greco, A., Brunetti, D., Renna, G., Mele, G. & Maffezzoli, A. Plasticizer for poly(vinyl chloride) from cardanol as a renewable resource material. in Polymer Degradation and Stability vol. 95 2169–2174 (2010).
83. Kanehashi, S. et al. Preparation and characterization of cardanol-based epoxy resin for coating at room temperature curing. Journal of Applied Polymer Science **130**, 2468–2478 (2013).
84. Suresh, K. I. Rigid Polyurethane Foams from Cardanol: Synthesis, Structural Characterization, and Evaluation of Polyol and Foam Properties. ACS Sustainable Chemistry & Engineering **1**, 232–242 (2013).
85. Kim, Y. H., An, E. S., Park, S. Y. & Song, B. K. Enzymatic epoxidation and polymerization of cardanol obtained from a renewable resource and curing of

epoxide-containing polycardanol. Journal of Molecular Catalysis B: Enzymatic **45**, 39–44 (2007).
86. Ionescu, M. & Petrović, Z. S. Phenolation of vegetable oils. Journal of the Serbian Chemical Society **76**, 591–606 (2011).
87. Pascault, J.-P. & Williams, R. J. J. General Concepts about Epoxy Polymers. in Epoxy Polymers 1–12 (John Wiley & Sons, Ltd, 2010). doi:https://doi.org/10.1002/9783527628704.ch1.
88. Liu, Y., Wang, J. & Xu, S. Synthesis and curing kinetics of cardanol-based curing agents for epoxy resin by in situ depolymerization of paraformaldehyde. Journal of Polymer Science, Part A: Polymer Chemistry **52**, 472–480 (2014).
89. Kathalewar, M. & Sabnis, A. Effect of molecular weight of phenalkamines on the curing, mechanical, thermal and anticorrosive properties of epoxy based coatings. Progress in Organic Coatings **84**, 79–88 (2015).
90. Darroman, E., Durand, N., Boutevin, B. & Caillol, S. Improved cardanol derived epoxy coatings. Progress in Organic Coatings **91**, 9–16 (2016).
91. Weinmann, D. J., Dangayach, K. C. B. & Smith, C. Amine-functional curatives for low temperature cure epoxy coatings. Journal of Coatings Technology **68**, 29–37 (1996).
92. Huang, K. et al. Preparation of a light color cardanol-based curing agent and epoxy resin composite: Cure-induced phase separation and its effect on properties. Progress in Organic Coatings **74**, 240–247 (2012).
93. Maffezzoli, A. et al. Cardanol based matrix biocomposites reinforced with natural fibres. Composites Science and Technology **64**, 839–845 (2004).
94. Aggarwal, L. K., Thapliyal, P. C. & Karade, S. R. Anticorrosive properties of the epoxy-cardanol resin based paints. Progress in Organic Coatings **59**, 76–80 (2007).
95. Kolb, H. C., Finn, M. G. & Sharpless, K. B. Click Chemistry: Diverse Chemical Function from a Few Good Reactions. Angewandte Chemie International Edition **40**, 2004–2021 (2001).
96. Binder, W. H. & Sachsenhofer, R. 'Click' Chemistry in Polymer and Materials Science. Macromolecular Rapid Communications **28**, 15–54 (2007).
97. Sumerlin, B. S. & Vogt, A. P. Macromolecular Engineering through Click Chemistry and Other Efficient Transformations. Macromolecules **43**, 1–13 (2010).
98. Hoyle, C. E., Lowe, A. B. & Bowman, C. N. Thiol-click chemistry: a multifaceted toolbox for small molecule and polymer synthesis. Chemical Society Reviews **39**, 1355–1387 (2010).
99. Pham, P. D., Lapinte, V., Raoul, Y. & Robin, J. J. Lipidic polyols using thiol-ene/yne strategy for crosslinked polyurethanes. Journal of Polymer Science, Part A: Polymer Chemistry **52**, 1597–1606 (2014).
100. Pötzsch, R., Stahl, B. C., Komber, H., Hawker, C. J. & Voit, B. I. High refractive index polyvinylsulfide materials prepared by selective radical mono-addition thiol–yne chemistry. Polymer Chemistry **5**, 2911–2921 (2014).
101. Lligadas, G. Renewable Polyols for Polyurethane Synthesis via Thiol-ene/yne Couplings of Plant Oils. Macromolecular Chemistry and Physics **214**, 415–422 (2013).

102. Hoyle, C. E., Lee, T. Y. & Roper, T. Thiol–enes: Chemistry of the past with promise for the future. Journal of Polymer Science Part A: Polymer Chemistry **42**, 5301–5338 (2004).
103. Luo, A., Jiang, X., Lin, H. & Yin, J. "Thiol-ene" photo-cured hybrid materials based on POSS and renewable vegetable oil. Journal of Materials Chemistry **21**, 12753–12760 (2011).
104. Carioscia, J. A. et al. Thiol–norbornene materials: Approaches to develop high Tg thiol–ene polymers. Journal of Polymer Science Part A: Polymer Chemistry **45**, 5686–5696 (2007).
105. Belgacem, M. N. et al. Monomers, Polymers and Composites from Renewable Resources. http://elsevier.com/locate/permissions (2008).
106. Reck, B. K. & Graedel, T. E. Challenges in metal recycling. Science vol. 337 690–695 (2012).
107. Hoyle, C. E. & Bowman, C. N. Thiol-ene click chemistry. Angewandte Chemie - International Edition vol. 49 1540–1573 (2010).
108. Stemmelen, M. et al. A Fully Biobased Epoxy Resin from Vegetable Oils: From the Synthesis of the Precursors by Thiol-ene Reaction to the Study of the Final Material. Journal of Polymer Science Part A: Polymer Chemistry **49**, 2434–2444 (2011).
109. Lligadas, G., Ronda, J. C., Galià, M. & Cádiz, V. Monomers and polymers from plant oils via click chemistry reactions. Journal of Polymer Science Part A: Polymer Chemistry **51**, 2111–2124 (2013).
110. Fu, C., Yang, Z., Zheng, Z. & Shen, L. Properties of alkoxysilane castor oil synthesized via thiol-ene and its polyurethane/siloxane hybrid coating films. Progress in Organic Coatings **77**, 1241–1248 (2014).
111. Chu, Z. et al. Bio-based polyfunctional reactive diluent derived from tung oil by thiol-ene click reaction for high bio-content UV-LED curable coatings. Industrial Crops and Products **160**, (2021).
112. Fu, C., Liu, J., Xia, H. & Shen, L. Effect of structure on the properties of polyurethanes based on aromatic cardanol-based polyols prepared by thiol-ene coupling. Progress in Organic Coatings **83**, 19–25 (2015).
113. Wazarkar, K. & Sabnis, A. Synthesis and characterization of UV oligomer based on cardanol. Journal of Renewable Materials **8**, 57–68 (2020).
114. Moon, R. J., Martini, A., Nairn, J., Simonsen, J. & Youngblood, J. Cellulose nanomaterials review: Structure, properties and nanocomposites. Chemical Society Reviews **40**, 3941–3994 (2011).
115. Habibi, Y. Key advances in the chemical modification of nanocelluloses. Chemical Society Reviews vol. 43 1519–1542 (2014).
116. Eichhorn, S. Cellulose nanowhiskers: Promising materials for advanced applications. Soft Matter **7**, 303–315 (2011).
117. Missoum, K., Belgacem, M. N. & Bras, J. Nanofibrillated cellulose surface modification: A review. Materials **6**, 1745–1766 (2013).
118. Capron, I., Rojas, O. J. & Bordes, R. Behavior of nanocelluloses at interfaces. Current Opinion in Colloid and Interface Science vol. 29 83–95 (2017).

119. Siqueira, G., Bras, J. & Dufresne, A. Cellulosic bionanocomposites: A review of preparation, properties and applications. Polymers vol. 2 728–765 (2010).
120. Miao, C. & Hamad, W. Y. Cellulose reinforced polymer composites and nanocomposites: A critical review. Cellulose vol. 20 2221–2262 (2013).
121. Lee, K. Y., Aitomäki, Y., Berglund, L. A., Oksman, K. & Bismarck, A. On the use of nanocellulose as reinforcement in polymer matrix composites. Composites Science and Technology vol. 105 15–27 (2014).
122. Ray, D. & Sain, S. In situ processing of cellulose nanocomposites. Composites Part A: Applied Science and Manufacturing vol. 83 19–37 (2016).
123. Oksman, K. et al. Review of the recent developments in cellulose nanocomposite processing. Composites Part A: Applied Science and Manufacturing **83**, 2–18 (2016).
124. Kargarzadeh, H. et al. Recent developments on nanocellulose reinforced polymer nanocomposites: A review. Polymer vol. 132 368–393 (2017).
125. Jonoobi, M. et al. Different preparation methods and properties of nanostructured cellulose from various natural resources and residues: a review. Cellulose vol. 22 935–969 (2015).
126. Menon, M. P., Selvakumar, R., Suresh, P. & Ramakrishna, S. Extraction and modification of cellulose nanofibers derived from biomass for environmental application. www.webometrics.info/en/node/58 (2017).
127. Uetani, K. & Yano, H. Nanofibrillation of Wood Pulp Using a High-Speed Blender. Biomacromolecules **12**, 348–353 (2011).
128. Zhao, Y., Moser, C., Lindström, M. E., Henriksson, G. & Li, J. Cellulose Nanofibers from Softwood, Hardwood, and Tunicate: Preparation–Structure–Film Performance Interrelation. ACS Applied Materials & Interfaces **9**, 13508–13519 (2017).
129. Deepa, B. et al. Structure, morphology and thermal characteristics of banana nano fibers obtained by steam explosion. Bioresource Technology **102**, 1988–1997 (2011).
130. Cherian, B. M. et al. Isolation of nanocellulose from pineapple leaf fibres by steam explosion. Carbohydrate Polymers **81**, 720–725 (2010).
131. Abe, K. & Yano, H. Comparison of the characteristics of cellulose microfibril aggregates isolated from fiber and parenchyma cells of Moso bamboo (Phyllostachys pubescens). Cellulose **17**, 271–277 (2009).
132. de Morais Teixeira, E. et al. Cellulose nanofibers from white and naturally colored cotton fibers. Cellulose **17**, 595–606 (2010).
133. Ek, R., Gustafsson, C., Nutt, A., Iversen, T. & Nystrom, C. Cellulose powder from Cladophora sp. algae. JOURNAL OF MOLECULAR RECOGNITION vol. 11 263–265 (1998).
134. Jonoobi, M., Mathew, A. P. & Oksman, K. Producing low-cost cellulose nanofiber from sludge as new source of raw materials. Industrial crops and products (Print) **40**, 232–238 (2012).
135. Berglund, L., Noël, M., Aitomäki, Y., Öman, T. & Oksman, K. Production potential of cellulose nanofibers from industrial residues: Efficiency and nanofiber characteristics. Industrial Crops and Products **92**, (2016).

136. Eichhorn, S. J. et al. Review: current international research into cellulose nanofibres and nanocomposites. Journal of Materials Science vol. 45 http://doc.rero.ch (2010).
137. Ansari, F., Galland, S., Johansson, M., Plummer, C. J. G. & Berglund, L. A. Cellulose nanofiber network for moisture stable, strong and ductile biocomposites and increased epoxy curing rate. Composites Part A: Applied Science and Manufacturing **63**, 35–44 (2014).
138. Zhao, J. et al. Grafting of polyethylenimine onto cellulose nanofibers for interfacial enhancement in their epoxy nanocomposites. Carbohydrate Polymers **157**, 1419–1425 (2017).
139. Niu, Q., Gao, K., Lin, Z. & Wu, W. Surface molecular-imprinting engineering of novel cellulose nanofibril/conjugated polymer film sensors towards highly selective recognition and responsiveness of nitroaromatic vapors. Chemical Communications **49**, 9137–9139 (2013).
140. Bideau, B., Lucie CherpozatauthorIUT Moselle-Est 12 rue Victor Demange 57500 Saint-Avold France, U. de L., Eric LorangerauthorLignocellulosic Materials Research Center 3351 boul. des Forges C.P. 500 Trois-Rivires QC G9A 5H7 Canada, U. du Q. T.-R. & Claude DaneaultauthorLignocellulosic Materials Research Center 3351 boul. des Forges C.P. 500 Trois-Rivires QC G9A 5H7 Canada, U. du Q. T.-R. Conductive nanocomposites based on TEMPO-oxidized cellulose and poly(N-3-aminopropylpyrrole-co-pyrrole). (2015).
141. Hakalahti, M. et al. Direct Interfacial Modification of Nanocellulose Films for Thermoresponsive Membrane Templates. ACS Applied Materials & Interfaces **8**, 2923–2927 (2016).
142. Salas, C., Nypelö, T., Rodriguez-Abreu, C., Carrillo, C. & Rojas, O. J. Nanocellulose properties and applications in colloids and interfaces. Current Opinion in Colloid and Interface Science vol. 19 383–396 (2014).
143. Nishiyama, Y., Sugiyama, J., Chanzy, H. & Langan, P. Crystal Structure and Hydrogen Bonding System in Cellulose I ?? from Synchrotron X-ray and Neutron Fiber Diffraction. J Am Chem Soc **125**, 14300–14306 (2003).
144. Roy, D., Semsarilar, M., Guthrie, J. T. & Perrier, S. Cellulose modification by polymer grafting: a review. Chem Soc Rev **38 7**, 2046–64 (2009).
145. Malmström, E. & Carlmark, A. Controlled grafting of cellulose fibres - An outlook beyond paper and cardboard. Polymer Chemistry vol. 3 1702–1713 (2012).
146. Zarrelli, M., Skordos, A. A. & Partridge, I. K. Investigation of cure induced shrinkage in unreinforced epoxy resin. in Plastics, Rubber and Composites vol. 31 377–384 (2002).
147. Jana, S. & Zhong, W. FTIR study of ageing epoxy resin reinforced by reactive graphitic nanofibers. Journal of Applied Polymer Science **106**, 3555–3563 (2007).
148. Omrani, A., Simon, L. C. & Rostami, A. A. Influences of cellulose nanofiber on the epoxy network formation. Materials Science and Engineering A **490**, 131–137 (2008).
149. Liu, D., Pourrahimi, A. M., Olsson, R. T., Hedenqvist, M. S. & Gedde, U. W. Influence of nanoparticle surface treatment on particle dispersion and interfacial

adhesion in low-density polyethylene/aluminium oxide nanocomposites. European Polymer Journal **66**, 67–77 (2015).
150. Lu, T. et al. Effect of surface modification of bamboo cellulose fibers on mechanical properties of cellulose/epoxy composites. Composites Part B: Engineering **51**, 28–34 (2013).
151. Vijayan P, P., Tanvir, A., El-Gawady, Y. H. & Al-Maadeed, M. Cellulose nanofibers to assist the release of healing agents in epoxy coatings. Progress in Organic Coatings **112**, 127–132 (2017).
152. Saba, N. et al. Mechanical, morphological and structural properties of cellulose nanofibers reinforced epoxy composites. International Journal of Biological Macromolecules **97**, 190–200 (2017).
153. Vacche, S. D., Vitale, A. & Bongiovanni, R. Photocuring of epoxidized cardanol for biobased composites with microfibrillated cellulose. Molecules **24**, (2019).

# CHAPTER 2: Synthesis and Characterization of Novel Bio-based Epoxy Polymers Derived from Cardanol

## 2.1 Abstract

A novel bio-based epoxy polymer was synthesized at ambient temperature using cardanol derivatives, epoxy prepolymer, and phenalkamine. FT-IR and $^{1}$H NMR spectroscopy were used to investigate the chemical structures of cured epoxy polymers. The drying, physical, thermal, optical, and mechanical characteristics of epoxy polymers were explored in terms of epoxy and amine compound composition, epoxy prepolymer molecular weight, and post-curing technique. The resulting epoxy polymers were flexible and thermally stable (thermal breakdown temperature of 300°C, for example). Furthermore, the epoxy polymers were anti-microbial against *E. coli* and *S. aureus.* The drying property was also greatly impacted by the molecular weight of the epoxy prepolymer, implying that the drying time may be regulated by the prepolymer's molecular weight. Thermal post-curing of polymers was a successful method for increasing hardness, thermal stability, and mechanical strength. As a result, this new epoxy polymer based on cardanol derivatives may be predicted to be extremely green functional epoxy polymers for coating, film, and resin applications.

## 2.2 Introduction

Global warming and plastic pollution are major environmental issues today, harming whole ecosystems, marine life, and human health and well-being [1-3]. Over the last several decades, the manufacturing of petroleum-based plastics has skyrocketed, presently exceeding 300 million tonnes per year [4], with an estimated 8 million tonnes of plastic garbage entering the seas each year [5]. To address these global environmental issues, there is a rising emphasis on the utilization of renewable resources to manufacture chemicals and materials that can replace fossil fuels [6]. Today, a broad range of functional polymers renewable resources are being researched to support long-term development. Because of their great performance, epoxy materials are widely used in industrial applications such as adhesives, coatings, and resins [7]. Recent epoxy polymer research has focused on

ecologically friendly processes, renewable resources, and additional functionality [8]. Due to the facilitation of additional crosslink reaction and rearrangement, the post-curing process of epoxy polymers is one of the effective techniques to improving mechanical and thermal characteristics [9]. Cashew nuts shell liquid (CNSL) is a non-edible plant oil derived from the processing of cashew nuts (*Anacardium occidentale*). Natural CNSL is a combination of phenolic chemicals, the primary component being anacardic acid, with minor components including cardanol, cardol, and 2-methyl cardol [10]. Thermal refining converts anacardic acid to cardanol, allowing industrial resources to be used. Cardanol has a phenolic compound structure with a meta-substituted unsaturated long alkyl side chain (C15) and a variety of functionalisable sites. Cardanol's structural properties give heat resistance, chemical resistance, and flexibility. CNSL is now available in epoxy resins and coatings. Coatings developed from CNSL, for example, are utilized as synthetic lacquers because they offer attributes comparable to natural lacquer, "Urushi," such as superb gloss and long-term durability [11, 12]. This is because urushiol, a phenolic lipid found in natural lacquer, and cardanol have a similar chemical structure.

We previously described the production of a new epoxy cardanol prepolymer (ECP) through direct oxidative polymerization of epoxidized cardanol double bonds [13-16]. UV-crosslinking or petroleum-based amine-crosslinking were used to create epoxy polymers from this epoxy prepolymer. These epoxy prepolymers demonstrated flexibility, chemical resistance, thermal stability, and antibacterial action against *E. coli* and *S. aureus* [13-15]. Phenalkamine is a cardanol-derived compound that has been used as an epoxy hardener in resins and coatings [17, 18]. The crosslink point with the epoxy groups is caused by the amine side chain in phenalkamine.

We attempted to improve the more environmentally-friendly synthesis process of epoxy polymers using phenalkamine, a biomass-based amine monomer. Herein, we have prepared novel “green” epoxy polymers derived from cardanol derivatives, epoxy cardanol prepolymer and phenalkamine. The influence of molecular weight of epoxy prepolymer and post curing process on the natures of epoxy polymers was investigated in terms of effective curing process, physical, thermal, optical, and mechanical properties.

## 2.3 Experiment

### 2.3.1 Materials

Purified cardanol and phenalkamine (Figure 2.1) were procured from Tohoku Chemical Industry Co., Ltd. in Japan and Kusumoto Chemical, Ltd. in Japan, respectively. Tokyo Chemical Industry Co., Ltd. in Japan supplied epichlorohydrin (>99.0 percent) and diethylenetriamine (>98.0 percent). All compounds were utilized without additional purification. The chemical makeup of the cardanol utilized in this investigation is given in Table 2.1. The chemical composition and degree of unsaturation were assessed using $^{1}H$ NMR and HPLC analyses. As a comparison, CNSL-based polymer for coating (No. 53, Cashew Co., Ltd., Japan) was employed in this research.

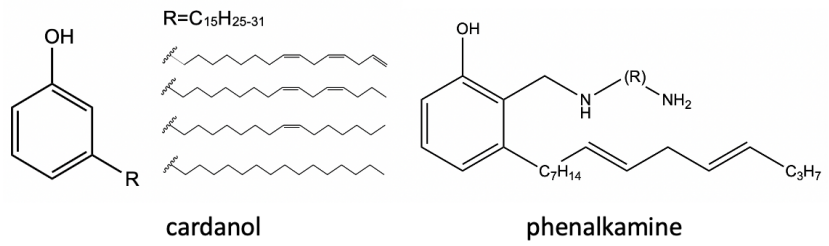


Figure 2.1 Chemical structures of cardanol and phenalkamine.

Table 2.1 Properties of purified cardanol

| Purity | Tri-ene (%) | di-ene (%) | Mono-ene (%) | Saturation (%) | Unsaturation degree |
|---|---|---|---|---|---|
| 96% | 29 | 30 | 38 | 3 | 1.9 |

### 2.3.2 Synthesis of epoxy cardanol and epoxy cardanol prepolymers

The synthetic route of epoxy cardanol (EC) and epoxy cardanol prepolymers (ECP) is shown in Scheme 2.1. These epoxy compounds were prepared in accordance with our earlier research [13, 14]. 9.25 g (0.3 eq.) of cardanol, potassium hydroxide, and 30 mL of DMSO were poured in a 200 mL flask and agitated with a magnetic stirrer. Epichlorohydrin 4.40 g (2.0 eq) was progressively put on an ice bath, and the mixture was agitated at room temperature for a predetermined amount of time. Diethyl ether was used to extract the solution, and the organic phase was washed with saturated sodium chloride solution. To get the epoxy cardanol, the organic phase was dehydrated with magnesium sulphate and the solvent was evaporated. The resulting epoxy cardanol was purified using silica gel column chromatography with an eluent combination of n-hexane and ethyl acetate (9:1). $^{1}$H NMR validated the purification of epoxy cardanol. Meanwhile, epoxy cardanol prepolymer was created using the thermal oxidative polymerization of epoxy cardanol, as described below. A 100-mL flask was filled with 5.0 g (0.017 mol) of epoxy cardanol. The flask was then put in an oil bath (160°C) and the epoxy cardanol was agitated for the duration of the oil bath. In this study, two epoxy prepolymers with various molecular weights (ECP-low and ECP-high, respectively) were synthesized to investigate the influence of molecular weight on epoxy polymer characteristics.

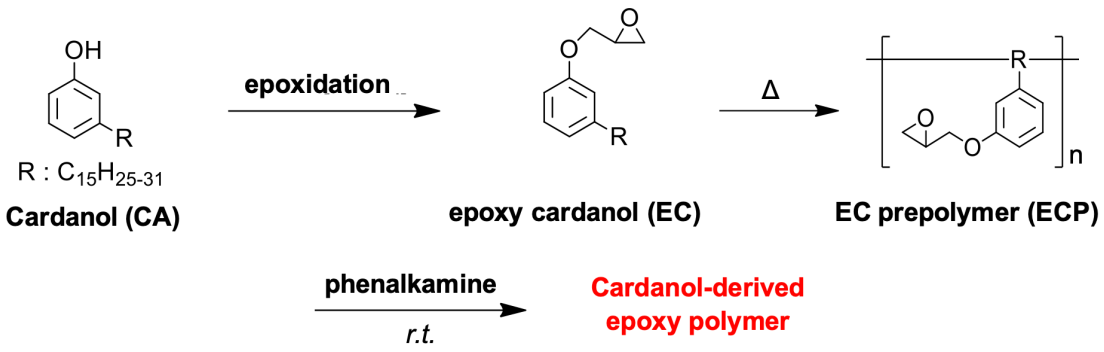


Scheme 2.1 Synthetic route of all cardanol-based epoxy polymer.

### 2.3.3 Preparation of epoxy film

In the indicated formulations, the epoxy prepolymer and phenalkamine, a phenylalkylamine molecule, were physically mixed for 15 minutes using a spatula. The epoxy polymer (epoxy prepolymer/phenalkamine) has a composition of 1:0.33 (P1), 1:0.5 (P2), 1:1 (P3), 1:2 (P4), and 1:3 (P5) (P5). The epoxy polymers produced by varying the molecular weight of the prepolymers were examined in this work. A vacuum pump was employed to remove the dissolved air from the resulting mixture. Following degassing, an applicator was used to distribute the liquid uniformly on a glass plate at room temperature (Yoshimitsu Seiki, Tokyo, Japan). When the epoxy polymer had dried, it was removed off the glass plate. Furthermore, the epoxy polymer was post-cured at 180°C for 30 minutes. In contrast, a cardanol-based polymer for coating (No. 53, commercial product) was also examined.

### 2.3.4 Structure Analysis

Molecular weight and polydispersity index (PDI) were assessed using gel permeation chromatography (GPC) in a system equipped with a UV detector (254 nm) (UV-2075 Plus, Tokyo, Japan) with chloroform as eluent, calibrated against a monodisperse polystyrene standard. A JNM-ECZR300 spectrometer was used to collect $^{1}H$ NMR spectra (JEOL Ltd., Tokyo, Japan). The samples were dissolved in deuterated chloroform solution, and chemical shifts were calculated using tetramethylsilane (TMS). An FT/IR-4100 was used to conduct attenuated total reflection (ATR) Fourier transform infrared (FT-IR) spectroscopy (Jasco Corporation, Tokyo, Japan). The spectra were obtained between 3500 $cm^{-1}$ and 600 $cm^{-1}$. Each spectrum was scanned 64 times with a resolution of 2 $cm^{-1}$.

### 2.3.5 Characterization

The chemical structure, physical, mechanical, and thermal characteristics of all samples were investigated. To measure the degree of the crosslink reaction, the gel content of the cured epoxy polymers was evaluated. The gel content was determined using the equation: $Gel\ content\ (\%) = w_{insol}/w_{initial} \times 100$, where $w_{insol}$ and $w_{initial}$ are the weight of the insoluble portion and the weight of the well-dried initial sample, respectively. At room temperature,

the polymer was submerged in acetone, an excellent solvent for epoxy prepolymer and phenalkamine. The non-dissolved components were filtered out after 24 hours and dried at room temperature for 24 hours to eliminate residual solvent before being weighed. At 23°C, epoxy polymers may be dried in three stages: dust-free drying (DF), touch-free drying (TF), and harden drying (HD). At 23°C and 60% relative humidity, the drying time for each step was measured using an automated drying time recorder (Paint Drying Time Recorder RC, Taiyu Corporation, Osaka, Japan). The hardness of the pencil lead was assessed using a designation consisting of letters and numbers in accordance with the current national standard GB/T6739-1996. The hardness of the pencil lead was determined at 23°C using a C-221 hardness tester (Yoshimitsu Seiki, Tokyo, Japan).

UV-vis analysis of epoxy films was carried out using a double-beam spectrophotometer V-670 (Jasco Corporation, Tokyo, Japan) with a slit width of 2 nm. The color of the cured epoxy polymers was detected using a spectro-guide (BYK Gardner GmbH, Germany) with an irradiance/observer of D65/10° and a geometry of 45°/0°.

Thermogravimetric analysis (TGA) was carried out using a TG8120 (Rigaku Corporation, Tokyo, Japan). Polymer samples were heated in platinum pans from 50 to 600°C at a heating rate of 10°C/min under nitrogen at a flow rate of 60 ml/min.

Mechanical properties were measured using a universal tensile tester EZ-SX (Shimadzu Corporation). The stress-strain (S-S) curve was measured. The test specimens were prepared in the form of dumbbells with a width of 5 mm and a central thickness of 2 mm. Dynamic mechanical analysis (DMA) was carried out using a Mettler Toledo DMA1. The DMA samples were rectangular in shape (length: 15 mm, width: 8 mm, thickness: 0.2 mm). The DMA samples were heated from 50°C to 100°C at a rate of 5°C/min while the frequency was kept at 10 Hz (viscoelastic range).

Anti-microbial activity of epoxy film against *E. coli* as gram negative and *S. Aureus* as gram positive bacteria was evaluated by international test (Japanese Industrial Standard, JIS Z 2801). Polyethylene film was used as control.

## 2.4 Results and discussion

### 2.4.1 Preparation of epoxy cardanol and epoxy cardanol prepolymer (ECP)

The chemical structures of cardanol, epoxy cardanol, and epoxy cardanol prepolymers were determined by $^{1}$H-NMR spectroscopy according to our previous work [13]. The properties of epoxy cardanol prepolymer are summarized in Table 2.2. The unsaturation degree of cardanol was estimated to be 1.9 by $^{1}$H NMR spectrum. This value was consistent with the literature values (1.98-2.61) [19]. While those of ECP prepared by different heating time were 1.34 and 0.92, respectively, indicating that the molecular weight of the epoxy cardanol prepolymer increased with decreasing unsaturation degree due to the oxidative polymerization at the side chains. For this oxidation of EC, 1,4-diene type structure is liable to occur during oxidation because of the ease of hydrogen loss in the active methylene group. The formed radicals produce hydroxyl and carbonyl group under the presence of oxygen and hydroxyl radical during the thermal polymerization. Furthermore, the crosslink reaction also generated between formed radicals at oxygen atmosphere in parallel [13]. We obtained the two types of different molecular weight of the prepolymers, ECP-low and ECP-high by changing the heating time. There was no chemical reaction in the epoxy groups during the oxidative polymerization, regardless of the heating time according to the $^{1}$H NMR and FT-IR measurements.

Table 2.2 Properties of cardanol epoxy prepolymer (ECP)

| Prepolymer | Unsaturation degree | $M_n$ | $M_w$ | $M_w/M_n$ |
|---|---|---|---|---|
| ECP-low | 1.34 | 2400 | 14400 | 6.0 |
| ECP-high | 0.92 | 5900 | 111000 | 18.8 |

### 2.4.2 Preparation and structure analysis of epoxy cardanol polymers

Epoxy polymers were prepared by the ECP with phenalkamine at various ratios, and the optimization of the epoxy: amine composition was investigated. Photographic image of the epoxy polymer (P2-low) is shown in Figure 2.2. The presented epoxy polymer was flexible, light yellow, and highly transparent. The time dependence of the gel content of the epoxy polymers prepared with ECP-low is shown in Figure 2.3. The gel content indicates the degree of progress of the crosslink reaction. Up to 5 days from initiation of curing, the gel content increased significantly and then remained constant, indicating that the curing was completed within 5 days. The gel content of P2-low was highest among P1-P3 prepared with ECP-low. Table 2.3 summarizes the time until harden dry as drying property and gel content of the epoxy polymers prepared from ECP-low. From the drying time and gel content, P2-low was found to have a better composition since P2-low showed the shortest drying time and the highest gel content among P1-P5. P4 and P5 did not cure completely which might be regarding the excess amount of phenalkamine. The theoretical value of amine hydrogen equivalent weight (AHEW)/ epoxy equivalent weight (EEW) for this curing system was estimated to be 0.41. Therefore, P2-low would be the suitable composition from the structural properties and theoretical composition.

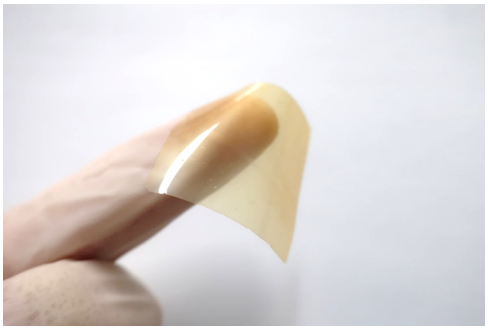

Figure 2.2 Photographs of cardanol-derived epoxy film.

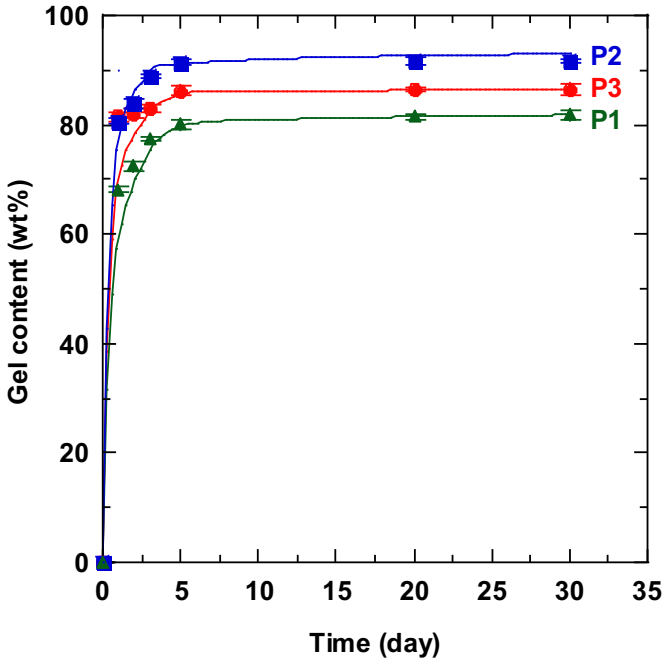


Figure 2.3 Gel content of cardanol-derived epoxy films (P1-P3) prepared with ECP-low.

Table 2.3 Properties of cardanol-derived epoxy polymers prepared with ECP-low

| Sample | Composition[a)] | Drying time (h)[b)] | Gel content (wt%)[c)] | Remark |
|---|---|---|---|---|
| P1-low | 1:0.33 | 14 | 79.8±0.8 | cured |
| P2-low | 1:0.5 | 12 | 91.3±0.8 | cured |
| P3-low | 1:1 | 12 | 86.1±0.9 | cured |
| P4-low | 1:2 | > 24 | < 50 | uncured |
| P5-low | 1:3 | > 24 | < 50 | uncured |
| cardanol-based polymer[d)] | — | 8.0 | 98.3±0.6 | cured |

a) composition of epoxy cardanol prepolymer: phenalkamine
b) time until harden dry (HD)
c) cured for 5 days
d) commercially available cardanol-based polymer (No.53)

FT-IR spectra of P2 epoxy polymers prepared from ECP-low and ECP-high are presented in Figure 2.4. The characteristic peaks of epoxy polymer appeared at 3500-3100 $cm^{-1}$ (OH group), 3040 $cm^{-1}$ C–H (aromatic), 3005 $cm^{-1}$ N–H (secondary), 2922, 2852 $cm^{-1}$ C-H

(aliphatic), 1729 $cm^{-1}$, C=O (ester), 1588, 1583, 1455 $cm^{-1}$ C=C (aromatic), 1258, 1045 $cm^{-1}$ C–O (aromatic), 1157 $cm^{-1}$ (C–N), 876 $cm^{-1}$ (epoxy), 871,773, and 693 $cm^{-1}$ C-H (*m*-aromatic). The appearance of OH group and secondary amine peaks in the FT-IR spectra was attributed to the reaction between epoxy and amine groups. There was no obvious difference in the FT-IR spectra of the epoxy polymers prepared from ECP-low and ECP-high. On the other hand, some peak changes in the FT-IR spectra after thermal treatment were observed. The peaks of OH group (3500-3100 $cm^{-1}$), C=O (1729 $cm^{-1}$), aliphatic C–O (1120 $cm^{-1}$) increased, while epoxy group (876 $cm^{-1}$) and secondary amine (3005 $cm^{-1}$) decreased. These results indicated that further crosslink reaction proceeded between epoxy and secondary amines. The new peaks appeared at 1655 $cm^{-1}$ C=C, which attributed to the dehydration of OH groups by thermal treatment [20]. These structure analyses expect the possible crosslinked structure of the epoxy polymer as shown in Figure 2.5. Further crosslink reaction proceeded by thermal treatment in P2-high (180), resulting in highly crosslink structure.

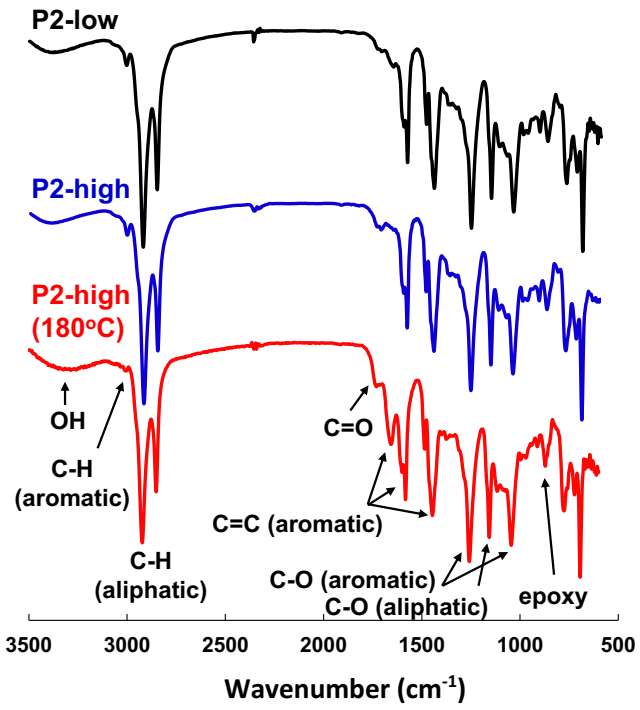


Figure 2.4 FT-IR spectra of cardanol-derived epoxy polymers prepared with different molecular weight of the prepolymer (ECP-low and ECP-high)

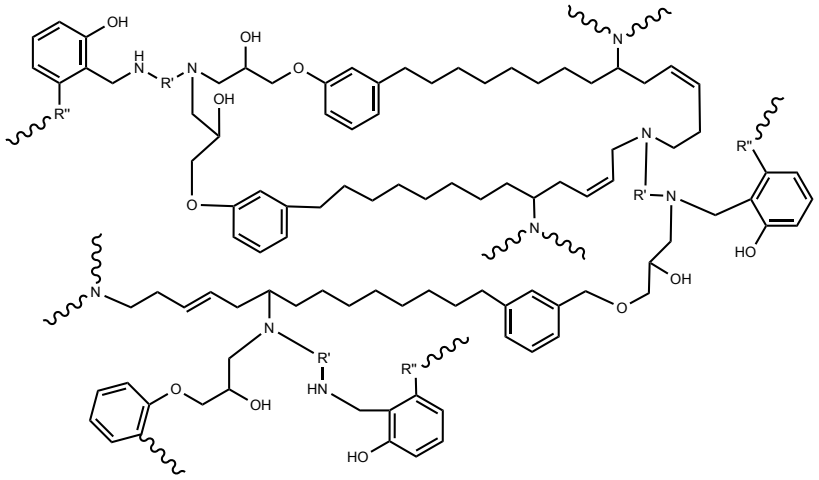

Before thermal treatment

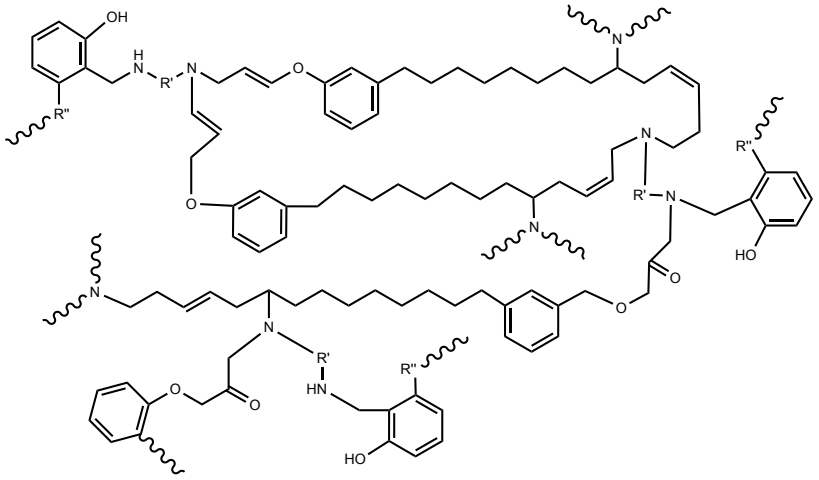

After thermal treatment

Figure 2.5 Plausible crosslink structure of epoxy polymer after thermal treatment.

The influence of the molecular weight of the ECP and the post-heat treatment on the physical, thermal and mechanical properties of epoxy polymers are summarized in Table 2.4. The gel contents of P2-low and P2-high cured for 5 days were 91.3 and 93.2 wt%, respectively. The epoxy polymer prepared with ECP-high gave higher gel content, indicating the highly crosslink density. The time to harden dry state of P2-high was dramatically shorter than that of P2-low. The time of P2-high was 5.6 times shorter than that of P2-low, suggesting that the higher molecular weight of prepolymer results in the accelerated crosslinking reaction. Effect of molecular weight and structures of phenalkamine as curing agent on the various properties of epoxy coatings was investigated [21]. The high molecular weight of phenalkamines resulted in faster drying time util HD state compared with conventional cardanol-based polymer because of the rapid increase in the molecular weight by crosslink reaction. Therefore, this result suggested that higher molecular weight of epoxy prepolymer worked effectively in curing process as seen in phenalkamine with different molecular weights. In the present work, the different molecular weight of epoxy prepolymer can be easily prepared by changing the heating time. In addition, the P2-high (180) increased the gel content to 96.7 wt% from 93.2 wt%, suggesting that further crosslink reaction proceeded by thermal treatment as discussed in the structure analysis. The pencil hardness of the cardanol-derived epoxy polymers showed very flexible nature compared with conventional cardanol-based polymer or other petroleum-based epoxy polymers, indicating that this flexible property of the cardanol-derived epoxy polymers was attributed to the flexible crosslinked structure of the prepolymer.

Table 2.4 Properties of cardanol-derived epoxy polymers prepared with different molecular weight of the prepolymer (ECP-low and ECP-high)

| Sample | Drying condition | Gel content (wt%) [a)] | Drying time (h) | | | Pensile hardness | Color indices | | |
|---|---|---|---|---|---|---|---|---|---|
| | | | DF | TF | HD | | *L** | *a** | *b** |
| P2-low | *r.t.* | 91.3±0.4 | 3.0 | 4.5 | 14 | < 10B | 81.3 | -3.6 | 14.8 |
| | 180°C | — | — | — | — | < 10B | 78.2 | -0.3 | 43.7 |
| P2-high | *r.t.* | 93.2±0.6 | 1.0 | 1.5 | 2.5 | < 10B | 77.5 | -2.7 | 37.7 |
| | 180°C | 96.7±0.5 | — | — | — | 10B | 68.4 | 11.8 | 64.1 |
| cardanol-based polymer[b)] | *r.t.* | 98.3±0.6 | 0.8 | 4.0 | 8.0 | H | 29.1 | 45.0 | 48.0 |

a) cured after 5 days
b) commercially available cardanol-based polymer (No.53)

### 2.4.3 Optical property

The UV-vis spectra of the epoxy polymer films are presented in Figure 2.6. Visible light absorption of the epoxy polymers increased by thermal treatment. The increase in the absorption toward the longer wavelengths was due to the increase in OH, carbonyl groups, and C=C bonds after thermal treatment. The color index (CIE-Lab color) of the epoxy polymer is optical appearance property as presented in Table 4. The *b** value in CIE-Lab color which presents degree of yellow/blue index, increased with molecular weight of the prepolymer and further increased by thermal treatment. The color of the cardanol-derived epoxy prepolymer was changed from light yellow to dark brown with increasing molecular weight, which reflected the degree of the oxidative polymerization. Therefore, the molecular weight of the ECP affected the optical nature of the epoxy polymers. Even the cardanol epoxy polymers after thermal treatment were lighter in color than conventional cardanol-based polymers.

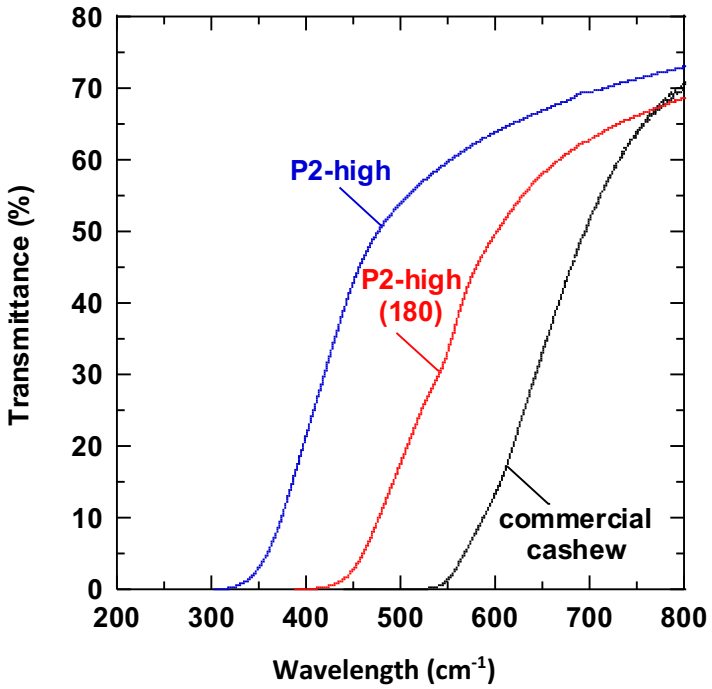


Figure 2.6 UV-vis spectra of cardanol-derived epoxy films (P2).

### 2.4.4 Thermal property

The TGA curves of epoxy polymers are presented in Figure 2.7. The thermal properties of epoxy polymers determined by TGA are also summarized in Table 2.5. TGA curves provides the thermal stability and thermal degradation behavior of crosslinked structure. As shown in Figure 2.7, the 2- step thermal decomposition was observed in the epoxy polymers. The thermal decomposition at 300-500°C was assigned to the cleavage of the ether bond and crosslinked alkyl chains of epoxy cardanol prepolymer [12,13]. The temperature at weight loss in 5 wt%, 10 wt% and thermal decomposition temperatures of P2-high were greater than that of P2-low, indicating that the crosslink structure among alkyl side chains in oxidative polymerization affected the thermal stability of the whole epoxy polymer. The pyrolysis temperature of all epoxy polymers was over 30°C higher than the $T_5$, suggesting degradation of free alkyl chains in phenalkamine or ECP prior to

pyrolysis of the main chain backbone. The result showed that these cardanol-derived epoxy polymers can be acceptable for general coatings as thermal resistance.

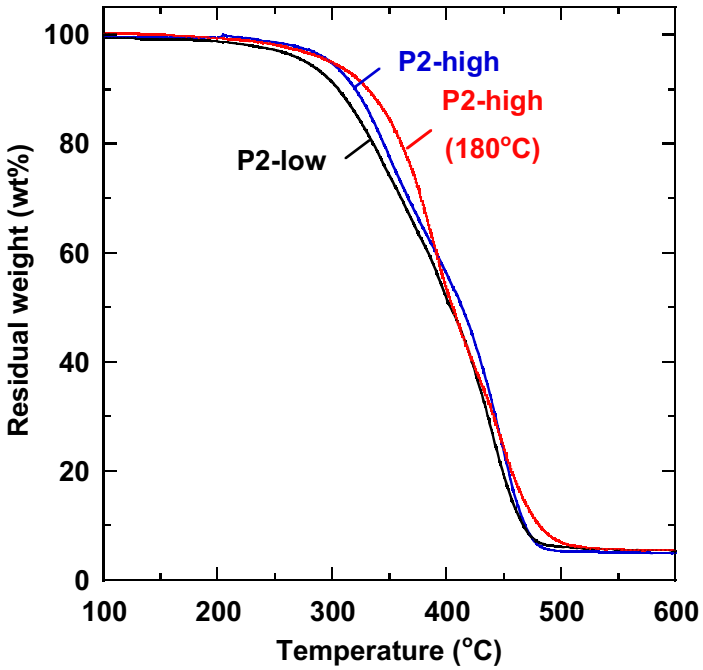


Figure 2.7 TGA curves of cardanol-derived epoxy films (P2).

Table 2.5 Thermal properties of cardanol-derived epoxy films prepared with different molecular weight of the prepolymer

| Sample | Drying condition | $T_5$ (°C) | $T_{10}$ (°C) | $T_d$ (°C)[a)] | $W_{R600}$ (wt%) | $T_g$ (°C)[b)] |
|---|---|---|---|---|---|---|
| P2-low | *r.t.* | 277 | 305 | 310 | 5 | 20.8 |
| P2-high | *r.t.* | 300 | 320 | 335 | 5 | 30.6 |
| | 180°C | 300 | 331 | 350 | 5 | 43.6 |
| cardanol-based polymer[c)] | *r.t.* | 208 | 288 | 432 | 12 | 96.3 |

a) Onset temperature
b) Determined by dynamic mechanical analyses (DMA)
c) commercially available cardanol-based polymer (No.53)

### 2.4.5 Mechanical property

The mechanical property of epoxy polymers was investigated by the tensile test and dynamic mechanical analysis (DMA) measurement. The stress-strain curves of the epoxy polymers are presented in Figure 2.8. The mechanical properties are also summarized in Table 2.6. The tensile strength of P2-high was 1.8 times greater than that of P2-low, indicating that the epoxy polymer prepared with ECP-high had more highly crosslink density. Tensile strength and Young's modulus of previous ECP-diethylenetriamine (DETA) system were 12.5 MPa and 1.2 MPa. Both values of P2 were higher than that of the ECP-DETA, suggesting that phenalkamine as curing amine component improved their mechanical property due to the presence of rigid aromatic structure. Furthermore, the tensile strength and Young's modulus of the epoxy polymers could be enhanced by thermal treatment. Particularly, the Young's modulus of P2-high (180) was nearly 8 times higher than that of P2-high before thermal treatment.

The DMA curves of the epoxy polymers are presented in Figure 2.9. The temperature at which the maximum tan δ is obtained is defined as the glass transition temperature (Tg). The Tg of the P2-low, P2-high and P2-high (180) were 20.8°C, 30.6°C, and 43.6°C, respectively. It can be seen that the high molecular weight of ECP and thermal treatment increased the Tg of the epoxy polymer. Therefore, the influence of thermal treatment on Tg which presents the polymer stiffness was greater than that of molecular weight of prepolymer. This result suggested that the further crosslink structure provided more rigid structure by thermal treatment. The maximum tan δ value of the epoxy polymer decreased after thermal treatment, indicating that the viscosity of the epoxy polymer decreased while the elastic energy increased.

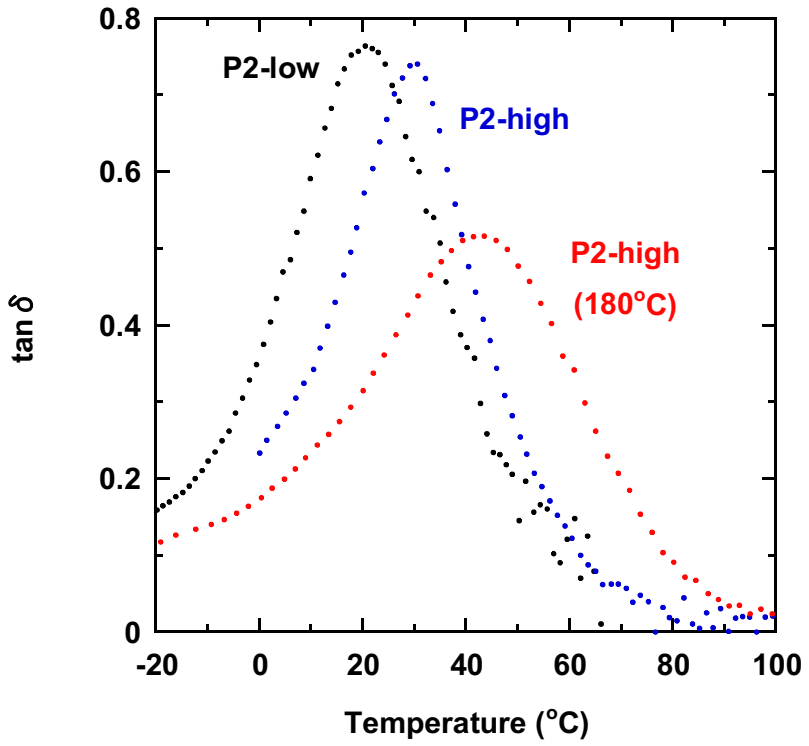


Figure 2.8 DMA curves of cardanol-derived epoxy films (P2).

Table 2.6 Mechanical properties of cardanol-derived epoxy films prepared with different molecular weight of the prepolymer

| Sample | Drying condition | $T_g$ (°C) | Tensile strength (MPa) | Young's modulus (MPa) |
|---|---|---|---|---|
| P2-low | *r.t.* | 20.8 | 16.8 ± 1.6 | 3.9 ± 0.2 |
| P2-high | *r.t.* | 30.6 | 29.8 ± 2.4 | 8.5 ± 0.5 |
| | 180°C | 43.6 | 32.3 ± 1.8 | 65.0 ± 7.0 |
| cardanol-based polymer[a)] | *r.t.* | 96.3 | N.A. | N.A. |

a) commercially available cardanol-based polymer (No.53)

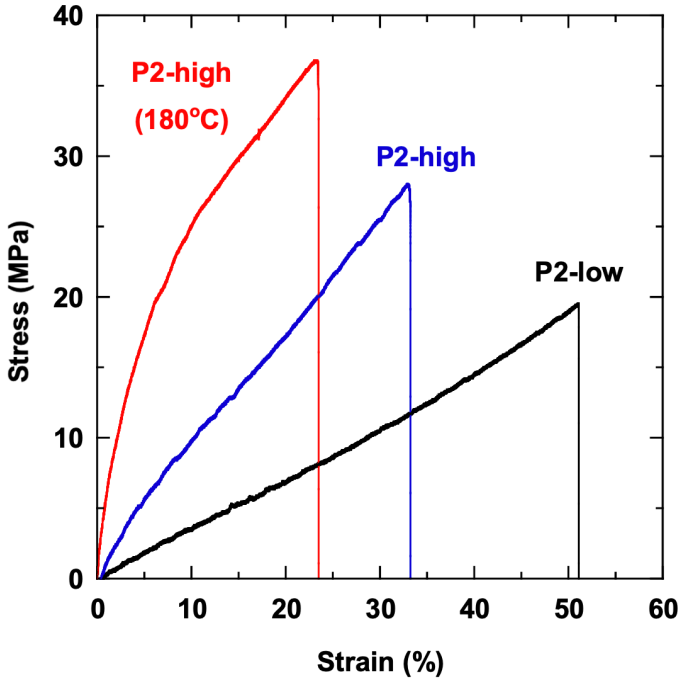


Figure 2.9 Stress-Strain curves of cardanol-derived epoxy films (P2).

### 2.4.6 Anti-microbial property

The anti-microbial activity against *E. coli*. and *S. aureus* are summarized in Table 2.7. Purifed CNSL and anacardic acid showed anti-microbial activity [22, 23]. As reported in our previous works, ECP-DETA polymer showed the anti-microbial activity against E. coli. and S. aureus [14]. The present cardanol derivative-based epoxy polymers also showed anti-microbial activity against *E. coli* and *S. aureus.* One possible reason for this anti-microbial property would be attributed to the unsaturated long alkyl chains [24] and/or amine compound (phenalkamine) [25] which generally showed anti-microbial property. Interestingly, the anti-microbial activity increased after thermal treatment, suggesting that the further crosslinked structure and rearrangement of polymer segments by thermal treatment were effective for the activity. Therefore, this cardanol-derived epoxy polymer can be expected as a flexible anti-microbial polymer for coatings, films, and resins.

Table 2.7 Anti-microbial activities for *S. aureus* and *E. coli.* of cardanol-derived epoxy films prepared with ECP-high

| Sample | Drying condition | *S. aureus* | | *E. coli* | |
|---|---|---|---|---|---|
| | | initial [a)] | after [a)] | initial [a)] | after [a)] |
| Control | − | 3.89 | 4.21 | 4.14 | 5.70 |
| P2-high | as cast | 3.89 | < 0.20 | 4.14 | 1.93 |
| | 180°C | 3.89 | 0.30 | 4.14 | 0.30 |

a) logarithm value of number of bacteria in area unit

## 2.5 Conclusion

Novel epoxy polymers were synthesized from cardanol derivatives, epoxy cardanol prepolymer and phenalkamine. The effects of the molecular weight of the prepolymer used for the epoxy polymer and the thermal treatment on the physical properties of the epoxy polymers were investigated. The optimal composition of epoxy and amine compounds determined from the drying time and the gel content of the epoxy polymers was close to the theoretical ratio. The drying time to harden dry state of the epoxy polymers strongly depended on the molecular weight of the prepolymer. This result indicates that the molecular weight of the prepolymer could control the drying time of the epoxy polymer. The epoxy polymer showed flexible nature and thermally stable up to 300°C. The glass transition temperature of the epoxy polymer determined from dynamic viscoelasticity measurements was nearly room temperature. The molecular weight of the prepolymer had a significant influence on the drying properties of the epoxy polymer according to the optical, thermal, and mechanical properties of epoxy polymer, suggesting that high molecular weight of the prepolymer more likely to form the cross-linked structure. Furthermore, the thermal treatment of epoxy polymers as post curing process significantly enhanced the mechanical strength and glass transition temperature. The epoxy polymers were found to exhibit anti-microbial activity against E. coli and S. aureus. Hence, this novel cardanol-derived epoxy polymer has high potential as flexible, thermal resistance, and anti-microbial coatings and resins.

## 2.6 References


1. Koelmans, A. A. *et al.* Risks of Plastic Debris: Unravelling Fact, Opinion, Perception, and Belief. *Environmental Science & Technology* **51**, 11513–11519 (2017).
2. Ivleva, N. P., Wiesheu, A. C. & Niessner, R. Microplastic in Aquatic Ecosystems. *Angewandte Chemie International Edition* **56**, 1720–1739 (2017).
3. Maris, J. *et al.* Mechanical recycling: Compatibilization of mixed thermoplastic wastes. *Polymer Degradation and Stability* **147**, 245–266 (2018).
4. Ellen, M. Beyond plastic waste. *Science (1979)* **358**, 843 (2017).
5. Payne, J., Mckeown, P. & Jones, M. D. *A Circular Economy Approach to Plastic Waste*.
6. Gandini, A. The irruption of polymers from renewable resources on the scene of macromolecular science and technology. *Green Chemistry* **13**, 1061–1083 (2011).
7. Pascault, J.-P. & Williams, R. J. J. General Concepts about Epoxy Polymers. in *Epoxy Polymers* 1–12 (John Wiley & Sons, Ltd, 2010). doi:https://doi.org/10.1002/9783527628704.ch1.
8. Auvergne, R., Caillol, S., David, G., Boutevin, B. & Pascault, J.-P. Biobased Thermosetting Epoxy: Present and Future. *Chemical Reviews* **114**, 1082–1115 (2014).
9. Moller, J. C., Berry, R. J. & Foster, H. A. On the nature of epoxy resin post-curing. *Polymers (Basel)* **12**, (2020).
10. Anilkumar, P. *Cashew nut shell liquid: A goldfield for functional materials*. *Cashew Nut Shell Liquid: A Goldfield for Functional Materials* (Springer International Publishing, 2017). doi:10.1007/978-3-319-47455-7.
11. Kobayashi, S., Uyama, H. & Ikeda, R. Artificial Urushi. *Chemistry – A European Journal* **7**, 4754–4760 (2001).
12. Lu, R. & Miyakoshi, T. *Lacquer chemistry and applications*. (Elsevier, 2015).
13. Kanehashi, S. *et al.* Preparation and characterization of cardanol-based epoxy resin for coating at room temperature curing. *Journal of Applied Polymer Science* **130**, 2468–2478 (2013).
14. Kanehashi, S. *et al.* Development of a cashew nut shell liquid (CNSL)-based polymer for antibacterial activity. *Journal of Applied Polymer Science* **132**, (2015).
15. Kanehashi, S. *et al.* Photopolymerization of Bio-Based Epoxy Prepolymers Derived from Cashew Nut Shell Liquid (CNSL). *Journal of Fiber Science and Technology* **73**, 210–221 (2017).
16. Kanehashi, S., Oyagi, H., Ogino, K. & Miyakoshi, T. Development of Room Temperature Curable Natural Polyphenols-Based Hybrid Epoxy Polymers. *Journal of Fiber Science and Technology* **73**, 192–201 (2017).
17. Pathak, S. K. & Rao, B. S. Structural effect of phenalkamines on adhesive viscoelastic and thermal properties of epoxy networks. *Journal of Applied Polymer Science* **102**, 4741–4748 (2006).
18. Sahoo, S. K., Khandelwal, V. & Manik, G. Renewable Approach To Synthesize Highly Toughened Bioepoxy from Castor Oil Derivative–Epoxy Methyl Ricinoleate and Cured with Biorenewable Phenalkamine. *Industrial & Engineering Chemistry Research* **57**, 11323–11334 (2018).

19. Tyman, J. H. P. Long-chain phenols: IV. Quantitative determination of the olefinic composition of the component phenols in cashew nut-shell liquid. *Journal of Chromatography A* **111**, 277–284 (1975).
20. Grassie, N., Guy, M. I. & Tennent, N. H. *Degradation of Epoxy Polymers: Part 4 Thermal Degradation of Bisphenol-A Diglycidyl Ether Cured with Ethylene Diamine*. *Polymer Degradation and Stability* vol. 14 (1986).
21. Kathalewar, M. & Sabnis, A. Effect of molecular weight of phenalkamines on the curing, mechanical, thermal and anticorrosive properties of epoxy based coatings. *Progress in Organic Coatings* **84**, 79–88 (2015).
22. Ashraf, S. M., Mahanty, S. & Rathinasamy, K. Securinine induces mitotic block in cancer cells by binding to tubulin and inhibiting microtubule assembly: A possible mechanistic basis for its anticancer activity. *Life Sciences* **287**, 120105 (2021).
23. Kubo, Isao. *et al.* Structure-antibacterial activity relationships of anacardic acids. *Journal of Agricultural and Food Chemistry* **41**, 1016–1019 (1993).
24. Zheng, C. J. *et al.* Fatty acid synthesis is a target for antibacterial activity of unsaturated fatty acids. *FEBS Letters* **579**, 5157–5162 (2005).
25. Li, C. *et al.* Antimicrobial activities of amine- and guanidine-functionalized cholic acid derivatives. *Antimicrob Agents Chemother* **43**, 1347–1349 (1999).

# CHAPTER 3: Development of Cellulose Nanofiber-reinforced Cardanol Epoxy Composites

## 3.1 Abstract

Novel bio-based epoxy nanocomposites reinforced with cellulose nanofiber (CNF) were developed. The epoxy nanocomposites were prepared from cashew nut shell liquid (CNSL)-derived epoxy prepolymer and phenalkamine using two types of CNFs. CNF were immobilized with epoxy cardanol prepolymer (ECP) and phenalkamine before curing. Fourier transform infrared spectroscopy (FTIR) analysis showed that new amide bonding was formed between CNF and phenalkamine, while there was no chemical interaction between CNF and ECP. The thermal stability and glass transition temperature of the epoxy nanocomposites were higher than that of the base epoxy polymer. In addition, the tensile strength and Young's modulus of the epoxy nanocomposites were in the range of 47.3–84.6 MPa and 254–496 MPa, respectively, which are 59-185% and 378-837 % greater than these of the epoxy resin (29.7 and 53 MPa). The epoxy nanocomposites prepared from CNF-immobilized phenalkamine were more enhanced those properties, suggesting that the new amide bonding between CNF and phenalkamine showed effective improvement of the thermal and mechanical properties. Therefore CNSL-based epoxy nanocomposites reinforced with CNFs possess high potential as bio-based epoxy coating, film and resin.

## 3.2 Introduction

One of the most significant industrial thermosetting polymers is epoxy resins [1]. They are currently extensively used as high-performance thermosetting resins in a broad range of industrial applications, including coating, adhesive, and electrical insulation. Industrial epoxy resins have been created using petroleum resources in recent decades. However, in response to increasing environmental concerns, epoxy products with environmentally friendly production processes that result in a reduced carbon footprint [2] have gained great attention from petroleum to biomass resources. Plant oils containing triglycerides, such as soybean, linseed, and canola, for example, have been explored for use in the production of bio-based epoxy composites [3]. Cashew nut shell liquid (CNSL), a phenolic plant oil

derived from biomass waste in the cashew nut industry, is one of the potential precursors utilized to make several kinds of epoxy bio-based resins [4]. We have created CNSL-based polymers with flexibility, thermal stability, chemical resistance, and antimicrobial properties [5-7].

Cellulose nanofibers (CNFs) have generated intense research interest as natural nanofibers derived from cellulose, the most abundant natural resource on the planet. CNFs have a cross-sectional diameter of a few nanometers and a length of hundreds of nanometers [8]. CNFs with highly ordered crystalline structures have been explored as additives to improve mechanical, thermal, and gas/water vapor barrier qualities [9,10]. Epoxy composites based on CNFs have been extensively researched to increase their performance in areas such as thermal, mechanical, gas barrier, and water tolerance [11,12]. There have been a few publications recently for CNSL-based composites using CNF, such as photopolymerization of epoxy cardanol [13] and cardanol methacrylate [14].

In the present work, we have developed CNSL-derived epoxy nanocomposites composed of epoxy cardanol prepolymer (ECP), phenalkamine, and CNF. The effect of immobilized-CNF compound in the preparation of the epoxy nanocomposites as investigated in terms of the structural, thermal, and mechanical properties of the reinforced epoxy nanocomposites loaded with CNF.

## 3.3 Experiment

### 3.3.1 Materials

CNSL (industrial grade) and phenalkamine were obtained from Tohoku Chemical Industry Co., Ltd., Japan and Kusumoto Chemical, Ltd., Japan, respectively. Cellulose nanofiber (CNF) (RHEOCRYSTA, 2 wt% solid content in water suspension) was kindly supplied by DKS Co. Ltd., Japan. Two types of CNF, CNF (S) (RHEOCRYSTA I-2SX) which is standard type and CNF (A) (RHEOCRYSTA I-2AX) which has better polar solvent compatibility compared with CNF (S), were used in this work. Epichlorohydrin, dimethyl sulfoxide (DMSO), potassium hydroxide and acetone were purchased from Tokyo Chemical Industry Co., Ltd., Japan. All chemicals were used as received.

### 3.3.2 Preparation of EC

The synthesis of epoxy cardanol (EC) and ECP was conducted based on our previous work [5]. For example, 9.0 g (0.030 mol) of cardanol, potassium hydroxide and 30 mL of DMSO were placed in a 200 mL flask and stirred by magnetic stirrer. 8.9 g (0.096 mol) of epichlorohydrin was added slowly on an ice bath, then stirred at room temperature for 24 hours. The solution was extracted with diethyl ether, and the organic phase was washed with saturated sodium chloride solution. The organic phase was dehydrated with magnesium sulphate and evaporated to give EC. The product was purified by silica gel column chromatography using a mixture of *n*-hexane and ethyl acetate (9:1) as an eluent. The chemical structure of purified EC was confirmed by $^{1}$H NMR. ECP was synthesized by thermal polymerization of EC. The 5.0 g (0.017 mol) of EC placed in a 100-mL flask was stirred at 160 °C for 24 hours, yielding ECP as a high viscous liquid. In the present work, ECP with a molecular weight (Mn) of 5900 g/mol were used to prepare the epoxy polymers.

### 3.3.3 Preparation of CNF-immobilized ECP and phenalkamine

The immobilized ECP and phenalkamine wre prepared, respectively on the two types of CNF, i.e., CNF(S) and CNF(A), obtaining the following four types of CNF-immobilized compounds: CNF(S)-immobilized ECP (i-SE), CNF(A)-immobilized ECP (i-AE), CNF(S)-immobilized phenalkamine (i-SP), and CNF(A)-immobilized phenalkamine (i-AP). In this work, we used commercially available CNF water suspension (CNF-S and CNF-A) which is well-dispersed in water. Immobilization of CNFs into epoxy or amine compounds was performed by mixing methods. 3.0 g of CNF were gradually added into 1.0 g of ECP or 1.0 g of phenalkamine with stirred by magnetic stirring bar (1350 rpm, Koike Precision Instruments Mfg.Co., Ltd, Japan, model HERALES20G) at 120°C for 3 hours according to modified method of previous work [15]. During stirring, the water content was gradually evaporated. Then, the immobilized ECP and phenalkamine solution were ultrasonicated for 15 minutes to get better dispersion state of CNF. The obtained products were dried at vacuum to remove water completely. After drying, we prepared the

immobilized ECP and phenalkamine solution. The immobilization of CNF into each matrix were confirmed by FT-IR measurements.

### 3.3.4 Preparation of epoxy nanocomposites

The preparation protocol of the epoxy nanocomposites is presented in Figure 3.1. The epoxy nanocomposites were prepared by crosslinking the CNF-immobilized compound with an agent of ECP or phenalkamine added at weight ratios summarized in Table 3.1. For P5(AP) preparation, well-dispersed 1.1 g of CNF-immobilized phenalkamine (i-AP) and 2.0 g of ECP were physically mixed until the mixture became homogeneous. After degassing, the mixture was coated onto a glass plate by 200 μm applicator (Yoshimitsu Seiki, Tokyo, Japan) at 25°C. The epoxy nanocomposites were post-cured for 30 minutes at 180°C to promote further crosslink reaction. The samples were peeled from the glass plate after curing at room temperature to give the self-standing film. Eventually we prepared several epoxy (P1) and epoxy nanocomposites prepared with CNF(S)- and CNF(A)-immobilized ECP which are denoted as P2(SE) and P3(AE,) respectively. Similarly, we obtained the epoxy nanocomposites prepared with CNF(S)- and CNF(A)-immobilized phenalkamine which are denoted as P4(SP) and P5(AP), respectively. The CNF content of the epoxy nanocomposites was about 2.0 wt% in this work.

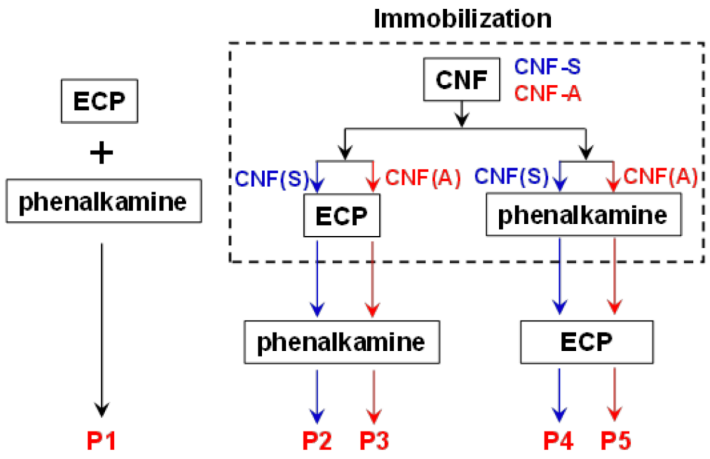


Figure 3.1 Preparation protocols of epoxy nanocomposites with CNF.

Table 3.1 Composition (weight ratio) of epoxy nanocomposites

| Sample[1)] | i-SE[2)] | i-AE[3)] | i-SP[4)] | i-AP[5)] | ECP | phenalkamine |
|---|---|---|---|---|---|---|
| P1 (epoxy) | 0 | 0 | 0 | 0 | 2 | 1 |
| P2 (SE) | 1 | 0 | 0 | 0 | 1 | 1 |
| P3 (AE) | 0 | 1 | 0 | 0 | 1 | 1 |
| P4 (SP) | 0 | 0 | 1 | 0 | 2 | 0 |
| P5 (AP) | 0 | 0 | 0 | 1 | 2 | 0 |

1) weight % ratio
2) i-SE: CNF(S)-immobilized ECP
3) i-AE: CNF(A)-immobilized ECP
4) i-SP: CNF(S)-immobilized phenalkamine
5) i-AP: CNF(A)-immobilized phenalkamine

### 3.3.5 Structure Analysis and characterization

The Fourier transform infrared (FT-IR) spectroscopy was performed on a FT/IR-4100 (JASCO Co., Tokyo, Japan). Each spectrum was averaged over 64 scans at a resolution of 2 $cm^{-1}$.

The gel content of the epoxy nanocomposite was determined from the weight fraction of the insoluble part after immersion in acetone for 24 h at room temperature. The gel content was calculated based on the following equation; $Gel\ content\ (\%) = w_{insol}/w_{initial} \times 100$, where $w_{insol}$ and $w_{initial}$ are the weight of the insoluble part and the weight of the well-dried initial sample, respectively.

Thermogravimetric analysis (TGA) was performed on a TG8120 (Rigaku Co., Tokyo, Japan). The polymer sample was heated in a platinum pan from 50 to 600 °C at a heating rate of 10°C/min under a nitrogen atmosphere at a flow rate of 60 mL/min.

The dynamic moduli of a film sample were measured at a frequency of 10 Hz using a Mettler Toledo DMA instrument. The film with dimensions of 15 mm in length, 8 mm in width, and 0.2 mm in thickness was heated from 50 to 100 °C at a rate of 5 °C/min. The amplitude of the sinusoidal strain was 0.05.

The tensile strength was measured using universal testing machine (UTM) Shimadzu EZ Test EZ-SX (Shimadzu Corporation, Kyoto, Japan) with 500 N load cell. The samples were prepared in films then cut into specimen, which was standard dumbbell shape, 38 mm length × 15 mm width × 0.2 mm thickness with a 20 mm gauge length for tensile test. In the process of measurement, the displacement was applied at a speed of 1 mm/min, and at least 5 specimens were measured for each sample. The average results of tensile strength, elongation at break and Young's modulus of the epoxy nanocomposites were calculated from the stress-strain curves.

## 3.4 Results and discussion

### 3.4.1 CNF-immobilized ECP and phenalkamine

In the present work, 4 types of CNF-immobilized compounds, i-SE, i-AE, i-SP, and i-AP were prepared. FT-IR measurement for these samples was conducted to confirm the immobilization of CNF into ECP and phenalkamine. Figure 3.2 presents FT-IR spectra of CNF, ECP, phenalkamine, and CNF-immobilized ECP and phenalkamine. For CNF(S) and CNF(A) showed a broad peak at 3600-3100 $cm^{-1}$ (OH stretching), sharp peaks at 1604 cm-1 (carboxylate $COO^{-}$) and 1100-900 $cm^{-1}$ (C–O stretching). For the CNF-immobilized ECP, characteristic peaks at 910 $cm^{-1}$ (epoxy) decreased while at 3500 $cm^{-1}$ (OH) and 1716 $cm^{-1}$ (C=O, ester) increased after the immobilization, indicating that epoxy groups reacted with $COO^{-}$ of CNF and formed ester bonding and OH group during the immobilization process. Furthermore, the formation of new hydrogen bonding was expected between ECP and CNF. On the other hand, for the CNF-immobilized phenalkamine, there were specific peaks of phenalkamine at 3300 $cm^{-1}$ (N–H) and 713 $cm^{-1}$ (C–N). In addition, a new peak at 1640 $cm^{-1}$ (C=O, amide) was appeared after immobilization, indicating the formation of amide linkage resulting from the chemical reaction between $COO^{-}$ of CNF and amine group of phenalkamine. Amine groups reacted with OH groups of CNFs to give amide linkage which can be expected as self-healing property [16, 17]. Therefore, the FT-IR measurement showed that new chemical bonding was formed in CNF-immobilized phenalkamine, while the absence of any chemical interaction between CNF and ECP.

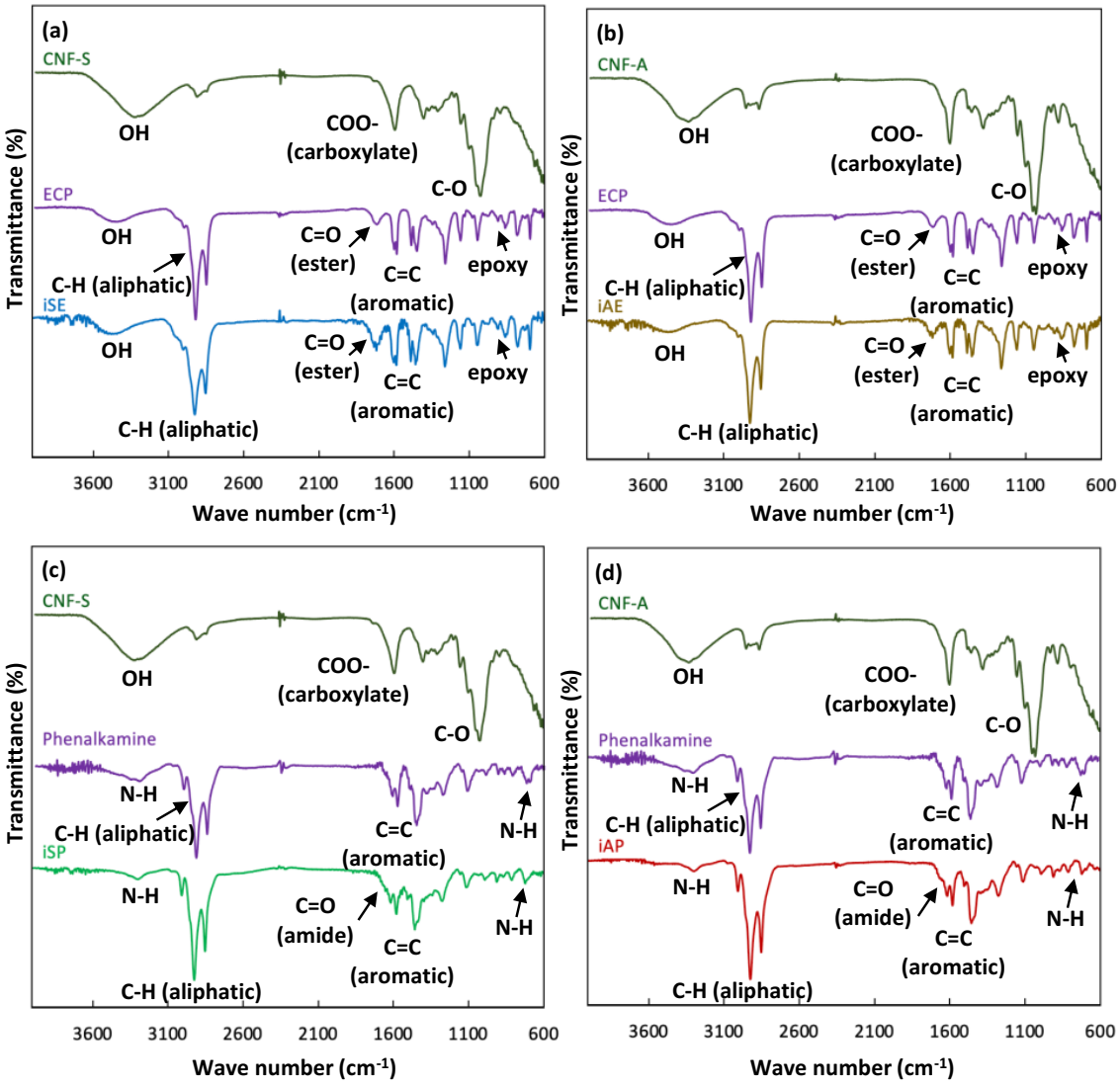


Figure 3.2 FT-IR spectra of CNF-immobilized ECP and phenalkamine (a) i-SE, (b) i-AE, (c) i-SP, and (d) i-AP.

### 3.4.2 Epoxy nanocomposites

The photographic images of the base epoxy polymer and the epoxy nanocomposite films are presented in Figure 3.3. The epoxy polymer film without CNF (before thermally post-curing) was very flexible and soft, while the epoxy composite film was stiff and hard.

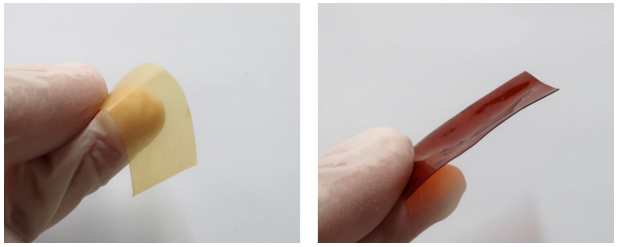

Figure 3.3 Photographs of base epoxy (left) and epoxy nanocomposite films (right).

The gel content of the polymer films was determined to evaluate the curing behavior of the epoxy nanocomposites in terms of the presence of CNF. Figure 3.4 presents the gel content of the epoxy nanocomposites. The gel content of P4(SP) and P5(AP) was greater than that of P2(SE) and P3(AE). The epoxy nanocomposites prepared with CNF(S) (i.e., P2(SE) and P4(SP)) showed lower gel contents compared with those prepared with CNF(A) (i.e., P3(AE) and P5(AP)), indicating that CNF(A) would be suitable in this epoxy polymer than the hydrophilic CNF(S) to give highly crosslinked epoxy nanocomposites.

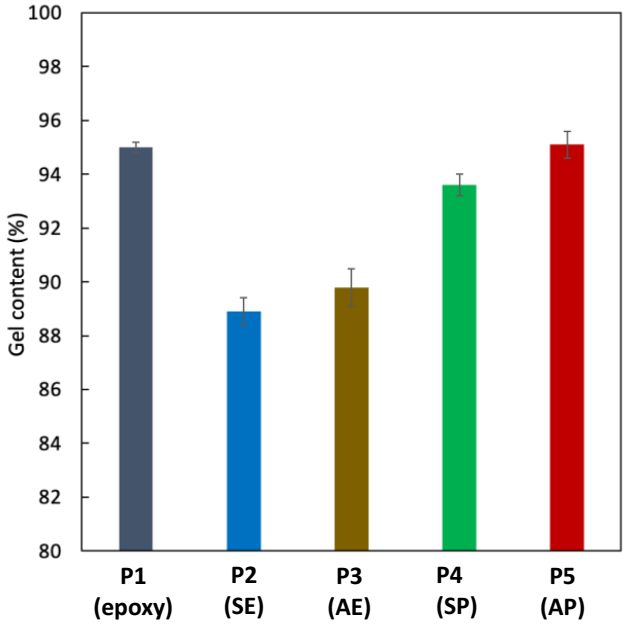


Figure 3.4 Gel content of epoxy nanocomposites.

The epoxy nanocomposites were analyzed by FT-IR measurement to investigate in more detail the curing process of the epoxy nanocomposites. Figure 3.5 presents FT-IR spectra of P1(epoxy) and P5(AP). For both P1(epoxy) and P5(AP), the characteristic peaks at 3500-3100 $cm^{-1}$ (OH group), 2974 $cm^{-1}$ (N–H, secondary), 1718 $cm^{-1}$ (C=O, ester), 1650 cm-1 (C=C), 1157 $cm^{-1}$ (C–N) were observed. The C=C was formed by dehydration of OH groups under thermally post-curing process [18]. The FT-IR analysis showed that the crosslink reaction in both P1(epoxy) and P5(AP) between epoxy and amine progressed, and the dehydration of OH group also occurred, suggesting that the epoxy nanocomposites films became more rigid and hydrophobic nature.

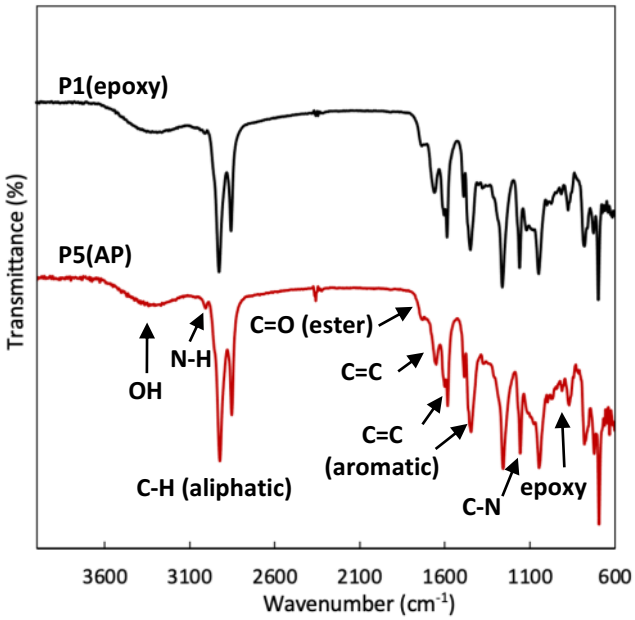


Figure 3.5 FT-IR spectra of epoxy nanocomposites.

### 3.4.3 Thermal property

The thermal stability of the epoxy nanocomposites was analyzed by TGA. The TGA curves and thermal properties of the epoxy nanocomposites are presented in Figure 3.6 and Table 3.2, respectively. The weight loss and thermal decomposition temperatures were denoted as $T_5$, $T_{10}$, and $T_d$, respectively. $W_{R600}$ is the retained weight at 600°C. The thermal stability of the epoxy nanocomposites was improved by addition of CNF. Generally, stiffness or rigidity of polymer segments is related with thermal properties of polymers such as thermal stability and glass transition temperature [19]. This result implies that the addition of CNF into epoxy polymers enhanced the rigidity or stiffness of the polymer segments. To clarify this result, it was investigated in terms of the mechanical property. In addition, new linkage between CNF and ECP or phenalkamine by chemical reaction could reduce strong hydrogen bonding formation among CNFs. This can lead to the less aggregation of CNFs in the composites [20]. The epoxy nanocomposites prepared with CNF(A) (i.e., P3(AE) and P5(AP)) showed better thermal stability than the epoxy nanocomposites prepared with CNF(S) (i.e., P2(SE) and P4(SP)), suggesting that CNF(A) could be well-embedded in the epoxy matrix than CNF(S) because of the better compatible property of CNF(A) in the epoxy nanocomposite. TGA measurement exhibited that the improvement of the thermal stability of the epoxy nanocomposites can be attributed to the covalent bonding with CNF.

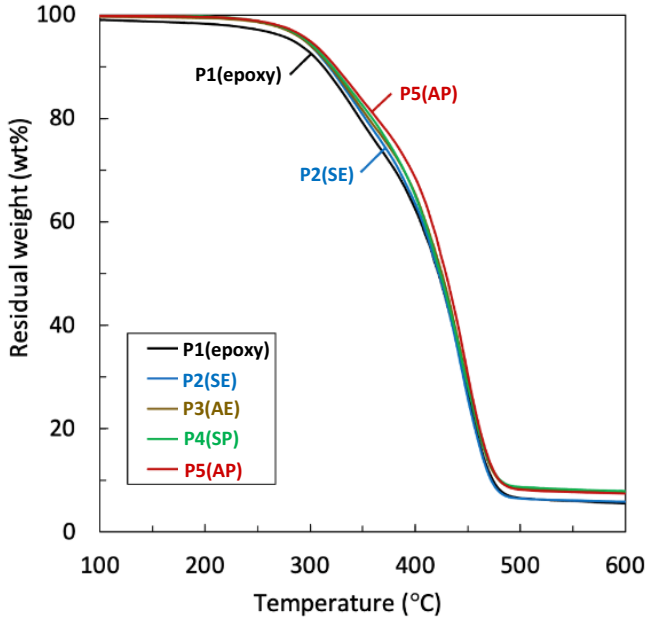


Figure 3.6 TGA curves of epoxy nanocomposites.

Table 3.2 Thermal properties of epoxy nanocomposites

| Sample | $T_5$ (°C) | $T_{10}$ (°C) | $T_d$ (°C) | $W_{R600}$ |
|---|---|---|---|---|
| P1 (epoxy) | 284 | 313 | 364 | 5.5 |
| P2 (SE) | 295 | 318 | 371 | 5.9 |
| P3 (AE) | 295 | 319 | 375 | 7.7 |
| P4 (SP) | 297 | 321 | 378 | 7.9 |
| P5 (AP) | 300 | 324 | 380 | 7.5 |

### 3.4.4 Mechanical property

The mechanical properties of the epoxy nanocomposites were evaluated by DMA and tensile strength. DMA curve of epoxy nanocomposites is presented in Figure 3.7. The glass transition temperature (Tg) of the epoxy nanocomposites was determined from maximum tanδ in DMA curve and is summarized in Table 3.3. The order of the Tg of the polymer films was P2(SE) < P1(epoxy) < P3(AE) < P4(SP) < P5(AP). Tg also represents the rigidity of polymer segments [19]. For example, Tg of P5(AP) was 56°C which was 12°C higher than of the P1(epoxy) base epoxy polymer, whereas Tg of P2(SE) was 5°C lower than of the P1(epoxy). Storage modulus (*E'*) values of P1(epoxy) and P5(AP) at rubbery state were about 600 and 4000 MPa. The difference of *E'* values between P1 and P5 can was about 3400 MPa which was affected by the chemical bonding between CNF and phenalkamine.

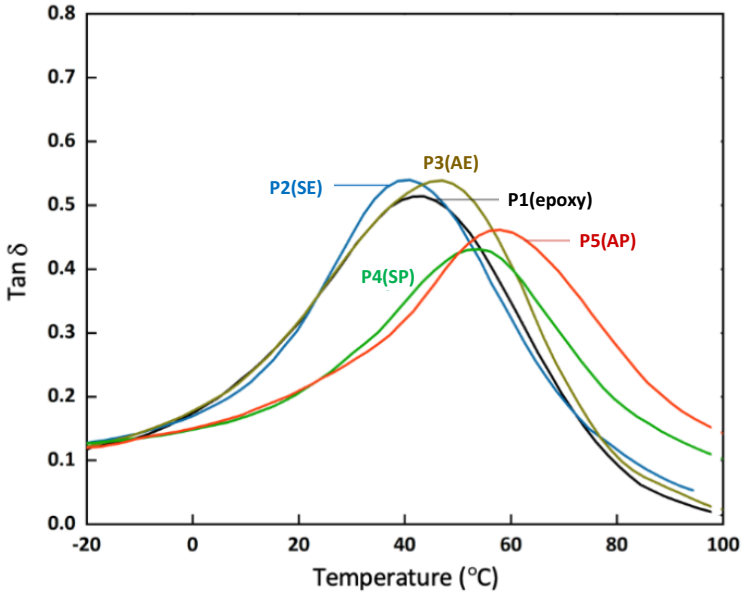


Figure 3.7 DMA curves of epoxy nanocomposites.

Table 3.3 Mechanical properties of epoxy nanocomposites

| Sample | $T_g$ (°C) | Tensile strength (MPa) | Young`s modulus (MPa) |
|---|---|---|---|
| P1 (epoxy) | 43.6 | 29.7±3.1 | 53.0±12.9 |
| P2 (SE) | 40.9 | 47.3±4.8 | 253.5±40.3 |
| P3 (AE) | 49.0 | 56.9±7.5 | 266.8±47.3 |
| P4 (SP) | 51.8 | 64.4±5.4 | 378.8±39.9 |
| P5 (AP) | 56.0 | 84.6±2.6 | 496.4±22.5 |

Figure 3.8 presents stress-strain curve of epoxy nanocomposites. The mechanical property of epoxy nanocomposites is also presented in Figure 3.9 and Table 3.3. The tensile strength and Young's modules in the epoxy nanocomposites (i.e., P2-P5) were 59-185% and 378-837% greater than those of the P1(epoxy). This result indicates that the presence of CNF obviously associates the enhancement of the stiffness of the epoxy nanocomposites. In addition, the P5(AP) showed highest values for tensile strength and Young's modules. The amide linkage between CNF and phenalkamine was more effective than the linkage between CNF and epoxy to enhance the mechanical property. Furthermore, CNF(A) would be preferable than CNF (S) because of the better compatible property of CNF(A) with this epoxy nanocomposites. Previously, the mechanical property of epoxy composite using modified graphene was improved by uniform dispersion of the modified graphene and strong interfacial bonding between the graphene and epoxy resin [21]. Therefore, in the present case, these results indicates that the improved mechanical properties of epoxy nanocomposites were could be attributed to the better dispersion of CNF in the epoxy matrix by the covalent bonding between CNF and epoxy polymer. Hence, it was found that the CNSL-based epoxy nanocomposites reinforced with CNF-immobilized phenalkamine was effective approach to improve the thermal and mechanical properties.

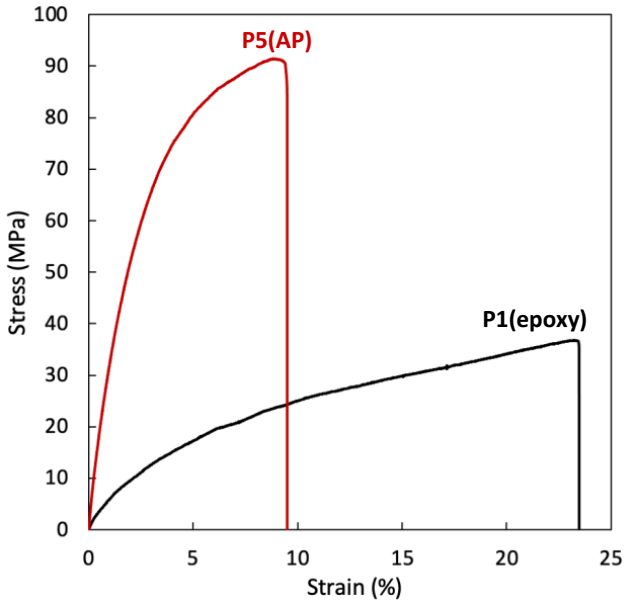


Figure 3.8 Stress-Strain curves of epoxy nanocomposites.

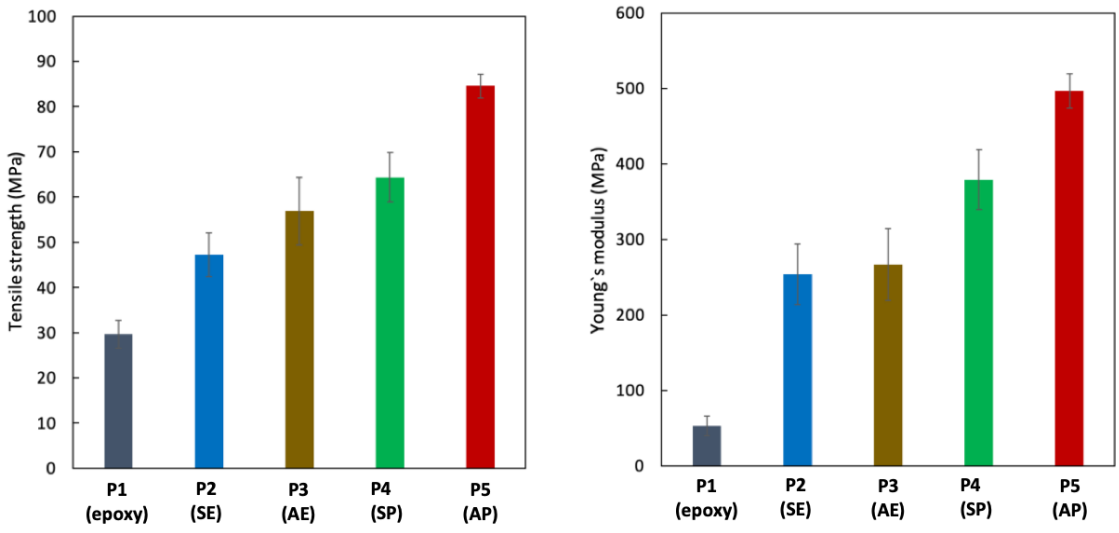


Figure 3.9 Tensile strength and Young's modulus of epoxy nanocomposites.

## 3.5 Conclusion

The novel bio-based epoxy nanocomposites were successfully prepared by using CNF. The immobilization of CNF was confirmed by FT-IR analysis, suggesting that the new amide bonging between CNF and phenalkamine was formed, while there was no chemical bonding between CNF and ECP. The epoxy nanocomposite prepared with CNF-immobilized phenalkamine greatly improved the thermal and mechanical properties. This enhancement could be attributed to the new amide bonding between CNF and phenalkamine, leading to the reduction of the hydrogen bonding among CNFs, that is, less aggregation of CNF in the epoxy nanocomposite. Therefore, the novel CNSL-derived epoxy nanocomposite reinforced with CNF has high potential as bio-based coating, film and resin.

## 3.6 References


1. Jin, F.-L., Li, X. & Park, S.-J. Synthesis and application of epoxy resins: A review. *Journal of Industrial and Engineering Chemistry* **29**, 1–11 (2015).
2. Babu, R. P., O'Connor, K. & Seeram, R. Current progress on bio-based polymers and their future trends. *Prog Biomater* **2**, 8 (2013).
3. Baroncini, E., Yadav, S., Palmese, G. & III, J. Recent Advances in Bio-based Epoxy Resins and Bio-based Epoxy Curing Agents. *Journal of Applied Polymer Science* **133**, (2016).
4. Anilkumar, P. *Cashew nut shell liquid: A goldfield for functional materials*. *Cashew Nut Shell Liquid: A Goldfield for Functional Materials* (Springer International Publishing, 2017). doi:10.1007/978-3-319-47455-7.
5. Kanehashi, S. *et al.* Preparation and characterization of cardanol-based epoxy resin for coating at room temperature curing. *Journal of Applied Polymer Science* **130**, 2468–2478 (2013).
6. Kanehashi, S. *et al.* Development of a cashew nut shell liquid (CNSL)-based polymer for antibacterial activity. *Journal of Applied Polymer Science* **132**, (2015).
7. Kanehashi, S. *et al.* Photopolymerization of Bio-Based Epoxy Prepolymers Derived from Cashew Nut Shell Liquid (CNSL). *Journal of Fiber Science and Technology* **73**, 210–221 (2017).
8. Nechyporchuk, O., Belgacem, M. N. & Bras, J. Production of cellulose nanofibrils: A review of recent advances. *Industrial Crops and Products* **93**, 2–25 (2016).
9. Isogai, A. Cellulose Nanofibers: Recent Progress and Future Prospects. *Journal of Fiber Science and Technology* vol. 76 310–326 (2020).
10. Aulin, C., Gällstedt, M. & Lindström, T. Oxygen and oil barrier properties of microfibrillated cellulose films and coatings. *Cellulose* **17**, 559–574 (2010).
11. Miao, C. & Hamad, W. Y. Cellulose reinforced polymer composites and nanocomposites: A critical review. *Cellulose* vol. 20 2221–2262 (2013).
12. Sharma, A., Thakur, M., Bhattacharya, M., Mandal, T. & Goswami, S. Commercial application of cellulose nano-composites – A review. *Biotechnology Reports* vol. 21 (2019).

13. Vacche, S. D., Vitale, A. & Bongiovanni, R. Photocuring of epoxidized cardanol for biobased composites with microfibrillated cellulose. *Molecules* **24**, (2019).
14. Vitale, A. *et al.* Biobased Composites by Photoinduced Polymerization of Cardanol Methacrylate with Microfibrillated Cellulose. *Materials* **15**, (2022).
15. Vijayan P, P., Tanvir, A., El-Gawady, Y. H. & Al-Maadeed, M. Cellulose nanofibers to assist the release of healing agents in epoxy coatings. *Progress in Organic Coatings* **112**, 127–132 (2017).
16. Mangalam, A. P., Simonsen, J. & Benight, A. S. Cellulose/DNA Hybrid Nanomaterials. *Biomacromolecules* **10**, 497–504 (2009).
17. Borsoi, C., Zimmernnam, M. V. G., Zattera, A. J., Santana, R. & Ferreira, C. A. Thermal degradation behavior of cellulose nanofibers and nanowhiskers. *Journal of Thermal Analysis and Calorimetry* **126**, 1867–1878 (2016).
18. Grassie, N., Guy, M. I. & Tennent, N. H. *Degradation of Epoxy Polymers: Part 4 Thermal Degradation of Bisphenol-A Diglycidyl Ether Cured with Ethylene Diamine*. *Polymer Degradation and Stability* vol. 14 (1986).
19. van Krevelen, D. W. & te Nijenhuis, K. *Properties of polymers: their correlation with chemical structure; their numerical estimation and prediction from additive group contributions*. (Elsevier, 2009).
20. Zhao, J. *et al.* Grafting of polyethylenimine onto cellulose nanofibers for interfacial enhancement in their epoxy nanocomposites. *Carbohydrate Polymers* **157**, 1419–1425 (2017).
21. Naebe, M. *et al.* Mechanical Property and Structure of Covalent Functionalised Graphene/Epoxy Nanocomposites. *Scientific Reports* **4**, (2014).

# CHAPTER 4: Synthesis and Characterization of Cardanol-derived Polymers via Thiol-ene Reaction

## 4.1 Abstract

Novel UV-curable bio-based polymers were prepared from cashew nut shell liquid (CNSL), natural phenol compound, at room temperature via thiol-ene reaction. The physical, thermal, optical, and mechanical properties of UV-cured polymers and the structure-property relationship of these properties were investigated. The resultant UV-cured polymers showed flexibility, transparency with high gloss, thermal resistance, and long-term stability as compared with other CNSL-based polymers. This is because that one step reaction of UV-click thiol-ene from transparent CNSL-derived monomer proceeded effectively among S–H and C=C of allyl and alkyl sidechains, leading to much higher flexible crosslinked structure. This UV-curable bio-based polymer can be very advantageous in application of flexible coating and film.

## 4.2 Introduction

Recent global environmental problems such as global warming, depletion of petroleum resources, and plastic pollution have to be solved to achieve sustainable economy. Development of chemicals and polymers from renewable resources has received great attention [1-3]. The utilization of biomass resources is highly significant for reducing greenhouse gas emissions as well as saving fossil resources. Among agricultural biomass resources, plant oil is one of the candidates for the feedstocks of bio-based materials, since plant oils have various nature such as abundant renewable resources, cost effectiveness, availability of chemical reaction, etc. Particularly, unutilized non-edible biomass resources have received particular attention since these biomasses are not competitive as food.

Cashew nuts shell liquid (CNSL) is a natural plant oil that is obtained from non-edible biomass waste produced in cashew nuts industry [4]. CNSL is a mixture of phenolic compounds such as anacardic acid, cardanol, and cardol. Main component of purified CNSL is cardanol. Recent researches for utilization of CNSL have been focused on the polymers such as phenolic resins [5-7], epoxy [8,9], polyurethane [10,11], benzoxazine

resins [12,13]. However, these polymers are prepared with formaldehyde or heavy metal catalysts. Previously, some researches for formaldehyde-free polymers, cardanol-furfural [14-16], acryl [17,18], epoxy [19-21], crosslinked resins with enzyme and oxidative polymerizations have been reported. These polymers are generally yellow to brown in color. Therefore, the transparent materials derived from CNSL is also interesting in film, packaging, and coating applications.

Thiol-ene photo-click reaction has advantages such as simple reaction and high yields [22]. This thiol-ene reaction have been employed in the synthesis of bio-based polymers using plant oils [23-27].

In the present work, it was investigated novel UV curable cardanol-derived polymer via thiol-ene reaction to give novel transparent flexible polymer without formaldehyde, heavy metal catalysts, and volatile organic solvents, which is advantageous in that it is environmentally-friendly. The UV-cured polymer derived from cardanol was investigated in terms of physical, optical and thermal properties through the comparison of previous our epoxy polymer and commercial CNSL-based polymer.

## 4.3 Experiment

### 4.3.1 Materials

Purified cardanol (3-pentadecadienylphenol) was purchased from Tohoku Chemical Industries, Ltd., Japan. The total unsaturation degree of cardanol was 2.1 determined by $^{1}$H NMR. Allyl bromide (>98%), methyl benzoylformate, and 2, 2-dimethoxy-2-phenylacetophenone (DMPA) (>98%) were purchased from Tokyo Chemical Industry Co., Ltd., Japan. Irgacure2959 was purchased from Aldrich Inc. Trimethylolpropane tris(3-mercaptopropionate) (TTMP) was purchased from Fujifilm Wako Pure Chemical Corporation, Japan. Commercially available CNSL-based polymer for painting (No. 53, Cashew Co., Ltd., Japan) was used as a comparison. Other chemicals were obtained commercially available. All the chemicals were used as received.

### 4.3.2 Synthesis of allyl cardanol

Preparation of UV-curable CNSL-derived polymer via thiol-ene reaction is presented in Scheme 4.1. Allylation of cardanol was performed according to similar manner of previous work [19]. Into a 300-mL round-bottom flask, cardanol 48.12g (0.16 mol), potassium hydroxide, 18.01 g (0.32 mol) and 42.0 mL DMF solution were mixed by magnetic stirrer. The mixed solution was cooled in an ice bath to maintain the low temperature during allyl bromide, 42.0 mL (0.50 mol) was slowly added drop by drop. Then, the mixture was stirred for 24 hours at room temperature. After stirring, distilled water was added and the mixture was stirred for 30 minutes, then extracted with ethyl acetate. The extracted organic layer was washed with water, dried over magnesium sulfate, evaporated, separated by column (hexane: ethyl acetate = 19:1), and dried in vacuum. After purification, a clear liquid was obtained (41.32 g, 93.6% yield). The allyl cardanol was confirmed by $^{1}$H NMR as shown in Scheme 4.1.

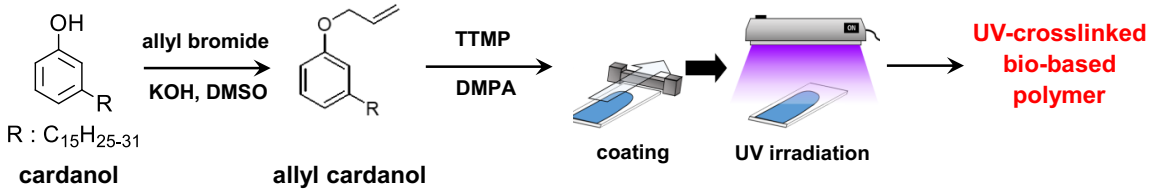


$^{1}$H-NMR [400 MHz , CDCl3, δ (ppm)] 7.21-7.15 (t, 1H, Ar-H), 6.78-6.72 (m, 3H, Ar-H), 6.11-6.02 (m, 1H, O-CH2-CH=), 5.86-5.77 (m, CH2-CH=CH2), 5.45-5.30 (m, -CH2=CH2-, O-CH2-CH=CH2), 5.08-4.96 (m, -CH=CH2), 4.54-4.51(m, 2H, Ar-O-CH2-)2.85-2.76(m, =CH-CH2-CH=), 2.59-2.54(t, 2H, Ar-CH2-CH2-), 2.07-1.98(m, CH2-CH2-CH=), 1.62-1.55(m, Ar-CH2-CH2-), 1.39-1.25(m, -CH2-), 0.93-0.86(m, -CH3)

Scheme 4.1 Preparation of UV-curable CNSL-derived polymer via thiol-ene reaction.

### 4.3.3 Preparation of crosslink film

The 1.00 g (2.94 mmol) of allyl cardanol (unsaturation degree: 2.80) and 1.09 g (2.75 mmol) of TTMP were mixed, then given amount of photo-initiator was mixed physically and treated under ultrasonication until completely dissolved. The well-mixed solution was uniformly coated onto a glass plate by applicator (75 and 750 μm, Yoshimitsu Seiki, Tokyo, Japan). UV irradiation (250W, 365 nm, ML-251D/B, Ushio lighting, Inc., Japan)

was performed at room temperature under atmosphere for given time until the solution was cured.

### 4.3.4 Structure Analysis

$^{1}$H NMR spectroscopies were conducted on a JNM-ECZR300 and JNM-ECZR500 spectrometer (JEOL Ltd., Tokyo, Japan). Samples were dissolved in deuterated chloroform solution with chemical shifts referenced from tetramethylsilane (TMS). The fluid of epoxy cardanol and epoxy cardanol prepolymer were analyzed to confirm the structure. The soluble part of the UV-cured polymers was measured to investigate the curing state.

Fourier transform infrared (FT-IR) spectroscopy was performed on a FT/IR-4100 (JASCO Co., Tokyo, Japan). Each spectrum was averaged over 64 scans at a resolution of 2 $cm^{-1}$.

Raman spectra of UV-cured polymers were conducted using the film coated on a glass plate on a Nicolet Almega XR (Thermo Scientific, USA) instrument with a 532 nm laser as the excitation source.

### 4.3.5 Characterization

The gel content of the UV-cured polymers was determined. The polymer film was immersed in acetone which is good solvent of UV-cured polymers, at room temperature. After 24 h, the non-soluble parts were filtered and dried under vacuum for 24 h to remove residual solvent before weighing. The gel content was calculated using the following equation: $Gel\ content\ (\%) = w_{insol}/w_{initial} \times 100$, where $w_{insol}$ and $w_{initial}$ are the weight of the insoluble portion and the weight of the well-dried initial sample, respectively.

At The UV–vis analysis of UV-cured films was conducted with a double beam spectrophotometer V-670 (JASCO Co., Tokyo, Japan), using a slit width of 2 nm.

Thermogravimetric analysis (TGA) was performed on a TG8120 (Rigaku Co., Tokyo, Japan). The polymer sample was heated in a platinum pan from 50 to 600°C at a heating rate of 10°C/min under a nitrogen atmosphere at a flow rate of 60 mL/min.

Dynamic mechanical analyses (DMA) were carried out on a Mettler Toledo DMA1. The DMA samples had a rectangular geometry (length: 15 mm, width: 8 mm, thickness: 0.2 mm). The samples were performed while heating at a rate of 5 °C/min from 50 to 100 °C, keeping frequency at 10 Hz (viscoelastic region) and strain at 0.05 %.

## 4.4 Results and discussion

### 4.4.1 Allyl cardanol

Allyl cardanol was confirmed by $^{1}$H-NMR and FT-IR, as shown in Scheme 4.1. The $^{1}$H NMR spectra of the allyl cardanol, the signals of the unsaturated parts (C=C) observed at 4.9-5.1, 5.3-5.5, and 5.7-5.9, and 6.0-6.1 ppm. The unsaturation degree calculated based on this NMR spectrum was estimated to be about 3.1. Throughout the allylation of cardanol, the unsaturated side chains were stable because that the value of cardanol was 3.1.

### 4.4.2 UV-cured polymer

The gel content of the UV-cured polymers obtained using various photo-initiators is summarized in Table 4.1. The highest gel content was observed in the UV-cured polymer obtained using DMPA. In addition, the transparent film was obtained only when DMPA was used (Figure 4.1). Therefore, further characterization of the UV-cured polymer prepared with DMPA was performed. Regardless of the film thickness, a self-standing colorless film with transparency and flexibility was obtained. The optimized condition for the thiol-ene reaction was determined based on the gel content of the UV-cured film. Figure 4.2 and Table 4.2 presents the gel content of the UV-cured films (75 μm) prepared using different concentrations of the photo initiator. The gel content of the UV-cured film increased with the increased concentration of the photo initiator until the concentration reached 6 %. When 6% of the photo initiator was used, it took 3 minutes to give a UV-cured film with a high gel content (96%). Based on this result, we tested for all characterization using the UV-cured film prepared using 6 % of the photo initiator with UV irradiation for 3 minutes. We also measured the gel content of the UV-cured film with a thicker film thickness (750 μm) that is prepared using 6 % of the photo initiator,

summarized in Table 4.1. The thick film required 5 minutes to get high gel content, indicating that 5 minutes UV irradiation was enough to complete the UV crosslink reaction even in the thick sample.

Figure 4.1 Photographic images of UV-curable CNSL-derived polymer films prepared with DMPA photo-initiator (left: 75 μm, right: 750 μm)

Table 4.1 Gel content of UV-cured polymers prepared with various photo-initiators

| Photo-initiator | Gel content (%) |
|---|---|
| Irgacure2959 | 73.9 |
| Methylbenzoylformate | 74.3 |
| DMPA | 94.2 |

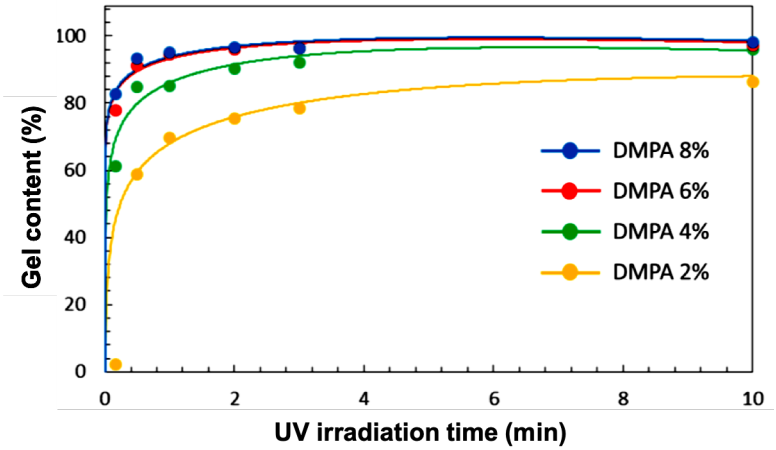


Figure 4.2 Gel content of UV-cured films (75 μm) with different amount of initiator

Table 4.2 Gel content of UV-cured films (750 μm) with 6% of photo initiator

| UV irradiation time (min) | Gel content (%) |
|---|---|
| 1 | 83 |
| 3 | 96 |
| 5 | 98 |
| 10 | 97 |
| 30 | 97 |

The chemical structure of UV-cured films and thiol-ene reaction were analysed by Raman spectroscopy. The Raman spectra of UV-cured polymers were presented in Figure 4.3. The peaks characteristic to the UV-cured film, such as 3062, 1610, 1275 $cm^{-1}$ (aromatic), 2576 $cm^{-1}$ (S–H), 1668 $cm^{-1}$ (C=C), were observed. The peaks corresponding to aromatic ring and C=C were observed in allyl cardanol, while those of S–H, C–H, C–$H_2$ were observed in thiol monomer. The peak corresponding to C=C and S-H groups decreased in UV-cured polymer after UV irradiation. The spectra also showed that residual unreacted C=C and S–H groups were still present after UV irradiation. According to structure analysis of UV-cured polymer by Raman spectroscopy, the plausible crosslink structure is presented in Figure 4.4. The reactivity of alkene with allyl ether in ene-thiol reaction is generally higher than the other C=C bonding [28]. In the present case, thiol groups reacted with the allyl position of cardanol as well as the reaction with the double bond of the side chain of cardanol, leading to the formation of three-dimensional cross-linked structure. On the other hand, it seems that it is difficult to perfectly react all the double bonds and thiol groups due to steric hindrance of C=C positions, and therefore the unreacted thiol groups and C=C were present as shown in the Raman spectra of the UV-cured polymer. This suggests that the UV-cured polymer with sufficient crosslink density was obtained to form the self-standing film as evidenced by the quite high gel content after thiol-ene reaction even some of the double bonds and the thiol groups remain unreacted.

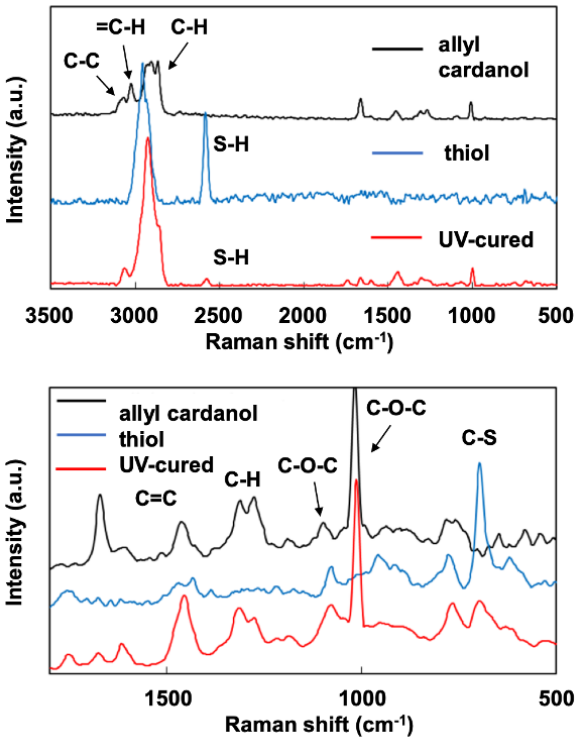


Figure 4.3 Raman spectrum of allyl cardanol, thiol compound (TTMP), and UV-cured polymer

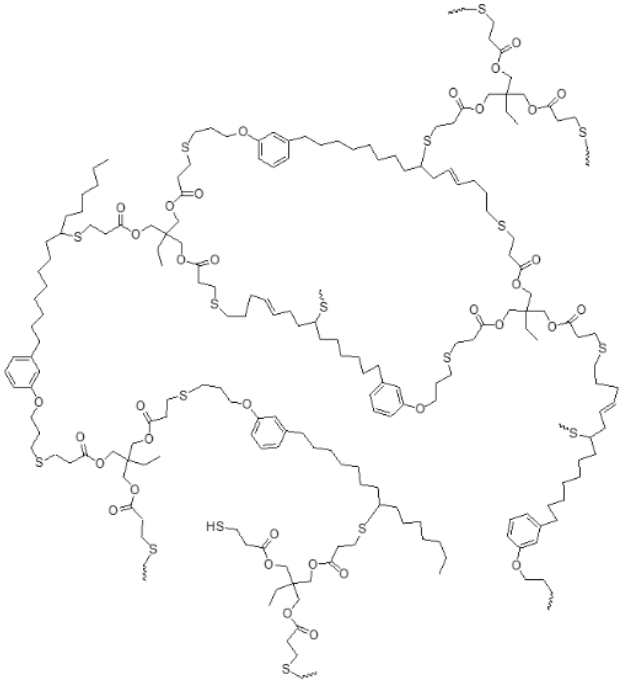

Figure 4.4 Plausible crosslink structure of UV-curable cardanol-derived polymer via thiol-ene reaction

The gel content and physical properties of the UV-cured polymer are summarized in Table 4.3, along with the physical properties of previous epoxy cardanol-amine polymer prepared with epoxy cardanol prepolymer and diethylenetriamine [21,22] and CNSL-based polymer [21,22] as comparison. For gel content, the value in the UV-cured polymer was over 95%, which was higher than that in epoxy cardanol-amine polymer but lower than that in CNSL-based polymer. The film density of the UV-cured polymer was greater than that of epoxy cardanol-amine polymer, and similar with CNSL-based polymer. In addition, the UV-cured polymer showed lowest value of the water uptake, indicating more hydrophobic and water tolerant properties. These results indicates that thiol-ene reaction of allyl cardanol provided more hydrophobic crosslink structure.

Table. 4.3 Gel content and physical properties of UV-cured polymer and other related polymers

| Polymer | Gel content/% | Density/ g $cm^{-3}$ | Water uptake/wt% |
|---|---|---|---|
| UV-cured[a] | 95.0 | 1.119 | 1.31 |
| Epoxy-amine[b] | 85.9 | 1.020 | 1.72 |
| CNSL-based polymer[c] | 98.5 | 1.111 | 1.56 |

a) this work
b) epoxy cardanol prepolymer-diethylenetriamine [21]
c) CNSL-based polymer for coating (No.53) [21]

Figure 4.5 presents UV-vis spectra of the UV-cured film along with UV-vis spectra of epoxy-amine cardanol polymer and CNSL-based polymer as comparison. The optical properties of the UV-cured polymer are also summarized in Table 4.4. The light absorption edge in the UV-cured film was as short as 288 nm, which was significantly shorter than the other polymers, indicating that the absorption in the visible light region (290-360 nm) was greatly reduced. To evaluate specific color property of the polymer films, color indices were measured. The color indices represent the optical nature of the samples. The parameter, *b* represents blue/yellow nature, wherein negative *b* value corresponds to blue and positive *b* value corresponds to yellow. Positive *b* value of other CNSL polymers was obtained, indicating the yellowness of these polymers. On the other hand, the UV-cured polymer film showed negative b value and was similar to that of glass substrate. The gloss of the UV-cured polymer film was same as CNSL-based polymer for coating, indicating

that the UV-cured polymer has a high potential for coating and film applications. These results suggest that the UV-cured polymer possesses highly transparent property.

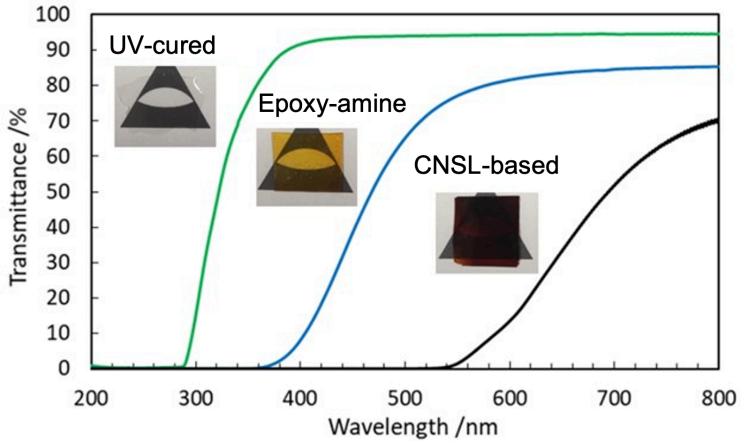


Figure 4.5 UV-vis spectrum of UV-curable CNSL-derived polymer and other related polymer films (75μm).

Table 4.4 Optical properties of UV-cured polymer and other related polymers

| Sample | Absorption edge (nm) | Refractive index at 532 nm | Color indices | | |
|---|---|---|---|---|---|
| | | | *L** | *a** | *b** |
| UV-cured | 288 | 1.548 | 89.6 | −1.1 | 1.1 |
| Epoxy-amine | 360 | 1.537 | 74.3 | −4.3 | 34.5 |
| CNSL-based polymer | 540 | 1.578 | 29.1 | 45.0 | 48.0 |

Figure 4.6 presents wavelength dependence on the refractive index of CNSL-based polymers. The wavelength dependence on the refractive index was estimated based on Cauchy's equation using 3 values of the refractive index at 532, 633, and 780 nm [29]. The refractive indices of UV-cured polymer film are summarized in Table 4.4. The refractive index at 532 nm was larger in the order of CNSL-based polymer > UV-cured polymer > epoxy cardanol-amine polymer. The refractive index of general phenolic resins, which is known as a high refractive index material, is 1.5 to 1.7. The refractive index of the CNSL-

based polymer was as high as that of the general phenolic resins. meanwhile, the refractive indices of the UV-cured polymers and epoxy cardanol-amine polymers were lower than that of the CNSL-based polymer. In general, the introduction of aromatic groups and sulfur elements increases the refractive index due to the enhancement of molar refraction [30]. The greater refractive index of the UV-cured polymer than those of epoxy-amine polymers may be because the UV-cured polymer had sulfur elements in the crosslinked structure formed by thiol-ene reaction. The refractive index of the UV-cured polymer was 1.490 which was greater than polymethyl acrylate (PMMA) [31].

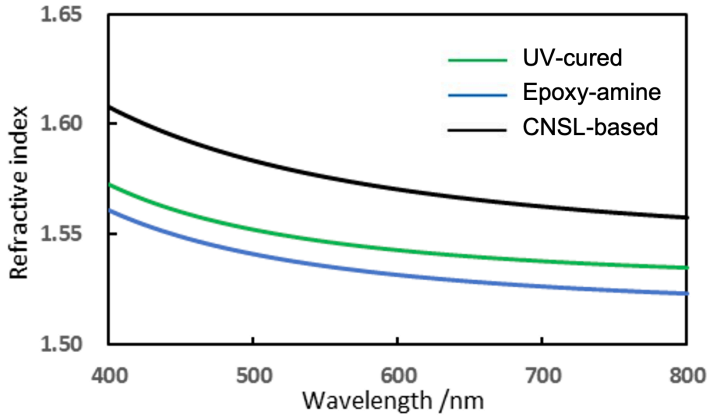


Figure 4.6 Wavelength-dependent refractive index of UV-curable CNSL-derived polymer and other related polymer films

TGA curves of UV-cured polymer were presented in Figure 4.7. The thermal property of UV-cured polymer is also summarized in Table 4.5. The UV-cured polymer and epoxy cardanol-amine polymer showed 2 step thermal decomposition behavior, as shown by the decomposition at around 300-350 °C, and at 400 °C, while CNSL product showed 1 step decomposition. The thermal decomposition temperature of the UV-cured polymer was higher than that of the epoxy-amine polymer, indicating that new C–S bonding formed by thiol-ene reaction improved the thermal stability with flexible crosslink network. The crosslink density of UV-cured polymer was greater than that of epoxy-amine polymer as shown in Table 4.3. This dense structure of the UV-cured polymer could improve the thermal stability. The possible expected crosslink structure of UV-cured and epoxy-amine polymer are presented in Figure 4.8.

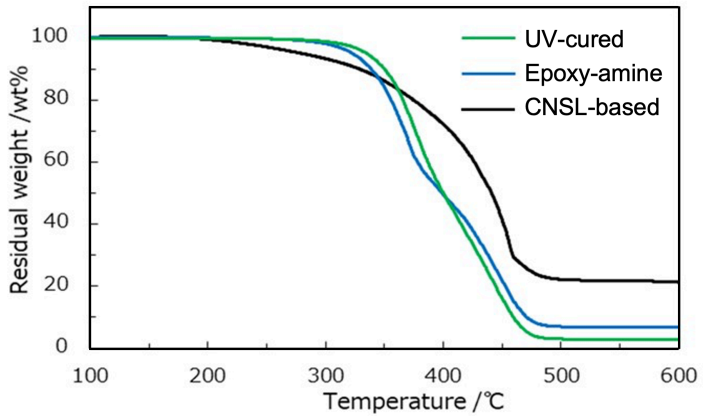


Figure 4.7 TGA curves of UV-curable CNSL-derived polymer and other related polymer films.

Table 4.5 Thermal properties of UV-cured polymer and other related polymers

| Sample | $T_5$ (°C) | $T_{10}$ (°C) | $T_d$ (°C) |
|---|---|---|---|
| UV-cured | 335 | 350 | 350 |
| Epoxy-amine | 323 | 339 | 332 |
| CNSL-based polymer | 281 | 329 | 432 |

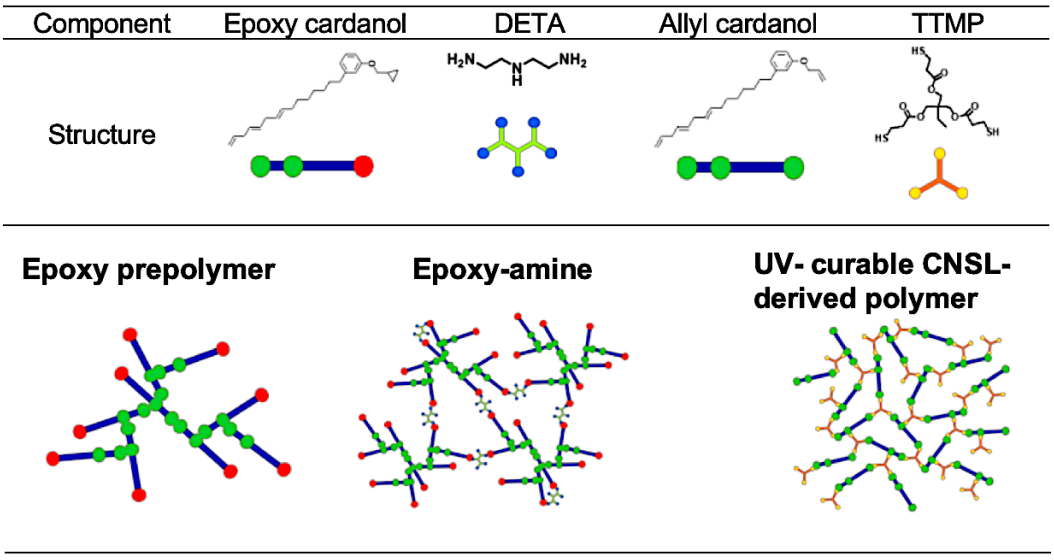


Figure 4.8 Possible crosslink structure of UV-curable CNSL-derived polymer and epoxy-amine polymer

Figure 4.9 presents DMA curves of UV-cured polymer. Mechanical property of UV-cured polymer is also summarized in Table 4.6. The glass transition temperature of UV-cured polymer was negative which was lower than that of epoxy polymer, indicating that the elastic modulus of the UV-cured polymer was greater than that of epoxy polymer at rubbery state. Furthermore, UV-cured polymer has flexible C–S bonding leading to less molecular interaction. C–S bonding as well as long alkyl side chains gives flexible nature, therefore, relatively high elastic modulus at room temperature with highly crosslink structure.

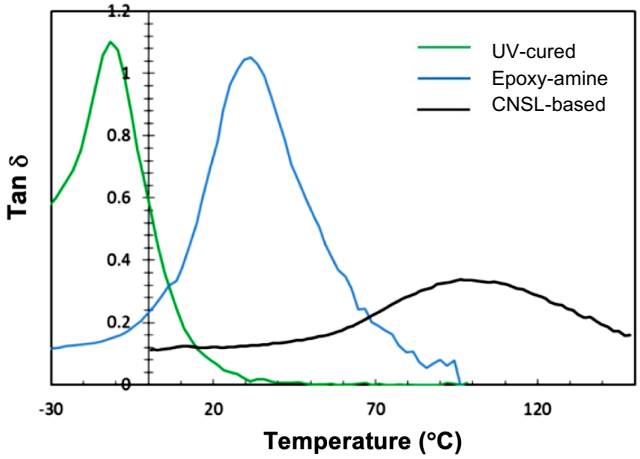


Figure 4.9 DMA curves of UV-cured polymer

Table 4.6 Glass transition temperature and storage modulus of UV-cured polymer and other related polymers

| Component | $T_g$ /°C | Storage modulus /MPa | | |
|---|---|---|---|---|
| | | 20°C | 30°C | 40°C |
| UV-cured | −11.8 | 6 | 6 | 7 |
| Epoxy-amine | 31.6 | 97 | 18 | 5 |
| CNSL-based polymer | 96.3 | 770 | 676 | 572 |

### 4.4.3 Stability (Time dependence behavior)

The stability or time depensence behavior of UV-cured polymer was investgated by the gel content and UV transmittance which it was compared with epoxy-amine and CNSL-based polymer. The time dependence on gel content of UV-cured and epoxy polymers in Figure 4.10. The gel content of UV-cured polymers after UV irradiation was almost constant, indicating that the crosslink structure was stable (i.e., no autoxidative reaction at unsaturation part). Moreover, the time-dependence on the UV-vis spectrum of UV-cured film is presented in Figure 4.11. The UV-vis spectrum of the UV-cured polymer was no change for 2 months, while those of the epoxy cardanol-amine polymer and CNSL-based polymer shifted to long-wavelength side with time due to the typical autoxidation at residual unsaturation parts occurred [19]. This is because that the thiol groups effectively reacted with C=C bonding in UV-cured polymer, leading to the suppression of the autoxidation.

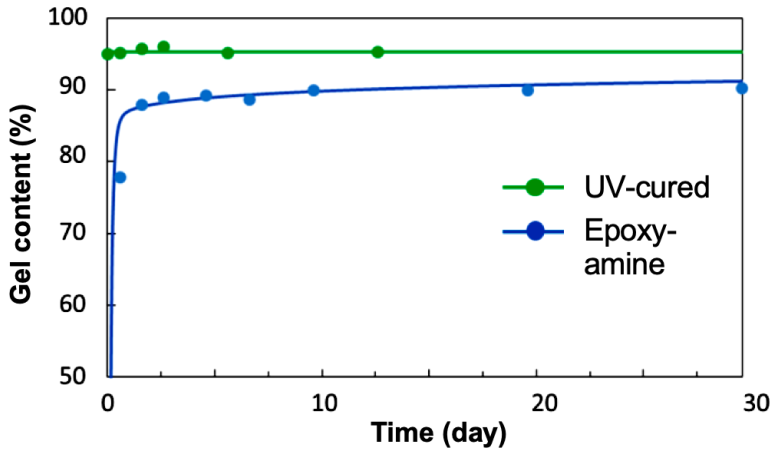


Figure 4.10 Time dependence of gel content of UV-cured and epoxy polymers

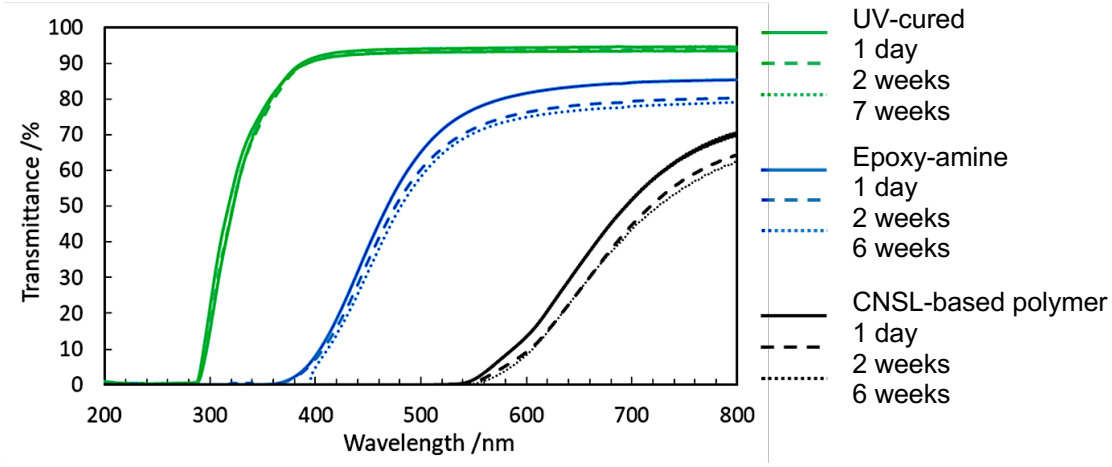


Figure 4.11 Time dependence of UV-vis spectra of UV-cured and epoxy polymers

## 4.5 Conclusion

Novel environmentally-friendly UV-curable polymer derived from CNSL via thiol-ene photo-click reaction. By converting the phenolic hydroxyl group to an allyl group, the thiol-ene reaction proceeded effectively among thiol, allyl groups and unsaturation parts in the alkyl side chains. The obtained UV-cured polymer film was flexible transparent with highly thermal stability. Furthermore, there was no change in UV-vis spectrum of this polymer for 2 months, indicating that thiol-ene reaction proceeded among thiol compound and allyl as well as unsaturation groups in the cardanol side chains. Therefore, this UV-curable bio-based polymer can be very advantageous in application of flexible coating and film.

## 4.6 References

1. Meier, M. A. R., Metzger, J. O. & Schubert, U. S. Plant oil renewable resources as green alternatives in polymer science. *Chem. Soc. Rev.* **36**, 1788–1802 (2007).
2. Zhu, Y., Romain, C. & Williams, C. K. Sustainable polymers from renewable resources. *Nature* vol. 540 354–362 (2016).
3. Miller, S. A. Sustainable Polymers: Opportunities for the Next Decade. *ACS Macro Letters* **2**, 550–554 (2013).
4. Anilkumar, P. *Cashew nut shell liquid: A goldfield for functional materials*. *Cashew Nut Shell Liquid: A Goldfield for Functional Materials* (Springer International Publishing, 2017). doi:10.1007/978-3-319-47455-7.

5. Campaner, P., D'Amico, D., Longo, L., Stifani, C. & Tarzia, A. Cardanol-based novolac resins as curing agents of epoxy resins. *Journal of Applied Polymer Science* **114**, 3585–3591 (2009).
6. Cardona, F., Lau, K. tak & Fedrigo, J. Novel Phenolic Resins with Improved Mechanical and Toughness Properties. *Journal of Applied Polymer Science* **123**, (2012).
7. Barreto, A. C. H., Rosa, D. S., Fechine, P. B. A. & Mazzetto, S. E. Properties of sisal fibers treated by alkali solution and their application into cardanol-based biocomposites. *Composites Part A: Applied Science and Manufacturing* **42**, 492–500 (2011).
8. Raju & Kumar, P. Cathodic electrodeposition of self-curable polyepoxide resins based on cardanol. *Journal of Coatings Technology and Research* **8**, 563–575 (2011).
9. Yadav, R., Srivastava, P. & Srivastava, D. Studies on synthesis of modified epoxidized novolac resin from renewable resource material for application in surface coating. *Journal of Applied Polymer Science* **114**, 1471–1484 (2009).
10. Gopalakrishnan, S. & Fernando, T. Influence of polyols on properties of bio-based polyurethanes. *Bulletin of Materials Science* **35**, (2012).
11. Mythili, C., Retna, M. & Gopalakrishnan, S. Physical, mechanical, and thermal properties of polyurethanes based on hydroxyalkylated cardanol–formaldehyde resins. *Journal of Applied Polymer Science* **98**, (2005).
12. Lochab, B., Varma, I. K. & Bijwe, J. Cardanol-based bisbenzoxazines: Effect of structure on thermal behaviour. *Journal of Thermal Analysis and Calorimetry* **107**, 661–668 (2012).
13. Rao, B. S. & Palanisamy, A. A new thermo set system based on cardanol benzoxazine and hydroxy benzoxazoline with lower cure temperature. *Progress in Organic Coatings* **74**, 427–434 (2012).
14. Souza, F. G. *et al.* Effect of pressure on the structure and electrical conductivity of cardanol-furfural-polyaniline blends. *Journal of Applied Polymer Science* **119**, 2666–2673 (2011).
15. John, G. & Pillai, C. K. S. Synthesis and characterization of a self-crosslinkable polymer from cardanol: Autooxidation of poly(cardanyl acrylate) to crosslinked film. *Journal of Polymer Science Part A: Polymer Chemistry* **31**, 1069–1073 (1993).
16. Ikeda, R., Tanaka, H., Uyama, H. & Kobayashi, S. *Enzymatic Synthesis and Curing of Poly(cardanol)*. *Polymer Journal* vol. 32 (2000).
17. Ikeda, R., Tanaka, H., Uyama, H. & Kobayashi, S. Synthesis and curing behaviors of a crosslinkable polymer from cashew nut shell liquid. *Polymer (Guildf)* **43**, 3475–3481 (2002).
18. Otsuka, T., Fujikawa, S. I., Yamane, H. & Kobayashi, S. Green polymer chemistry: The biomimetic oxidative polymerization of cardanol for a synthetic approach to "artificial urushi." *Polymer Journal* **49**, 335–343 (2017).
19. Kanehashi, S. *et al.* Preparation and characterization of cardanol-based epoxy resin for coating at room temperature curing. *Journal of Applied Polymer Science* **130**, 2468–2478 (2013).
20. Kanehashi, S. *et al.* Photopolymerization of Bio-Based Epoxy Prepolymers Derived from Cashew Nut Shell Liquid (CNSL). *Journal of Fiber Science and Technology* **73**, 210–221 (2017).
21. Kanehashi, S. *et al.* Development of a cashew nut shell liquid (CNSL)-based polymer for antibacterial activity. *Journal of Applied Polymer Science* **132**, (2015).
22. Hoyle, C. E. & Bowman, C. N. Thiol-ene click chemistry. *Angewandte Chemie - International Edition* vol. 49 1540–1573 (2010).
23. Wang, H. & Zhou, Q. Synthesis of Cardanol-Based Polyols via Thiol-ene/Thiol-epoxy Dual Click-Reactions and Thermosetting Polyurethanes Therefrom. *ACS Sustainable Chemistry & Engineering* **6**, 12088–12095 (2018).

24. Fu, C., Liu, J., Xia, H. & Shen, L. Effect of structure on the properties of polyurethanes based on aromatic cardanol-based polyols prepared by thiol-ene coupling. *Progress in Organic Coatings* **83**, 19–25 (2015).
25. Shrestha, M. L. *et al.* Biobased Aromatic-Aliphatic Polyols from Cardanol by Thermal Thiol-Ene Reaction. **6**, 87–101 (2018).
26. Darroman, E., Bonnot, L., Auvergne, R., Boutevin, B. & Caillol, S. New aromatic amine based on cardanol giving new biobased epoxy networks with cardanol. *European Journal of Lipid Science and Technology* **117**, 178–189 (2015).
27. Wazarkar, K. & Sabnis, A. Synthesis and characterization of UV oligomer based on cardanol. *Journal of Renewable Materials* **8**, 57–68 (2020).
28. Northrop, B. H. & Coffey, R. N. Thiol–ene click chemistry: Computational and kinetic analysis of the influence of alkene functionality. *J Am Chem Soc* **134**, 13804–13817 (2012).
29. Jenkins, F. A. & White, H. E. Reflection. *Fundamentals of Optics* 523–543 (1981).
30. Liu, J. & Ueda, M. High refractive index polymers: fundamental research and practical applications. *Journal of Materials Chemistry* **19**, 8907–8919 (2009).
31. Ali, U., Karim, K. J. B. A. & Buang, N. A. A review of the properties and applications of poly (methyl methacrylate)(PMMA). *Polymer Reviews* **55**, 678–705 (2015).

# CHAPTER 5: Conclusions

Novel environmentally-friendly bio-based polymers derived from natural cardanol were developed from phenolic oil which obtained from cashew nut shells.

The conclusions for each topic are as follow;

**Synthesis and Characterization of Novel Bio-based Epoxy Polymers Derived from Cardanol**

Novel epoxy polymers were synthesized from cardanol derivatives, epoxy cardanol prepolymer (ECP) and phenalkamine. The optimum ratio of ECP and phenalkamine was 2:1 by weight, which determined by drying time and epoxy polymer gel concentration that close to the predicted ratio. The effects of the prepolymer's molecular weight and the heat treatment on the physical characteristics of the epoxy polymers were examined. It was found that, the drying time to harden dry state of the epoxy polymers was substantially dependent on the prepolymer's molecular weight. This finding suggests that the prepolymer's molecular weight may influence the drying time of the epoxy polymer. The epoxy polymer demonstrated flexibility and heat stability up to 300°C. The glass transition temperature of the epoxy polymer was almost ambient temperature, as revealed by dynamic viscoelasticity experiments. According to the optical, thermal, and mechanical characteristics of the epoxy polymer, the prepolymer's molecular weight had a substantial impact on the drying properties of the epoxy polymer, indicating that a prepolymer with a high molecular weight is more likely to form the cross-linked structure. Furthermore, as a post-curing step, heat treatment of epoxy polymers considerably improved mechanical strength and glass transition temperature. Antimicrobial activity of epoxy polymers against *E. coli* and *S. aureus* was discovered. As a result, this unique cardanol-derived epoxy polymer has a great potential for use in flexible, thermally resistant, and anti-microbial coatings and resins.

**Development of Cellulose Nanofiber-reinforced Cardanol Epoxy Composites**

For advanced cellulose nanofiber composites, epoxy resins are preferred polymer matrices for various applications. However, in order to generate high-performance composites, poor dispersion and compatibility between cellulose fibers and polymer matrix become critical concerns that must be addressed. In this study, to achieve environmental-friendly bio materials, synthesized cardanol and cardanol derivative, phenalkamine were applied for polymer matrices. The results show that the immobilization of CNF was confirmed by FT-IR analysis, suggesting that the new amide bonging between CNF and phenalkamine was formed, while there was no chemical bonding between CNF and ECP. The epoxy nanocomposite prepared with CNF-immobilized phenalkamine greatly improved the thermal and mechanical properties. This enhancement could be attributed to the new amide bonding between CNF and phenalkamine, leading to the reduction of the hydrogen bonding among CNFs, that is, less aggregation of CNF in the epoxy nanocomposite. Therefore, the novel CNSL-derived epoxy nanocomposite reinforced with CNF has high potential as bio-based coating, film and resin. In further work, the morphology of cellulose nanofiber-reinforced cardanol epoxy composites will be analyzed to describe the dispersion of CNF.

**Synthesis and Characterization of Cardanol-derived Polymers via Thiol-ene Reaction**

Novel UV-curable bio-based polymers were prepared from cashew nut shell liquid (CNSL), natural phenol compound, at room temperature via thiol-ene reaction. The physical, thermal, optical, and mechanical properties of UV-cured polymers and the structure-property relationship of these properties were investigated. The resultant UV-cured polymers showed flexibility, transparency with high gloss, thermal resistance, and long-term stability as compared with other CNSL-based polymers. This is because that

one step reaction of UV-click thiol-ene from transparent CNSL-derived monomer proceeded effectively among S–H and C=C of allyl and alkyl sidechains, leading to much higher flexible crosslinked structure. This UV-curable bio-based polymer can be very advantageous in application of flexible coating and film by its significantly transparent property.